COMPARATIVE SENSORY AND ENERGETIC ECOLOGY OF SCIAENID FISHES AND THEIR COMPETITORS IN CHESAPEAKE BAY, VA

A Dissertation

Presented to

The Faculty of the School of Marine Science

The College of William and Mary in Virginia

In Partial Fulfillment

Of the Requirements for the Degree of

Doctor of Philosophy

---

by

Andrij Zenon Horodysky

2009

APPROVAL SHEET

This dissertation is submitted in partial fulfillment of
the requirements of the degree of

Doctor of Philosophy

_____
Andrij Zenon Horodysky

Approved August 2009.

_____
Robert J. Latour, Ph.D.
Committee Chairman, co-Advisor

_____
John A. Musick, Ph.D.
co-Advisor

_____
Richard W. Brill, Ph.D.

_____
Mark R. Patterson, Ph.D.

_____
Sönke Johnsen, Ph.D.
Duke University
Durham, NC

DEDICATION

This dissertation is dedicated to the memory of my grandfather, John Zenon Horodysky, Ph. D., J.D. (1915-2002), who always made time to take me fishing and dreamed about seeing his grandson pursue a graduate education.

TABLE OF CONTENTS

ACKNOWLEDGMENTS

To my committee chair and co-advisor, Rob Latour, I offer limitless thanks for your friendship, patience, advice, and support throughout the past five years. You have worn a myriad of caps including mentor, friend, fishing partner, psychiatrist, programming guru, as well as one with a big red B on it. You gently fed me the bran flakes of quantitative analysis, and convinced me that it was good for me even if a bit distasteful at first. I thank you so humbly for all of it, Rob, and hope this synthesis is but an inkling of what is to come for us. I especially thank you for the times spent on Chesapeake Bay experiencing our fauna firsthand and collecting my research specimens with hook and line. I greatly look forward to our collaborations, our field adventures, and our philosophical "lab meetings" with peaty brown liquids.

To my coadvisor, Jack Musick, I offer sincere thanks for initiating my training as an ichthyologist on the banks of the Delaware, and for the many discussions of the conspiracies of fish behavior over ice cubes marinating in Islay malts. Your insights into the natural world have fundamentally molded both this dissertation and my comparative and evolutionary approach to fisheries science. Time spent in the field with you, whether in Virginia or in more exotic locales, has fueled my wonderment with the natural world and the delicate evolutionary balances that underlie behavior and ecology. I greatly look forward to the times we'll spend 'standing in a river and waving a stick' at pavement's end, tithing at the Temple of the Flowing Waters.

To Rich Brill, a coadvisor in all but title, I give tremendous thanks for your patience, forsight, rigor, support, and dedication to seeing these chapters morph from abstract ideas in my head to published manuscripts. Your incredible work ethic, seemingly limitless range of skills and techniques, unwavering devotion to student projects, and remarkable productivity are, in short, tremendous inspirations. None of my work would have been possible without you, Rich, and I thank you from the bottom of my heart. May this dissertation stand as a testament to your mentorship, and may it be a sign of the collaborative things to come.

Committee members Mark Patterson and Sönke Johnsen deserve special mention for gently making the biophysical tangible to a physics- and math-phobe, and for patient diligence in critically reviewing this work. Non-committee coauthors on papers from this dissertation, Mike Fine, Eric Warrant, and Peter Bushnell, deserve thanks for the many discussions. Collectively, thank you all for enduring my out-of-the-blue phone calls, office raids, and late night emails about the theory underlying these experiments, and for critically reviewing and refining these chapters.

Many contributed time, sweat, and resources to this project and my VIMS tenure. Patrick Lynch and Andre Buchheister were invaluable sounding boards, fellow animal husbanders, and great friends in the office, laboratory, field, and special 'lab meetings'. Fellow Ichthyology TAs Dave Portnoy, Chip Cotton, and Pat McGrath trips to Mountain Lake and points west unforgettable, and Chris Magel and Lenny Pace carved indelible

memories in Wachapreague for three summers of cohabitation, assisting tremendously with animal husbandry. Dr. Lenore Litherland very patiently and diligently taught me so much about the dark arts of electrophysiology and invaluably helped me endure their emotional rollercoaster. Tom Nania spent two internship summers assisting with AMR experiments, animal husbandry, and calorimetry while providing an unforgettable guitar soundtrack to this degree. My MS advisor, Dr. John Graves, served as a great friend, counsel *par excellence*, dissertation moderator, and an extremely productive collaborator that provided my support in the last several semesters of this degree. Cindy Forrester, Grace Walser, and Gail Reardon very patiently ensured that my paychecks kept coming and that all of my ordering and travel paperwork was correct, thereby enabling any and all of this dissertation. Jane Lopez and Connie Motley carefully proctored the small fruits of my grantwriting, and Bob Polley and Adam Miller generously gave of their time to repair the myriad of computers I totaled. Financial support for my research was provided by grants from NOAA-CMER, the VMRC Saltwater Recreational License fund, and the International Women's Fishing Association. A small army of labmates and friends from the collective 8 years at VIMS deserves humble thanks for forging lifelong memories in the moments not spent in front of computers. Those who remain unmentioned herein should still be aware I am indebted for your contributions.

Finally, to my family, I give sincere thanks for the unwavering love, unquestioned support, incredible patience, and steadying advice that was so central to the successful completion of this degree. From the bottom of my heart, my humblest thanks.

LIST OF TABLES

Page

CHAPTER 4: Comparative Metabolism in Sciaenid Fishes Common to Chesapeake Bay, VIRGINIA

LIST OF FIGURES

Page

ABSTRACT

Coastal fishes of the western North Atlantic, such as sciaenids and their competitors, support substantial commercial and recreational fisheries in waters that may vary widely in temperature, salinity, light intensity and spectral distrubution, and dissolved oxygen levels, yet their ecophysiological abilities to cope with such variability have received little attention. I therefore applied multidisciplinary comparative techniques to investigate aspects of the sensory and energetic ecophysiology of several sciaenid fishes and non-sciaenid competitors common in the western North Atlantic.

Auditory brainstem response experiments demonstrated that sciaenid fishes have greatest auditory sensitivity at low frequencies that match their vocalizations. Based upon both anatomy and auditory bandwidths, most sciaenids appear to be hearing generalists that are likely sensitive to the particle motion components of aquatic sounds.

Electroretinographic experiments revealed that the luminous sensitivities, temporal properties, and chromatic characteristics of the visual systems of phylogenetically-similar sciaenid fishes from different microhabitats, and those of phylogenetically-dissimilar piscivores from similar microhabitats, all correlated with lifestyle and ecology. The eyes of benthic and nocturnal fishes were typified by high luminous sensitivity, slow temporal resolution, and relative diel-invariance, consistent with foraging in dim photoclimates. By contrast, the eyes of pelagic diurnal piscivores had comparatively lower luminous sensitivity, higher temporal resolution, and exhibited higher diel variation, consistent with specific diurnal light niches. Accordingly, visually-foraging diurnal piscivores may be disadvantaged in eutrophied, turbid waters characteristic of many modern estuaries.

Intermittent-flow respirometry experiments revealed that the majority of sciaenid fishes had resting and active metabolic rates similar to those of most teleost fishes but significantly lower than high-demand species such as tunas. However, the metabolic rates of kingfishes (*Menticirrhus* sp.) were significantly higher than other sciaenids, but significantly lower than those of tunalike fishes. Estimates of standard metabolic rate from power performance curves fitted to active metabolic rate data did not differ significantly from experimentally-derived measurements in static chambers, validating the experimental approach.

Data from these chapters were analyzed with linear repeated measures and nonlinear mixed effects models that considered repeated measurement of subjects, modeled within-individual correlations, and the included random factors that improved the scope of inference. Although not novel approaches, these methods demonstrate quantitative advancements for future analyses of physiological data comprised of multiple measurements taken from individual experimental subjects. Collectively, the results of this dissertation underscore the potential power and utility of physiological techniques to provide a wide variety of information that may complement more traditional techniques used in fisheries science, particularly when coupled with appropriate analytical strategies. Sciaenid fishes are model organisms for investigations of the links between form, function, and the environment in coastal ecosystems.

AUTHOR'S NOTE

The primary research chapters of this dissertation were written in the format of the journal in which each is published, in review, or to be submitted. Said chapters are written in the third person to represent my co-authors. The citations for the chapters are as follows:

Chapter 1

Horodysky, A.Z., Brill, R.W., Fine, M.L., Musick, J.A., and Latour, R.J. (2008). Acoustic pressure and acceleration thresholds in six sciaenid fishes. *J. Exp. Biol*. **211(9)**, 1504-1511.

Chapter 2

Horodysky, A.Z., Brill, R.W., Warrant, E.J., Musick, J.A., and Latour, R.J. (2008). Comparative visual function in five sciaenid fishes. *J. Exp. Biol.* **211(22)**:3601-3612.

Chapter 3.

Horodysky, A.Z., R.W. Brill, E.J. Warrant, J.A. Musick, and R.J. Latour. (In prep). Comparative visual function in four piscivorous fishes inhabiting Chesapeake Bay. *J. Exp. Biol*.

Chapter 4.

Horodysky, A.Z., Brill, R.W., Bushnell, P.B., Musick, J.A. and Latour, R.J. (In review). Metabolic rates of sciaenid fishes common to Chesapeake Bay, VA. *J. Exp. Biol*.

COMPARATIVE SENSORY AND ENERGETIC ECOLOGY OF SCIAENID FISHES AND THEIR COMPETITORS IN CHESAPEAKE BAY, VA

PROJECT INTRODUCTION

Chesapeake Bay: a brief physical and ecological overview

The Chesapeake Bay is the largest estuary in the United States, presently covering an area of 6500 km^2 and draining a watershed of over 170,000 km^2 throughout parts of six states and the District of Columbia. This geologically recent estuary formed in the Pleistocene 7-9 kya when the dendritic river system of the paleo-Susquehanna River, itself formed by an Eocene bolide impact 35 mya, was flooded by post-glacial sea level rise (Willard et al., 2003). Along with the Susquehanna, which provides about half of Chesapeake Bay's freshwater input, the major tributaries of the modern bay include the Potomac (33%), James (13%), Rappahannock (3%), York (2%), Patuxent (1%), Choptank (1%) and Nanticoke (1%) (Schubel and Pritchard, 1986). The bay's main stem is approximately 320 km long and averages 10-15 m deep. The majority of the bay is fairly shallow (50% of its area < 6 m depth), however the bay's deepest point exceeds 50 m (Murdy et al. 1997). The estuary's name derives from the Algonquin '*Chesepiooc'* meaning "settlement at a big river" (Stewart, 1945); this watershed was the site of the first permanent English settlement (Jamestown, 1607). Chesapeake Bay bears a rich cultural history, but human inhabitants have had a profound impact on watershed over the last half-millennium. European settlers in the 17th and 18th centuries removed riparian buffer zones, increasing sedimentation rates to the Bay. Agricultural and population expansion from the mid 19th Century to present dramatically increased nutrient loadings to tributaries, leading to eutrophication (Cooper and Brush, 1993). More recently, industrialization and urbanization has increased runoff of pesticides and other organic and inorganic contaminants (Cooper and Brush, 1993; Ko and Baker, 1995). The anthropogenic degradation of Chesapeake Bay over time has been well documented;

consequences for ecosystem structure and function remain less tangibly understood (Cooper and Brush 1993; Kemp et al., 2005).

The present Chesapeake Bay is a partially-mixed salt wedge estuary with a latitudinal salinity gradient, strong seasonal pycnoclines, and extreme annual water temperature ranges (0-4ºC in late winter vs. 28-30ºC in late summer: Murdy et al., 1997). The stratification of bay waters is generally enhanced during the warmer, wetter seasons, when seaward-moving warm freshwaters overlie cooler saline bottom waters that are pushed up the bay and its tributaries by Chesapeake Bay's semidiurnal tides. This "salt wedge" conduit is exploited by the ingressing larvae of many fishes and invertebrates via the selection of favorable flows and avoidance of unfavorable flows, a process known as selective tidal stream transport (Forward and Tankersley, 2001; Hare et al., 2005). However, this stratification also reduces the transport and exchange of materials across the pycnocline, effectively isolating deeper layers from mixing with oxygenated surface waters. Nutrient-enriched freshwaters trapped at the surface overstimulate primary production in warmer, wetter months, resulting in a flux of organic materials into bottom waters where respiration processes exacerbate low oxygen conditions (Taft et al., 1980). Additionally, recent increases in sedimentation and eutrophication have decreased light attenuation and increased the frequency and extent of hypoxic/anoxic conditions, leading to losses of submerged aquatic vegetation and changes in benthic community structure (Orth and Moore, 1984; Cooper and Brush, 1993). Large inter- and intrannual variations in salinity, temperature, turbidity, and dissolved oxygen are caused by regional precipitation and discharge from tributaries (Cronin et al., 1999), nutrient dynamics

(Boynton and Kemp, 1985), physical processes such as tides (Breitburg, 1992), and ecological interactions (Kemp et al.2005).

Despite the hyperdynamic nature of temperature, salinity, and oxygen in Chesapeake Bay, this estuary is utilized by over 3,000 species of plants and animals, including 267 fish species (Murdy et al., 1997). Chesapeake Bay has only 32 year-round resident fishes, which is not surprising given its extreme 25-30ºC annual temperature range. The majority of the bay's fish fauna are seasonal visitors, which include boreal fauna in cooler months and tropical fauna in warmer months. Peak diversity in Chesapeake Bay occurs in late summer and early fall, when rare tropical visitors coincide with warm-temperate and subtropical fishes (Murdy et al., 1997). In addition to designations based on biomes, the fish fauna of Chesapeake Bay can also be delineated by salinity regime into freshwater, euryhaline estuarine, high salinity marine, and diadromous species, the latter classification based on specialized reproductive migrations of anadromous and catadromous fauna. Among the most abundant, diverse, ecologically important and often economically important fishes in Chesapeake Bay are warm temperate euryhaline fishes of the families Cyprinodontidae, Paralichthyidae and Sciaenidae (Murdy et al., 1997).

Sciaenid fishes of Chesapeake Bay

The 70 genera and 270 species of primarily marine fishes in the teleost family Sciaenidae are distributed globally along continental shelves and adjacent waters from tropical to temperate regions (Myers, 1960; Nelson, 1994). Sciaenids occupy a myriad of habitats in freshwater, estuarine, coastal neritic and reef-associated marine systems, but

are most speciose in coastal and estuarine waters (Myers, 1960). The oldest known fossils of the family Sciaenidae are from the Eocene (40-50 mya), suggesting a marine origin followed by invasion of freshwater habitats and strong radiation in the late Mesozoic and early Cenozoic (Berg, 1958; Myers, 1960; Boeger and Kritsky, 2003). Present debate over the phylogenetic position of this family within the order Perciformes questions whether the Haemulidae (grunts) or the Polynemidae (threadfins) are the sister group to the Sciaenidae (Chao, 1978; Johnson, 1983).

Approximately 14 sciaenid species utilize Chesapeake Bay as a nursery or seasonal foraging ground (Murdy et al., 1997). Species-specific ecomorphologies enable these fishes to utilize food resources from different microhabitats, presumably resulting in niche division and reduced competition where multiple species co-occur (Chao and Musick, 1977). While a few of these species are rare visitors to the Chesapeake Bay, the seven sciaenids studied in parts of this dissertation support substantial commercial and/or recreational fisheries within the region (Table 1). Recreational fisheries have maintained greater economic impact over the last few decades (Kirkley and Kerstetter, 1997). In Maryland and Virginia waters, average annual commercial and recreational landings of Atlantic croaker and spot are fairly comparable and generally an order of magnitude higher than other sciaenid species (Table 1). Weakfish are also highly important to both recreational and commercial fisheries. Average annual landings of the remaining species (spotted seatrout, red drum, kingfish spp.), are substantially lower and dominated by recreational harvest. A brief description of the ecology, life history and fisheries management of these species follows.

Spotted seatrout (*Cynoscion nebulosus* Cuvier, 1830) occur from Cape Cod, Massachussetts to the Florida Keys and Gulf of Mexico. Combined commercial and recreational landings have ranged from 1-7 million pounds annually, with the majority taken on recreational gear (ASMFC, 2008a). There has been no coastwide stock assessment for spotted seatrout due to the largely non-migratory nature of adults; however, several southeast states conduct age-structured analyses (ASMFC, 2008a). Euryhaline adult spotted seatrout are found throughout shallower Chesapeake Bay waters, associating with submerged aquatic vegetation and structure from April through late November and spawning *circa* age 1-2 near the bay mouth over a protracted season from April through September (Murdy et al., 1997). Young of the year recruit to tidal marsh creeks and shallow seagrass nurseries. Juveniles and adults emigrate from Chesapeake Bay southward to overwinter in coastal waters; fish in estuaries south of this region exhibit less seasonal migratory behavior (Bortone, 2003). Recent increases in coastal development, eutrophication, and sedimentation have fractioned seagrass habitats that this species uses throughout its life cycle; consequently, spotted seatrout populations have been considered a measure of seagrass ecosystem health (Bortone, 2003). Spotted seatrout forage on a variety of zooplankton, small fishes, and crustaceans, becoming increasingly piscivorous with age (Murdy et al. 1997).

Weakfish (*Cynoscion regalis* Bloch and Schneider, 1801) occur along the Atlantic coast of North America from Nova Scotia to southeastern Florida. Commercial and recreational landings combined have ranged from 2-36 million pounds year^{-1}, declining from 1999 to present (ASMFC, 2008b). The most recent stock assessment for the species conducted in 2006 concluded that the mid-Atlantic stock component is depleted, but

overfishing is not occurring (ASMFC, 2008b). Apparent increases in natural mortality have led to a declining biomass trajectory despite considerable reductions in harvest in both commercial and recreational fisheries (ASMFC, 2008a). Adult weakfish appear in lower Chesapeake Bay waters in April-May, forming dense schools throughout bay waters. Weakfish reach maturity circa age 1-2, spawning near the bay mouth over a protracted season from April through August (Barbieri et al., 1995). Young of the year recruit to low salinity river habitats in late summer where they grow rapidly and emigrate from the estuary southward to overwinter in coastal waters (Murdy et al., 1997). Weakfish forage on a variety of zooplankton, small fishes, and crustaceans, becoming increasingly piscivorous with age (Chao and Musick, 1977; Latour et al., in press)

Spot (*Leiostomus xanthurus* Lacepède, 1802) occur in coastal and estuarine waters from the Gulf of Maine through Mexico, and support large commercial and recreational fisheries in the along the US east coast. In the mid-Atlantic region, spot combined landings have varied between roughly 3 to 15 million pounds year^{-1} depending on environmental conditions at spawning and nursery sites (ASMFC, 2008c). At present, the condition of the stock component in the mid Atlantic region is unknown, as no coastwide stock assessments have been performed due to the lack of time series of basic demographic and fisheries data (ASMFC, 2008c). Adult spot migrate seasonally, entering bays and estuaries in spring and remaining until late fall, when they undertake offshore spawning migrations to coastal waters. Spawning by age-2 and older spot takes place from fall to spring, and young of the year recruit into low salinity tidal creeks in late summer, where they overwinter (Murdy et al., 1997). Spot are generalist foragers that frequently winnow sediments in search of small prey; larvae and small juveniles feed on

small planktonic and benthic organisms, while larger juveniles and adults forage small polychaetes, bivalves, crustaceans and meiofauna (Chao and Musick, 1977; Bonzek et al., 2009). Spot serve as important forage for many piscivores including striped bass, flounder, weakfish, and bluefish (Bonzek et al., 2009).

Atlantic croaker (*Micropogonias undulatus* Linnaeus, 1766) occur in coastal and estuarine waters from the Gulf of Maine to Yucatan, Mexico and are one of the most abundant inshore demersal fishes along the US southeast. Croaker support large commercial and recreational fisheries throughout this range. Croaker landings in both fisheries exhibit cyclical trends, ranging from two to over 30 million pounds $year^{-1}$ (ASMFC, 2005). At present, the stock component in the mid Atlantic region is not overfished and overfishing is not occurring (ASMFC, 2005). First spawning in the species occurs circa age-2 from July through February, peaking in August-October in both the lower Chesapeake Bay and in coastal waters (Barbieri et al., 1994). Young of the year recruit into low salinity tidal creeks in late summer, where they overwinter. Adults immigrate to Chesapeake Bay from overwintering habitats in southeastern continental shelf waters in spring, remaining in this estuary until 12-15ºC water temperatures in late autumn. Atlantic croaker are generalist foragers; larvae and small juveniles feed mainly on small planktonic organisms, while larger juveniles and adults forage on benthic organisms such as polychaetes, bivalves, crustaceans, and occasionally small fishes (Chao and Musick, 1977; Bonzek et al., 2009). Atlantic croaker are, in turn, forage for many species including striped bass, flounder, weakfish, and spotted seatrout (Bonzek et al., 2009).

The *Menticirrhus* complex in Chesapeake Bay involves mainly northern kingfish (*Menticirrhus saxatilis* Bloch and Schneider, 1801) and southern kingfish (*Menticirrhus americanus* Linnaeus, 1758). A third species, gulf kingfish (*Menticirrhus littoralis*), has been recorded in the mid-Atlantic, but will not be discussed herein (Murdy et al., 1997). Northern kingfish range from Maine to the Yucatan and southern kingfish from New York to Mexico. Both species co-occur in littoral zones in Chesapeake Bay, although southern kingfish are comparatively more eurythermal and euryhaline (Murdy et al., 1997). Both species are of limited commercial importance and are taken in a small directed recreational fishery prosecuted in littoral zones. Adults enter the bay in April and May, spawn circa age-2 in coastal waters from May-August, and emigrate southward in mid-autumn to overwintering grounds along the continental shelf (Murdy et al, 1997). Larvae settle in lower salinity tidal nurseries and migrate to the lower bay as juveniles. Both kingfishes are benthic generalist foragers that prey on a myriad of crustaceans, bivalves, and polychaetes (Chao and Musick, 1978; Bonzek et al., 2009).

Red drum (*Sciaenops ocellatus* Linnaeus, 1766) occur from Massachussetts to Key West, Florida and the Gulf of Mexico, and have supported large commercial and recreational fisheries at times during the past century. Commercial landings of red drum have been reported throughout this range since the 1880s but are presently low because harvest is prohibited in federal waters and several states likewise prohibit commercial retention. Red drum are prized sportfish, with recreational landings accounting for over 85% of all harvest; many states have enacted slot limit regulations, limiting recreational exploitation to the immature age 1-4 red drum (SEFMC, 2009). The most recent stock assessment, conducted in 2000, indicated that red drum in the mid-Atlantic region do not

appear to be overfished but it is unclear if overfishing is occurring due to difficulties estimating the stock size of adults (ASMFC, 2008d). Upon reaching sexual maturity circa age-4, red drum emigrate from estuarine nurseries to coastal waters, appearing in Chesapeake Bay from May through November. Spawning occurs in nearshore coastal waters from late summer through fall, with young of the year recruiting to shallow estuarine nursery areas from August through September (Murdy et al., 1997). Immature age 1-4 red drum use estuarine seagrass beds and marshes as nursery habitats. Red drum are benthic generalist foragers that prey on a myriad of crustaceans and invertebrates (Murdy et al. 1997).

Collectively, the life history traits of most of the sciaenid species examined in this work are fairly similar, with the majority reaching sexual maturity around age 2 or earlier at body sizes less than 250 mm total length (TL: Table 1). The clear exception are red drum, which reach sexual maturity between ages 3-6 at body sizes greater than 600 mm TL (Table 1; Waggy et al., 2006). Red drum also have a longer life span, attain a larger maximum size, higher batch fecundity, lower spawning frequency, and lower relative fecundity than the other species investigated (Waggy et al., 2006).

Non-sciaenid competitors in Chesapeake Bay

Several commercially and/or recreationally important perciform and pleuronectiform fishes overlap temporally and spatially with the sciaenid species above, co-occuring in sympatry in microhabitats and potentially competing for prey species. A brief description of the ecology, life history and fisheries management of several of non-sciaenid species examined in parts of this dissertation follows.

Striped bass (*Morone saxatilis* Walbaum, 1792) are an anadromous moronid species distributed from the St. Lawrence River, Canada to northern Florida. This species supports large commercial and recreational fisheries along the US Atlantic seaboard, with many states closing commercial fisheries in the 1980s during a period of low stock abundance. The most recent assessment conducted in 2007 concluded that Atlantic coast striped bass are not overfished and overfishing is not occurring (NEFSC, 2008a). The Chesapeake Bay stock of striped bass spend most of their adult lives from age-4 onward in coastal waters, undertaking seasonal north-south foraging migrations and springtime spawning migrations to freshwater tributaries (Murdy et al., 1997). Young of the year settle in nearshore nursery habitats in brackish waters and move downstream as they age, remaining in the estuary for several years (female: 2-3; male: 4-6) before joining the coastal migrant segment of the population (Secor and Piccoli, 1994). These movements, however, demonstrate a high degree of plasticity; striped bass in Chesapeake Bay are partial migrants meaning that only a fraction of individuals will leave estuarine habitats for coastal waters (Secor and Piccoli, 1994). Juvenile striped bass prey on a variety of fishes, crustaceans, and cephalopods; adults become increasingly more piscivorous with age (Hartman and Brandt, 1995; Bonzek et al., 2009).

Summer flounder (*Paralichthys dentatus* Linnaeus, 1766) are a migratory demersal species distributed from Nova Scotia to Florida. This species supports large commercial and recreational fishes along on the Atlantic coast. Combined commercial and recreational landings have ranged from 15 to more than 60 million pounds year^{-1} since 1980, with a trend of reduced harvest for the past decade (ASMFC, 2006). The summer flounder stock is not overfished and overfishing is not occurring, but the stock is

not yet rebuilt based on a peer-reviewed update of the most recent assessment (NEFSC, 2008b). This species exhibits pronounced inshore foraging migrations in warmer months and offshore spawning migrations to coastal waters circa during autumn and winter, with strong sexual dimorphism in growth and migration patterns. Smaller males maintain a more coastal distribution, while larger females move into estuarine habitats in the warmer months. Larvae settle in shallow higher salinity bay habitats from October through May, young juveniles inhabit fringes of submerged aquatic vegetation and sandy habitats through spring/summer, and adults occur in deep channels and ridges near the bay mouth (Murdy et al., 1997). Summer flounder prey upon a number of small fishes, crustaceans, and soft-bodied benthic invertebrates (Latour et al., 2008).

Bluefish (*Pomatomus saltatrix* Linnaeus, 1766) are a schooling migratory coastal pelagic species distributed circumglobally in tropical and warm temperate waters except the eastern tropical Pacific. Bluefish support large commercial and recreational fisheries in the mid-Atlantic region, with combined landings ranging from 0.02-0.8 million pounds yr^{-1} (ASMFC, 2007). Atlantic coast bluefish stock has experienced periods of hyperabundance interspersed with periods of relative rarity. The most recent stock assessment conducted in 2005 determined that bluefish are not presently overfished, nor is overfishing occurring (ASMFC, 2007). Adults of this apex piscivore rely on estuarine habitats for feeding and nursery grounds after coastal spawning from age-2 onward (Harding and Mann, 2001). Bluefish appear to have several spawning cohorts and undergo extensive inshore-offshore and north-south migrations, with peak spawning off Chesapeake Bay in July (Murdy et al., 1997). Young of the year bluefish enter the lower bay and its tributaries in late summer, grow rapidly, and emigrate southward in autumn

(Murdy et al., 1997). Bluefish are voracious predators of a myriad of fishes, cephalopods, and crustaceans (Gartland et al., 2006).

Cobia (*Rachycentron canadum* Linnaeus, 1766) are distributed circumglobally in tropical and warm temperate waters except the eastern tropical Pacific. Combined commercial and recreational landing of this species in Virginia waters are low (<20,000 pounds yr^{-1}) despite this species' status as a prized gamefish and the coveted status of its flesh (Murdy et al., 1997). There has been no coastwide assessment of cobia stocks. Adults and large juveniles use nearshore and bay waters as foraging and/or spawning grounds from May through October. Peak spawning occurs from age-2 onward from June through August prior to the autumn emigration to warmer southern coastal waters (Richards, 1967). Strongly migratory adults are pelagic but may be found throughout the water column in a variety of natural habitats and around manmade structures; young of the year recruit to shallow, high salinity coastal areas (Shaffer and Nakamura, 1989). Cobia are generalist foragers that prey on a myriad of fishes, crustaceans, and soft-bodied invertebrates (Arendt et al., 1999).

Collectively, the species examined in this dissertation demonstrate fairly fast growth, strong seasonal migrations, and substantial differences in the microhabitats used throughout ontogeny. The selection pressures exerted by physical properties of the waters used by these neritic fishes (i.e., temperature, salinity, light, dissolved oxygen) will thus exhibit high degrees of variability, impacting each species' ecophysiology differently in different life stages. Understanding the effects of any anthropogenic impacts on life history, production, and fisheries, necessitates first understanding the bounds of species-specific ecophysiology.

Rationale for work

This dissertation applies multidisciplinary ecophysiological techniques and a comparative approach to investigate aspects of the sensory and energetic ecology of several sciaenid fishes and non-sciaenid competitors that co-occur in Chesapeake Bay. A rationale for each of these themes follows.

Sensory ecology

Since industrialization, increases in sedimentation, eutrophication, turbidity, and anoxia in the Chesapeake Bay have been well-documented; complex effects of decreased water quality on organisms and their ecological interactions are less well known (Kemp et al., 2005). Sensory systems act as the interface between the processes that occur within animals and those occurring between animals and their environment (Browman, 2005). Accordingly, the study of sensory function can provide novel insights into various aspects of organismal ecology, including distributions and movement patterns, relationships among fellow conspecifics and competitors, predator-prey interactions, and even the vulnerability to capture (Weissburg, 2005). Consequently, a better understanding of sensory ecology of fishes can provide valuable information to researchers and resource managers, particularly in light of the continued anthropogenic degradation of coastal habitats such as the Chesapeake Bay.

Fishes are ideal subjects for sensory research. Evolutionary radiation has allowed species-rich taxonomic groups of fishes to inhabit a broad range of habitats possessing complex physical and environmental properties (Levine and MacNichol, 1979; Kamil, 1988; van der Emde et al., 2004). These habitats present a myriad of selective pressures

on the evolution of sensory and feeding structures, within phylogenetic constraints (Levine and MacNichol, 1979; Evans, 2004). The Sciaenidae demonstrate morphological and microhabitat specialization and are a model group in which to examine the relationships between form, function, and the environment (Chao and Musick, 1977). Relationships between feeding morphology and habitat have been described for specific life stages of some species (Chao and Musick, 1977), but surprisingly little is known about the sensory ecology of sciaenids. I therefore appliedstandard electrophysiological techniques and comparative methods to examine the functions of the auditory (Chapter 1) and visual systems (Chapter 2) of several Chesapeake Bay Sciaenidae within phylogenetically-related but ecologically distinct species. In a subsequent chapter (Chapter 3), I assess the visual systems of four taxonomically unrelated non-sciaenid competitors that use similar microhabitats and bear similar ecologies. Collectively, I seeks insights into the relationships among sensory function, microhabitat use, and lifestyle in phylogenetically similar and disparate groups.

Energetic ecology

Anthopogenic degradation of coastal and estuarine waters, including Chesapeake Bay, has resulted in ever-increasing eutrophication, hypoxia, and even anoxia events (Breitburg, 2002), with major implications for energy demand and utilization in aquatic flora and fauna. Metabolic rate is the largest and most labile component of catabolism in active species (Ney, 1993). Metabolic data are important input parameters for energetics, growth, and population models (Brill, 1989; Kitchell et al., 1977; Wuenschel et al., 2004); however, these data are lacking for many sciaenid species.

Comparative methods have also provided novel insights into the form-function-environment relationships of teleost metabolic systems. The morphological and microhabitat specialization in sympatric sciaenids renders this family a model group in which to examine the relationships between metabolic physiology, performance, behavior, and ecology in fishes. In the final dissertation chapter (Chapter 4), I therefore use stop flow respirometry to: (1) investigate the resting and active metabolic rates of spot and Atlantic croaker, benthic generalist species that are sympatric and fairly ubiquitous throughout Chesapeake Bay in warmer months, (2) place these fishes in context of the metabolic ecophysiology of other sciaenids, and finally, (3) place sciaenids in context of the metabolic ecophysiology of other non-sciaenid fishes.

REFERENCES

Arendt, M.D, Olney, J.E., and Lucy, J.A. (1999). Stomach analysis of cobia, *Rachycentron canadum*, from lower Chesapeake Bay. *Fishery Bulletin*. 99, 665–670.

Atlantic States Marine Fisheries Commission [ASMFC]. (2005). Atlantic croaker stock assessment and peer-review report. Washington, DC: Atlantic States Marine Fisheries Commission, 370 pp.

Atlantic States Marine Fisheries Commission [ASMFC]. (2006). 2006 Review of the Atlantic States Marine Fisheries Commission fishery management plan for summer flounder (*Paralichthys dentatus*). Washington, DC: Atlantic States Marine Fisheries Commission, 13 p.

Atlantic States Marine Fisheries Commission [ASMFC]. (2007). 2007 Review of the Atlantic States Marine Fisheries Commission fishery management plan for bluefish (*Pomatomus saltatrix*). Washington, DC: Atlantic States Marine Fisheries Commission, 10 p.

Atlantic States Marine Fisheries Commission [ASMFC]. (2008a). 2008 Review of the Atlantic States Marine Fisheries Commission fishery management plan for spotted seatrout (*Cynoscion nebulosus*). Washington, DC: Atlantic States Marine Fisheries Commission, 15 p.

Atlantic States Marine Fisheries Commission [ASMFC]. (2008b). 2008 Review of the Atlantic States Marine Fisheries Commission fishery management plan for weakfish (*Cynoscion regalis*). Washington, DC: Atlantic States Marine Fisheries Commission, 22 p.

Atlantic States Marine Fisheries Commission [ASMFC]. (2008c). 2008 Review of the Atlantic States Marine Fisheries Commission fishery management plan for spot (*Leiostomus xanthurus*). Washington, DC: Atlantic States Marine Fisheries Commission, 11 p.

Atlantic States Marine Fisheries Commission [ASMFC]. (2008d). 2008 Review of the Atlantic States Marine Fisheries Commission fishery management plan for red drum (*Sciaenops ocellatus*). Washington, DC: Atlantic States Marine Fisheries Commission, 18 p.

Barbieri, L.R., M.E. Chittenden, Jr. and S.K. Lowerre-Barbieri. (1994). Maturity, spawning, and ovarian cycle of Atlantic croaker, *Micropogonias undulatus*, in the Chesapeake Bay and adjacent coastal waters. *Fishery Bulletin*. **92**, 671-685.

Bonzek, C.F., Gartland, J., Johnson, R.A., and Latour, R.J. (2009). 2008 progress report: The Chesapeake Bay Multispecies Monitoring and Assessment Program. Virginia Institute of Marine Science, Gloucester Point, VA. Report F-130-R-4, 366 pp.

Bortone, S. A. (2003). Spotted seatrout as a potential indicator of estuarine conditions. In S. A. Bortone (ed). *Biology of the spotted seatrout.* CRC Press, New York: 297-301.

Boynton, W., and Kemp, M. (1985). Nutrient regeneration and oxygen consumption by sediments along an estuarine salinity gradient. *Marine Ecology Progress Series*. **23**, 45-55.

Breitburg, D.L. (1992). Episodic hypoxia in Chesapeake Bay: interacting effects of recruitment, behavior, and physical disturbance. *Ecological Monographs*. **62(4)**, 525-546.

Breitburg, D. (2002). Effects of hypoxia, and the balance between hypoxia and enrichment, on coastal fishes and fisheries. *Estuaries*. **25(4)**, 767-781.

Brill, R.W. (1987). On the standard metabolic rates of tropical tunas, including the effect of body size and acute temperature change. *Fishery Bulletin*. **85(1)**, 25-35.

Browman, H.I. (2005). Applications of sensory biology in marine ecology and aquaculture. In: *Sensory biology: linking the internal and external ecologies of marine organisms*. M.J. Weismann and H. I. Browman, eds. *Marine Ecology Progress Series*. **287**, 263-307.

Chao, L.N. (1978). A basis for classifying western Atlantic Sciaenidae (Teleostei: Perciformes). NOAA Tech . Rep. NMFS Tech Circ. 415:1-64.

Chao, L.N., and Musick, J. A. (1977). Life history, feeding habits, and functional morphology of juvenile sciaenid fishes in the York River estuary, Virginia. *Fishery Bulletin.* **75(4)**, 657-702.

Cronin, T., Willard, D., Karlsen, A., Ishman, S. Verardo, S., McGeehin, J., Kerhin, R., Holmes, C., Colman, S., and Zimmerman, A. (2000). Climatic variability in the eastern United States over the past millennium from Chesapeake Bay sediments. *Geology*. **28**, 3-6.

Cooper, S.R. and Brush, G.S. (1993). A 2,500 year history of anoxia and eutrophication in Chesapeake Bay. *Estuaries*. **16(3B)**, 617-626.

Evans, B.I. (2004). A fish's eye view of habitat change. P 1-30 In *The senses of fish: adaptations for the reception of natural stimuli*. (van der Emde, G., J. Mogdans, and B.G. Kapoor, eds). Klewer Academic Publishers, Boston, MA, 375 pp.

Forward, R. B., and Tankersley, R. A. (2001). Selective tidal-stream transport of marine animals. *Oceanography and Marine Biology: an Annual Review*, **39**: 305-353.

Gartland, J., R.J. Latour, A.D. Halvorson, and H.M. Austin. (2006). Diet composition of young-of-the-year bluefish (*Pomatomus saltatrix*) in the lower Chesapeake Bay and the coastal ocean of Virginia. *Transactions of the American Fisheries Society* **135**, 371-378.

Harding, J. M. and Mann, R. (2001). Diet and habitat use by bluefish, *Pomatomus saltatrix*, in a Chesapeake Bay estuary. *Environmental Biology of Fishes*. **60(4)**, 401-409.

Hare, J.A., Thorrold, S., Walsh, H., Reiss, C., Valle-Levinson, A., and Jones, C.

(2005). Biophysical mechanisms of larval fish ingress into Chesapeake Bay. *Marine Ecology Progress Series*. **303**, 295-310.

Hartman, K. and Brandt, S. (1995). Trophic resource partitioning, diets, and growth of sympatric estuarine predators. *Transactions of the American Fisheries Society*. **124**, 520-537.

Kamil, A.C. (1988). Behavioral ecology and sensory biology. P 189-201 In: *Sensory biology of aquatic animals*, (Atema, J., R.R. Fay, A.N. Popper, and W.N. Tavolga eds). Springer Verlag, NY. 936 pp.

Kemp, W.M., Boynton, W.R., Adolf, J.E., Boesch, D.F., Boicourt, W.C., Brush, G., Cornwell, J.C., Fisher, T.R., Glibert, P.M., Hagy, J.D., Harding, L.W., Houde, E.D., Kimmel, D.G., Miller, W.D., Newell, R.E.I., Roman, M.R., Smith, E.M., and Stevenson, J.C. (2005). Eutrophication of Chesapeake Bay: historical trends and ecological interactions. *Marine Ecology Progress Series*. **303**, 1-29.

Kitchell, J. F., Stewart, D. J., and Weininger, D. (1977). Application of a bioenergetics model to yellow perch (*Perca flavescens*) and walleye (*Stizostedion vitreum vitreum*). *Journal of the Fisheries Research Board of Canada*. **34**, 1922–1935.

Ko, F-C. and Baker, J.E. (1995). Partitioning of organic contaminants to resuspended sediments and plankton in the mesohaline Chesapeake Bay. *Marine Chemistry*, 171-188.

Kirkley, J. and Kerstetter, D. (1997). *Saltwater angling and its economic importance to Virginia*. College of William and Mary – Virginia Institute of Marine Science, Virginia Sea Grant Program, Publ. VSG-97-04, Gloucester Point.

Latour, R.J., Gartland, J., Bonzek, C.F., and Brasseur, E.A. (In press). Trophic interactions of weakfish *Cynoscion regalis* in Chesapeake Bay, with reference to dietary overlap among common piscivores. *Journal of Fish Biology*.

Latour, R.J., Gartland, J., Bonzek, C.F., and Johnson, R.A. (2008). The trophic dynamics of summer flounder (*Paralichthys dentatus*) in Chesapeake Bay. *Fishery Bulletin*. **106**, 47–57.

Levine, J.S. and MacNichol, E.F. (1979). Visual pigments in teleost fishes: effects of habitat, microhabitat, and behavior of visual system evolution. *Sens. Proc*. **3**, 95-131.

Lowerre-Barbieri, S. K., M. E. Chittenden, and Barbieri, L. R. (1996). The multiple spawning pattern of weakfish in the Chesapeake Bay and Middle Atlantic Bight. *Journal of Fish Biology* **48 (6)**, 1139-1163.

Johnson, G.D. (1983). Percomorph phylogeny: progress and problems. *Bulletin of Marine Science*. **52(1)**, 3-28.

Murdy, E. O., Birdsong, R. S., and Musick, J. A. (1997). *Fishes of Chesapeake Bay*, pp. 324. Washington, DC: Smithsonian Institution Press.

Myers, G.S. (1960). Restriction of the croakers (Sciaenidae) and anchovies (Engraulidae) to continental waters. *Copeia*, **1960(1)**: 67-68.

Nelson, J. (1994). *Fishes of the World* – third edition. New York, NY: John Wiley and Sons.

Ney, J.J. (1993). Bioenergetics modeling today: growing pains on the cutting edge. *Transactions of the American Fisheries Society*. **122**, 736-748.

Northeast Fisheries Science Center [NEFSC] (2008a). 47th Northeast Regional Stock

Assessment Workshop (47th SAW) Assessment Summary: Striped bass. US Department of Commerce, Northeast Fisheries Science Center Reference Document 08-03a, 258 p.

Northeast Fisheries Science Center [NEFSC] (2008b). 47th Northeast Regional Stock Assessment Workshop (47th SAW) Assessment Summary: Summer Flounder. US Department of Commerce, Northeast Fisheries Science Center Reference Document 08-11, 22 p.

Richards, C.E. (1967). Age, growth and fecundity of the cobia, *Rachycentron canadum*, from Chesapeake Bay and adjacent mid-Atlantic waters. *Transactions of the American Fisheries Society*. **96**, 343-350.

Secor, D.H., Piccoli, P.M. (1994). Oceanic migration rates of Upper Chesapeake Bay striped bass (*Morone saxatilis*), determined by otolith microchemical analysis. *Fishery Bulletin*. **105**, 62-73.

South Atlantic Fisheries Management Council [SAFMC]. (2009). Southeast Data South Atlantic Fisheries Management Council Assessment and Review (SEDAR). Data Workshop Report: Atlantic Red Drum. SEDAR 18. 145 pp.

Shaffer, R.V., Nakamura, E.L. (1989). Synopsis of the biological data on the cobia, *Rachycentron canadum* (Pisces: Rachycentridae). US Department of Commerce, NOAA Technical Report NMFS 82.

Taft, J.L., Hartwig, E.O., Loftus, R. (1980). Seasonal oxygen depletion in Chesapeake Bay. *Estuaries*. **3**, 242-247.

van der Emde, G., J. Mogdans, and B.G. Kapoor. (2004). *The senses of fish:*

*adaptations for the reception of natural stimu*li. Klewer Academic Publishers, Boston, MA, 375 pp.

Waggy, G.L., Brown-Peterson, N.J., Patterson, M.S. (2006). Evaluation of the reproductive life history of the sciaenidae in the Gulf of Mexico and Caribbean Sea: "greater" vs. "lesser strategies? *Proc. 57th Gulf Carib. Fish. Inst.* **57**, 263-282.

Weissburg, M. J. (2005). Introduction. In *Sensory Biology: Linking the internal and external ecologies of marine organisms* (eds. M. J. Weissburg and H. I. Browman), *Mar. Ecol. Progr. Ser.* **287**, 263-265.

Willard, D.A., Cronin, T.M., and Verardo, S. (2003). Late-Holocene climate and ecosystem history from Chesapeake Bay sediment cores, USA. *The Holocene*. **13(2)**, 201-214.

Wuenschel, M.J., Werner, R.G., and Hoss, D.E. (2004). Effect of body size, temperature, and salinity on the routine metabolism of larval and juvenile spotted seatrout. *Journal of Fish Biology*. **64**, 1088-1102.

Table 1 – General life history and fisheries overview for sciaenid species examined in this dissertation.

Common name	*Scientific name*	*Age at maturity*[A]	*Size at maturity (mm)*[B]	*Spawning season*[C]	*Common habitats*[C]	*Avg. Landings 1990-pres (MT)*[D]
Atlantic croaker	*Micropogonias undulatus*	M: 1-2 F: 1-2	M: 180 F: 170	Summer-winter	Sand, mud	C: 2600 – 5900 R: 414 – 4061
Spot	*Leiostomus xanthurus*	M: 2-3 F: 2-3	M: 170 F: 200	Fall-spring	Sand, mud	C: 1300 – 1900 R: 720 – 1526
Weakfish	*Cynoscion regalis*	M: 1 F: 1	M: 164 F: 170	Spring-summer	sand	C: 150 – 850 R: 13 – 541
Spotted seatrout	*Cynoscion nebulosus*	M: 1 F: 1	M: 260 F: 275	Spring-summer	seagrass	C: 2 – 20 R: 12 – 133
Red drum	*Sciaenops ocellatus*	M: 3 F: 4	M: 600 F: 800	Summer-fall	Seagrass, sand, oyster reef	C: 1 – 5 R: 1 – 77
Kingfish spp.	*Menticirrhus* spp.	M: 2-3 F: 2-3	M: 150 F: 150	Summer-fall	Surf, mud	C: 6 – 45 R: 9 – 140

[A, B]- Armstrong and Muller, 1996; Murdy et al., 1997; Barbieri et al., 1994 ; Lowerre-Barbieri et al., 1996; Ross et al., 1995, Waggy et al., 2006.

[C] - Murdy et al., 1997

[D] – Commercial landings from ASMFC ; Recreational landings from MRFFS statistics. Wilk, 1981.

CHAPTER 1:

Acoustic Pressure and Acceleration Thresholds in Six Sciaenid Fishes

INTRODUCTION

Sound in water is composed of two physically-linked components, propagating scalar pressure waves and directional particle motion, which differ in the pathways through which they reach the inner ears of fishes (Fay and Popper, 1975). The otoliths of all fishes are biological accelerometers that directly detect the particle motion components of sound as a result of inertial differences between sensory epithelia and otoliths (Lu and Xu, 2002; Popper and Fay, 1999). Additionally, the pressure component of sound may be detected indirectly by some fishes via accessory anatomical structures that transform sound pressure waves into particle displacements (Popper and Fay, 1993).

Fishes are categorized as hearing "specialists" and "generalists" on the basis of anatomy, the ability to detect the pressure component of sound, and the range of detectable bandwidth. Hearing specialist species have evolved projections of the swim bladder or skeletal connections that enable the indirect re-radiation of the pressure component of sound as particle displacement capable of stimulating the inner ear (Fay and Popper, 1974; Popper and Fay, 1999). Thus hearing specialist fishes, which include groups such as clupeids, otophysans, mormyrids, and osphronemids, may use both direct (particle motion) and indirect (pressure transduction) mechanisms to enhance their hearing sensitivity and extend their detectable auditory bandwidth (Mann et al., 1997; Popper and Fay, 1993; Yan, 1998; Yan and Curtsinger, 2000). In contrast, hearing generalist fishes lack such specialized structures coupling pressure-to-displacement transducers to the otic capsule, resulting in attenuation of the signal and reduced

stimulation of the ear via sound pressure (Casper and Mann, 2006). The unaided organs of the inner ear of hearing generalists are thought to be fairly insensitive to the indirect transduction of sound pressure (Sand and Karlsen, 2000; Yan et al., 2000); direct particle motion stimulation of the otoliths is likely more relevant to these fishes (Lu and Xu, 2002; Casper and Mann, 2006). However, few studies have examined the hearing thresholds of fishes with respect to both pressure and particle motion sensitivity (Myrberg and Spires, 1980; van den Berg, 1985; Lovell et al., 2005; Casper and Mann, 2006).

Sciaenid fishes are model organisms of teleost bioacoustics (Ramcharitar et al., 2006a; Roundtree et al., 2006), but comparatively little is known about their auditory abilities. Sciaenid saccular otoliths are enlarged relative to most fishes, and their morphology and proximity to the swim bladder vary widely (Chao, 1978; Ramcharitar et al., 2001). Both hearing specialists and generalists have been identified within the family (Ramcharitar et al., 2004; 2006b). Unfortunately, the pressure detection abilities of less than two percent of the 270 sciaenid species have been described (Ramcharitar, 2003: Atlantic croaker, spot, weakfish, black drum, silver perch), and the particle motion sensitivity of these fishes has not been examined. Comparative work on sciaenid fishes has great potential to elucidate form-and-function relationships in the teleost auditory system (Ramcharitar, 2003). We therefore performed auditory brainstem response (ABR) experiments using a hydrophone and geophone to categorize the pressure and particle acceleration detection thresholds of six sciaenid fishes. The simultaneous recording of the pressure and particle motion components of sound stimuli allowed us to express audiograms with respect to both. The former allows us to compare our data to previously published results for sciaenid fishes (Ramcharitar and Popper, 2004;

Ramcharitar et al., 2006b); the latter allows comparison to recent studies examining particle motion thresholds in other fishes (Casper and Mann, 2006; Mann et al., 2007).

MATERIALS AND METHODS

Experimental animals and design

Spotted seatrout (*Cynoscion nebulosus* Cuvier, 1830), weakfish *(Cynoscion regalis* Bloch and Schneider, 1801), red drum (*Sciaenops ocellatus* Linnaeus, 1766), Atlantic croaker (*Micropogonias undulatus* Linnaeus, 1766), spot (*Leiostomus xanthurus* Lacepede, 1802), and northern kingfish (*Menticirrhus saxatilis* Bloch and Schneider, 1801) were captured in Chesapeake Bay using hook-and-line (Table 1). Animals were maintained in recirculating 1855 L aquaria at 20°C ± 1°C (winter months) or 25°C ± 2°C (summer months) and fed a combination of frozen Atlantic menhaden (*Brevoortia tyrannus*), squid (*Loligo* sp.), and commercially-prepared food (AquaTox flakes; Zeigler, Gardners, PA, USA).

Experimental and animal care protocols were approved by the College of William and Mary's Institutional Animal Care and Use Committee, protocol no. 0423, and followed all relevant laws of the United States. ABR experiments were conducted on six animals of each species. All subjects were sedated with an intramuscular (IM) dose of the steriod anesthetic Saffan (Glaxo Vet, Glaxo Vet Ltd, Uxbridge, UK; 10 mg kg^{-1}) and immobilized with an IM injection of the neuromuscular blocking drug gallamine triethiodide (Flaxedil; Sigma, St. Louis, MO., USA; 10 mg kg^{-1}). Recording of vertebrate ABR waveforms in anaesthetized and/or immobile subjects is a common practice to minimize the obscuring effect of muscular noise on ABR recordings (Hall,

1992; Kenyon et al. 1998; Casper et al. 2003). Sedated/immobilized animals were suspended within a rectangular 61 x 31 x 16.5 cm plexiglass tank via foam straps, leaving <1mm of the top of the head protruding from the water. Subjects were ventilated (1 L min^{-1}) with filtered, oxygenated, and temperature-controlled sea water (25 ± 2°C). At the conclusion of each experiment, fishes were euthanized via a massive IM dose of sodium pentobarbital (~300 mg kg^{-1}).

Auditory brainstem response

Auditory brainstem response (ABR) is a non-invasive recording of the neural activity in the eighth cranial nerve and brainstem in response to synchronized acoustic stimuli (Corwin et al., 1982; Kenyon et al., 1998). The ABR experimental setup and procedure followed Kenyon et al. (1998). A speaker (Model: 40-1034, 27.5 cm in diameter, Radio Shack, Fort Worth, TX, U.S.A), suspended in air, was mounted 1.5 m directly above the test subject. Two platinum wire needle electrodes (Model: F-E7, 10 mm tip, Grass Technologies, West Warwick, RI, U.S.A.) were placed subdermally along the midline of each subject: the active electrode was positioned above the medulla, and the reference electrode in the dorsal musculature above the operculum. The system was grounded to the water of the experimental tank via a 6 cm by 26 cm stainless steel plate. An omnidirectional hydrophone (Reson A/S, Slangerup, Denmark; sensitivity: -211 dB re: 1V/µPa) was suspended with rubber straps 25 mm below the water surface (i.e. the depth of a subject's otic capsule) and positioned within 2.5 mm of the right opercle-preopercle margin of each subject to measure the sound pressure level of the stimulus and ambient noise.

In the absence of an anechoic chamber, all experiments were conducted in a concrete laboratory. We produced a stochastic differential white noise signal to characterize the echos produced from all reflective surfaces at the hydrophone positioned next to the subject. A custom Fourier/inverse Fournier transform algorithm (MATLAB version 6.5, Mathworks, Inc., Natick, MA, U.S.A.) was used to analyze these recordings and add to each frequency's pure tone stimulus the appropriate signals needed to destructively interfere with any recorded echos (B. Deffenbaugh, unpubl). Any alteration to the sound field in the laboratory since the last echo-cancellation (i.e. movements, small changes in the tank water level, etc.) required us to re-echo cancel before proceeding. Visual examination of stimulus waveforms recorded by the hydrophone during ABR experiments (Fig. 1) confirmed that our echo-cancelled stimuli were very similar to pure tone waveforms used in other fish hearing experiments (Kenyon et al., 1998).

A Tucker-Davis Technologies System II (TDT, Inc: Gainesville, FL, USA) and BioSig software were used to produce sound stimuli (10 ms stimulus tone bursts in 100 Hz steps from 100 Hz to 1.2 kHz) and record ABR waveforms. Sound bursts were gated using a Blackman window to provide a ramped onset/decay, preventing speaker transients. ABR traces were recorded twice each in two opposing polarities at each frequency and attenuation (250 sweeps each, four total recordings). The polarity of ABR response waveforms is independent of sound stimulus polarity (Kenyon et al., 1998) but the polarity of stimulus artifacts is not. ABR traces of opposite polarity were therefore summed to remove stimulus artifacts. Periodic experiments were also conducted with euthanized fish to ensure that identified ABR responses were not stimulus artifacts.

The two ABR responses at each frequency and sound pressure level were overlaid

to assess the response. Sound pressure levels were successively attenuated in roughly 5 dB steps until repeatable ABR waveforms were no longer produced; thresholds were defined as the lowest sound pressure level for which a repeatable ABR trace could be identified visually (Kenyon et al., 1998). Visual threshold assignment provides results similar to quantitative threshold-seeking algorithms (Yan, 1998) and remains the standard method of threshold determination in fish ABRs (Kenyon et al., 1998; Casper et al. 2003). Visually assigned thresholds for each subject of a study species were pooled to produce mean audiograms.

Sound pressure levels of all experimental stimuli were calculated from hydrophone recordings following Burkhard (1984). Cursors were placed one cycle apart (peak-to-peak) on either side of the largest (i.e., center) cycle of a tone-burst recording of the hydrophone (Kenyon et al., 1998). The Bio-Sig software then calculated the root mean square (RMS) of the waveform between the cursors, and the appropriate gain calibration factors were applied to determine actual sound pressure level in dB re: 1 μPa.

Particle velocity was calibrated using an underwater acoustic pressure-velocity probe (Mk. 2, Acoustech Corp, Philadelphia, PA, U.S.A.) containing two built-in units: a piezoelectric, omni-directional hydrophone (sensitivity: -200 dB re: 1V μPa^{-1}) and a bi-directional moving-coil geophone (sensitivity: 0.112 V cm^{-1} s^{-1}). The outer housing of this probe was secured in place of the fish ~25 mm below the water surface with rubberized clamps, and the inner unit of the probe, designed to approximate neutral buoyancy, moved freely in response to our sound stimuli. The omnidirectional hydrophone was suspended by rubber straps to within 2 mm of the pressure-velocity probe. This setup enabled the simultaneous recording of the sound pressure and particle

velocity components of the entire range of our experimental stimuli. Subsequently and separately, measurements of particle displacements were recorded in three orthogonal orientations following Casper and Mann (2006). The vertical component (z-axis) of particle velocity had substantially greater amplitudes than the x (horizontal: head-to-tail) or y axes (left-to-right) at each frequency and attenuation (Table 2). This vertical axis was therefore considered most appropriate for expressing thresholds and plotting particle acceleration audiograms.

The otolithic organ systems of fishes are thought to act as accelerometers, and particle motion audiograms have been increasingly expressed in units of acceleration (Kalmijn, 1988; Fay and Edds-Walton, 1997; Casper and Mann, 2006). Therefore, particle velocity (m s^{-1}) was quantified as above for acoustic pressure, and velocity values were converted to particle acceleration using equation 1:

$A = U * 2\pi * F$, where (Eq. 1)

A = particle acceleration (m s^{-2})

U = particle velocity (m s^{-1})

F = frequency (Hz)

Statistical analyses

Auditory thresholds are ideally analyzed with repeated measures ANOVA designs because thresholds at different frequencies are non-independent within individual subjects (Underwood, 2002). Considering responses of an individual fish to be independent across frequencies constitutes pseudoreplication (Hurlbert, 1984); valid analyses of such data require that the nature of within-individual autocorrelation is explicitly understood. Inadequate consideration of the variance-covariance structure

resulting from repeated measures may result in biased estimates of the variance of fixed effects (Littell et al., 2006). Pressure and particle acceleration thresholds were therefore analyzed separately using two-way repeated measures ANOVAs with *a priori* contrasts to investigate whether hearing varied between the six sciaenid species and among frequencies. All statistical analyses were conducted using SAS v 9.1 (SAS Institute, Cary, NC, U.S.A.). The model for these analyses is given in equation 2:

$Y_{ijk} = \mu + \alpha_i + \beta_j + \delta_k + \varepsilon_{ijk}$, where, (Eq. 2)

Y_{ijk}= value of the response variable (threshold) for the i^{th} species, j^{th} frequency, and the k^{th} level of their interaction

μ=overall mean of threshold for all species:frequency combinations.

α_i=species (fixed factor)

β_j=frequency (fixed factor)

δ_k=species:frequency interaction

ε_{ijk}=random error term associated with the observation at each combination of the i^{th} species, the j^{th} frequency, and the k^{th} level of their interaction.

We fitted models with three candidate covariance structures (unstructured, compound symmetry, and first order autoregressive (AR(1)) to the pressure and particle acceleration threshold data. In the unstructured model (UN), each covariance between measures was estimated individually, allowing the data to dictate the appropriate covariance structure. The second covariance structure, compound symmetry (CS), assumed equal covariances between all pairs of observations. The final covariance structure, first order autoregressive (AR(1)), assumed that the correlation between observations is a function of their lag in space or time; adjacent observations are more

likely to be correlated than those taken further apart (Littell et al., 2006). As a simple example involving the relationship between evoked potentials at 200, 300, and 900 Hz, the UN model would calculate the variance-covariance of every pair of observations individually, the AR(1) model would assume that evoked potentials at 200 and 300 Hz are likely more similar than responses at 200 *versus* 900 Hz, whereas the CS model would assume equal covariance.

After models were fitted to data, the appropriate covariance structure was selected using Akaike's Information Criterion (AIC_c):

$$AIC_c = -2\ln(L) + 2p + \frac{2p(p+1)}{n-p-1}, \text{ where} \qquad \text{(Eq. 3)}$$

AIC_c: Akaike's Information Criterion for small samples

L: the value of the likelihood function at its maximum

n: sample size (threshold of each fish of each species at each frequency)

p: number of estimated parameters

AIC_c is a parsimonious measure that strikes a balance between model simplicity and complex overparameterization (Burnham and Anderson, 2002). The small-sample adjustment (AIC_c) is recommended when the ratio of sample size to the number of parameters is less than 40 (Burnham and Anderson, 2002).

RESULTS

The ABR waveforms, and audiograms for sound pressure and acceleration were species-specific, but with some commonalities. Auditory evoked potentials of the six sciaenid fishes (Fig. 2) generally began 10-15 milliseconds after stimulus onset and were

complete by 30 ms (≥ 400 Hz) or 50 ms (100-300 Hz). Waveform latency varied inversely with frequency and sound pressure level. Sound pressure, particle velocity, and acceleration audiograms of all species (Fig. 3 A-C) exhibited lowest thresholds at low frequencies (100-500 Hz). Velocity and acceleration audiograms were notably flatter at low frequencies. AIC_c values supported the selection of the first order autoregressive (ar(1)) covariance model for both pressure and particle acceleration analyses (Table 3), supporting the assumptions of the AR(1) model. Visual inspection of sciaenid audiograms (Fig. 3) confirms inferences based on AIC_c; ABR responses at adjacent frequencies were therefore more similar to each other than responses at distant frequencies.

Two-way repeated measures ANOVAs demonstrated significant differences between species for both pressure ($F_{5,48.6}$=3.17, p<0.02) and particle motion (velocity: $F_{5,51.4}$=3.85, p<0.005; acceleration: $F_{5,52.3}$=3.00, p<0.02) thresholds. Sound pressure thresholds of spot were significantly higher ($F_{1,357}$=5.05, P<0.03) than those of other sciaenids from 300-700 Hz. Among species with swim bladders, thresholds of those with anteriorly-projecting diverticulae (weakfish, spotted seatrout, and Atlantic croaker) did not differ from those species without diverticulae (red drum and spot) (pressure: $F_{1,357}$=2.35, P=0.13). Surprisingly, thresholds of northern kingfish were among the lowest at higher frequencies (>600 Hz) even though the swim bladder atrophies in the adults we studied. Detection thresholds varied inversely with frequencies for both pressure ($F_{11,324}$=53.01, p< 0.001) and particle motion (velocity: $F_{11,317}$=78.47, p< 0.0001 acceleration; $F_{11,315}$=129.24, p< 0.0001). Interactions of species and frequencies were significant for both pressure ($F_{55,319}$=3.31, p<0.0001) and particle motion (velocity:

$F_{55,314}$=8.48, $p < 0.0001$; acceleration $F_{55,314}$=9.77, $p < 0.0001$) and are visually evident in the crossing of species-specific curves in within audiograms (Fig 3 A-C).

DISCUSSION

All fishes are able to directly detect the particle motion components of sound, yet fish auditory thresholds are generally assessed only for sound pressure levels (Popper and Fay, 1993). Few studies have examined hearing thresholds of fishes with respect to both pressure and particle motion sensitivity (Myrberg and Spires, 1988; van den Berg, 1985; Lovell et al., 2005; Casper and Mann, 2006). Moreover, direct particle motion simulation of the otoliths may be more relevant to hearing generalist fishes than the detection of sound pressure (Fay and Popper, 1975; Popper and Fay, 1993). In this study, we measured thresholds and expressed audiograms of six sciaenid fishes in terms of both sound pressure and acceleration using an omnidirectional hydrophone and a bi-directional geophone. Our experiments are the first to assess particle motion thresholds in sciaenid fishes and include first reports of pressure audiograms for spotted seatrout, red drum, and northern kingfish.

Sound stimuli during fish audition experiments contain both pressure and particle motion (Parvulescu, 1967; Lu et al., 1996; Casper and Mann, 2006). Small experimental tanks can have complex particle motion and sound pressure fields, potentially compromising laboratory investigations unless both components of sound stimuli are measured (Kalmijn, 1988; Popper and Fay, 1993). Kenyon et al. (1998) suggested that

placing stimulus-generating speakers in air rather than water reduces the particle motion. Our results, however, demonstrate that speakers in air can produce notable particle motion fields (Table 2). Similar conclusions were reached by Casper and Mann (2006). Particle displacements in small tanks are complex, and for an equal sound pressure level they may be greater in tanks than in an unbounded body of water (Parvulescu, 1967; Rogers and Cox, 1988). General comparisons across studies may be complicated by differences in the location of the sound source in air *versus* water, the proximity of subjects to the sound source and air-water interfaces (Fay and Edds-Walton, 1997). Such concerns demonstrate the utility of routine particle motion assessment of experimental sound stimuli. Submersible units capable of generating and measuring particle motion are available (Casper and Mann 2007a,b). Future fish audition experiments should attempt to measure and report both the pressure and particle motion components of their experimental stimuli if possible (Popper and Fay, 1993; Casper and Mann, 2006).

The frequency range detected by the six sciaenids we studied was similar to those of other hearing generalist fishes (100 to < 2000 Hz) (Popper and Fay, 1993; Kenyon et al., 1998; Ramcharitar, 2003; Ramcharitar et al., 2004a; Ramcharitar et al., 2006b). Pressure detection thresholds of sciaenid fishes were significantly lower at low frequencies from 100-300 Hz. Our mean pressure thresholds for spot, weakfish, and Atlantic croaker, obtained with a speaker in air, averaged about 6 dB higher than those of Ramcharitar et al. (2004, 2006b), who used a speaker in water. Whether the different results are a consequence of speaker location/type, different levels of background noise, individual variation due to the use of larger animals in our study, or a combination of these factors, is unclear. Overall, our results generally support the conclusion of

Ramcharitar et al. (2006b) that enhanced swim bladder-otolith relationships within the Sciaenidae can improve auditory sensitivity. Among sciaenids bearing swimbladders, those possessing diverticulae (weakfish, spotted seatrout, and Atlantic croaker) had generally but not significantly lower pressure thresholds than species lacking diverticulae (spot and red drum). Swim bladders lacking mechanical coupling to the otic capsule may not enhance sound pressure detection (Yan et al., 2000). Surprisingly, however, we found the lowest sound pressure thresholds at higher frequencies (800-1100 Hz) in northern kingfish, a species with low hair cell densities and swim bladder atrophy in adults (Chao, 1978; Ramcharitar et al., 2001). Since species lacking swim bladders are unlikely to detect sound pressure (Casper and Mann, 2006; Mann et al., 2007), lower "pressure" thresholds of kingfish at higher frequencies are most likely a response to particle motion during the simultaneous presentation of pressure and particle motion stimuli.

Otoliths are biological accelerometers most sensitive to particle motion on their longitudinal axis (Lu and Xu, 2002), and the larger otoliths of sciaenid fishes may confer higher sensitivity to the particle motion components of low frequency sounds (Lychakov and Rebane, 1993; Ramcharitar et al., 2006b). Our particle acceleration audiograms demonstrate significantly greater sensitivity at low frequencies (Fig. 3C) and are comparable to results obtained with elasmobranchs (Casper and Mann, 2006). Sciaenid species with enhanced connections between the swim bladder and otic capsule (Atlantic croaker, spotted seatrout, weakfish) may be able to obtain different information from the acoustic particle motion and sound pressure fields (van den Berg, 1985; Ramcharitar et al., 2001). In contrast, sciaenid fishes lacking connections between these organ systems

(spot, red drum) are more likely responsive solely to particle motion fields (Ramcharitar, 2003). Similar conclusions have been reached for elasmobranch and teleost fishes lacking swim bladders (Mann et al., 2007; Casper and Mann, 2006). Adult kingfish (lacking swim bladders) used in our study probably detect acoustic particle motion rather than pressure. The situation is less clear for juvenile kingfish, which do have swim bladders that are distant from the otic capsule (Chao, 1978; Ramcharitar, 2003). Unfortunately, little is known about ontogenetic differences in pressure and particle motion discrimination in most fishes, including sciaenids.

A better understanding of particle motion thresholds in fishes is required, particularly with respect to hearing relative to the direction of stimulus (*sensu* Fay and Edds-Walton, 1997). In our study, maximum particle displacement occurred along the vertical axis (Table 2). But are sciaenids most sensitive to particle motion on this axis? Spawning aggregations involve chorusing fish juxtaposed in close proximity (Mok and Gilmore, 1983; Ramcharitar et al., 2006a; Gilmore, 2003), more likely stimulating otoliths in a horizontal direction. Although density and orientation of hair cell bundles in sciaenid fishes differ among species (Ramcharitar, 2003), Lu et al. (1996) demonstrated that behavioral sensitivity of oscars (Cichlidae: *Astronotus ocellatus*) to particle motion did not differ among orthogonal axes. The individual presentation of particle motion stimuli in various orthogonal Cartesian planes to sciaenids would shed light on this question (Lovell et al., 2005; Casper and Mann 2007a, b).

Dominant frequencies of most sciaenid reproductive and disturbance vocalizations (100-500 Hz: Ramcharitar et al., 2006a) lie well within the frequency bandwidths of the six species we measured. Therefore, if they are within range, sciaenids

should be able to detect each others' species-specific vocalizations, which differ in their dominant frequency, pulse duration, repetition rate, number of pulses per call, and sound pressure level (Ramcharitar et al., 2006a). The extent to which these sciaenids use auditory cues to discriminate among species or between individuals in generally noisy estuarine environments remains unknown. This ability has, however, been demonstrated in other soniferous fishes (Ladich, 2000; Ripley et al., 2002; Wysocki and Ladich, 2003).

Sound pressure and particle motion detection thresholds in sciaenids were lowest at the lower frequencies at which they communicate, but whether these species primarily detect conspecific and congeneric vocalizations via their sound pressure, particle motion, or both components of these sounds remains unknown. Communication in sound-producing fishes occurs over relatively short distances and typically in fairly shallow water, where the acoustic near field is dominated by particle motion (Myrberg, 2001; Bass and Clark, 2002; Weeg et al., 2002). Although the characteristics of sciaenid spawning aggregations differ among species, most occur in waters from 3-50 m depth (Saucier and Baltz, 1993).

Sciaenids and other soniferous fishes communicate in shallow coastal and estuarine waters despite high levels of background noise and the theoretical short-distance propagation of low frequency sounds in shallow water (Lugli et al., 2003; Ramcharitar et al., 2006a). Under idealized conditions, we estimate that sciaenid calls may propagate 8-128 m from the source based their amplitudes, simple spherical spreading (a loss of 6 dB for every distance doubled), and auditory thresholds (Table 4). Further, our calculations assumed that background noise was below the auditory thresholds, which is unlikely. For example, Sprague and Luczkovich (2004) measured

background ambient noise levels of 110-125 dB re: 1 μPa in a North Carolina estuary. There is evidence for frequency selectivity amidst background masking within the Sciaenidae, suggesting that some species may still detect certain sounds amidst the masking din of background noise in coastal environments (Ramcharitar et al., 2004a). Therefore, the distances at which these vocalizations can be heard depend on the source's sound pressure level, the pressure sensitivity and masked hearing ability of the listener, and environmental variables such as background noise, depth, bottom type, and habitat complexity (Mann, 2006). Unfortunately, masked auditory thresholds are known for only two sciaenids (Atlantic croaker and black drum: Ramcharitar and Popper, 2004). Additionally, the propagation of pressure and particle motion fields and actual attraction distances of sound sources in shallow, complex, high-scattering, high-background estuarine habitats, are not well understood at present (Mann, 2006; Casper and Mann, 2006; Lugli and Fine, 2007).

In this study, we presented the pressure and particle motion thresholds of six sciaenid fishes, including the first reports of particle acceleration thresholds in this teleost family and first reports of pressure thresholds for three species. Together, emerging data on sciaenid auditory abilities and sonifery support growing efforts to identify and manage their spawning habitats in environments with ever-increasing anthropogenic noise (Wahlberg and Westerberg, 2005; Ramcharitar et al., 2006a; Vasconcelos et al., 2007). Sciaenid bioacoustics therefore remains a fruitful research avenue and critical link between sensory physiology and behavioral ecology (Popper et al., 2005; Ramcharitar et al., 2006a; Roundtree et al., 2006). Such research promotes multidisciplinary syntheses that can mechanistically link processes from the cellular to the individual to the

population level in support of fisheries management.

REFERENCES

Baltz, D. (2002). Spotted seatrout spawning requirements and essential fish habitat: a microhabitat approach using hydrophones. In: *Listening to fish: passive acoustic applications in marine fisheries* (Rountree, R., Goudey, C., and Hawkins, T., eds). Pp. 90-93. Massachusetts Institute of Technology, Cambridge, M.A.

Barimo, J. F. and Fine, M. L. (1998). Relationship of swim-bladder shape to the directionality pattern of underwater sound in the oyster toadfish *Can. J. Zool.* **76(1)**, 134–143

Bass, A. H. and Clark, C. W. (2002). The physical acoustics of underwater sound communication. In: *Acoustic communication*. (ed. Simmons, A.M., Popper, A.N., Fay, R.R.). pp. 15-64. New York: Springer, Berlin Heidelberg.

Bass, A. H. and McKibben, J. R. (2003). Neural mechanisms and behaviors for acoustic communication in teleost fish. *Prog. Neurobiol.* **69**, 1-26.

Burkard, R. (1984). Sound pressure level measurement and spectral analysis of brief acoustic transients. *Electoencephalogr. Clin. Neurophys.* **57**, 83-91.

Burnham, K. P. and D. R. Anderson. (2002). *Model selection and multimodel inference: a practical information-theoretic approach*. 2nd edition. 488 Pp. N.Y, N.Y., U.S.A.: Springer Science and Business Media, LLC.

Casper, B. M., Lobel, P. S. and Yan, H. Y. (2003). The hearing sensitivity of the little

skate, *Raja erinacea*: a comparison of two methods. *Env. Biol. Fish.* **68(4)**, 371-379.

Casper, B. M. and Mann, D. A. (2006). Evoked potential audiograms of the nurse shark (*Ginglymostoma cirratum*) and the yellow stingray (*Urobatis jamaicensis*). *Env. Biol. Fish.* **76**, 101-108.

Casper, B.M. and Mann, D. A. (2007a). Dipole measurements in elasmobranch fishes. *J. Exp. Biol*. **210**, 75-81.

Casper, B. M. and Mann, D. A. (2007b). The directional hearing abilities of two species of bamboo sharks. *J. Exp. Biol*. **210**, 505-511.

Connaughton, M. A., Fine, M. L. and Taylor, M. H. (1997). The effects of seasonal hypertrophy and atrophy on fiber morphology, metabolic substrate concentration and sound characteristics of the weakfish sonic muscle. *J. Exp. Biol.* **200**, 2449–2457.

Corwin, J. T., Bullock, T. H., Schweitzer, J. (1982) The auditory brainstem response in five vertebrate classes. *Electroenceohalog. Clin. Neurophysiol*. **54**, 629-641.

Fay, R.R. and Edds-Walton, P.L. (1997). Directional response properties of sacular efferents of the toadfish, *Opsanus tau*. *Hearing Res.* **111**, 1-21.

Fay, R. R. and Popper, A. N. (1974). Acoustic stimulation of the ear of goldfish. *J. Exp. Biol.* **61**, 243-260.

Fay, R. R. and Popper, A. N. (1975). Modes of stimulation of the teleost ear. *J. Exp. Biol.* **62**, 379-387.

Fine, M. L., Shrinel, J., Cameron T. M. (2004). The effect of loading on disturbance

sounds of the Atlantic croaker *Micropogonias undulatus*: air versus water. *J. Acoust. Soc. Am.* **116**, 1271–1275.

Gilmore R. G. (2003). Sound production and communication in the spotted seatrout. In: *Biology of the spotted seatrout* (S. A. Bortone, ed.) Pages 177–195. CRC Press, Boca Raton, FL, U.S.A.

Hall, J. W. (1992). *Handbook of auditory evoked responses*. Allyn and Bacon, Boston MA, U.S.A.

Hurlbert S H. (1984). Pseudoreplication and the design of ecological field experiments. *Ecol Monogr.* **54**, 187-211.

Kenyon, T. N., Ladich, F., and Yan, H. Y. (1998). A comparative study of the hearing ability in fishes: the auditory brainstem response approach. *J. Comp. Physiol A.* **182**, 307-318.

Ladich, F. (2000). Acoustic communication and the evolution of hearing in fish. *Proc. Trans R. Soc. Lond. B.* **355**, 1285-1288.

Littell, R.C., G. A. Milliken, W. W. Stroup, R.D. Wolfinger, and O. Schabenberger. (2006*). SAS for mixed models*, 2nd Edition. 814 Pp. Cary, N.C., U.S.A.: SAS Institute.

Lovell, J. M., Findlay, M. M., Moate, R. M., Nedwell, J. R., and Pegg, M. A. (2005). The inner ear morphology and hearing abilities of the paddlefish (*Polyodon spathula*) and the lake sturgeon (*Acipenser fulvescens*). *Comp. Biochem. Physiol. A*. **142**, 286-296.

Lu, Z. and Xu, Z. (2002). Effects of saccular otolith removal on hearing sensitivity of the sleeper goby (*Dormitator latifrons*). *J. Comp. Physiol. A.* **188**, 595-602.

Lu, Z., Popper, A. N., and Fay, R. R. (1996). Behavioral detection of acoustic particle motion by a teleost fish (*Astronotus ocellatus*): sensitivity and directionality. *J. Comp. Physiol. A.* **179**, 227-233.

Lugli, M., and Fine, M. L. (2007). Stream ambient noise, spectrum and propagation of sounds in the goby *Padogobius martensii*: Sound pressure and particle velocity. *J. Acoust. Soc. Am.* **122(5)**, 2881-2892.

Lugli, M., Yan, H. Y., and Fine, M. L. (2003). Acoustic communication in two freshwater gobies: the relationship between ambient noise, hearing thresholds and sound spectrum. *J. Exp. Biol.* **189**, 309-320.

Lychakov, D. V. and Rebane, Y. T. (1993). Effect of otolith shape on directional sound perception is fish. *J. Evol. Biochem. Physiol.* **28**, 531-536.

Mann, D. A. (2006). Propagation of fish sounds. In: *Communication in fishes* (Ladich, F., Collin, S. P., Moller, P., and Kapoor, B.G. eds). Pp. 107-120. Science Publishers, Enfield, N. H.

Mann, D. A., Cott, P. A., Hanna, B. W., and Popper, A. N. (2007). Hearing in eight species of northern Canadian freshwater fishes. *J. Fish Biol.* **70**, 109-120.

Mann, D. A., Lu, Z., and Popper, A. N. (1997). Ultrasound detection by a teleost fish. Nature **389**, 341.

Mok, H. K., and Gilmore, R. G. (1983). Analysis of sound production in estuarine aggregations of *Pogonias cromis*, *Bairdiella chrysoura*, and *Cynoscion nebulosus* (Sciaenidae). *Bull. Inst. Zool. Acad. Sinica* **22**, 157-186.

Myrberg, A. A. (2001). The acoustical biology of elasmobranchs. *Env. Biol. Fishes.* **60**, 31-45.

Myrberg, A. A., and Spires, J.Y. (1980). Hearing in damselfishes: an analysis of signal detection among closely related species. *J. Comp. Physiol*. **140**, 135-144.

Parvulescu, A. (1967). The acoustics of small tanks. In: *Marine Bioacoustics*, vol 2 (Tavolga, W. N,. ed.). Pp. 7-13. Oxford: Pergamon Press.

Popper, A. N. and Fay, R. R. (1993). Sound detection and processing by fish: critical review and major research questions. *Brain Behav. Evol.* **41**, 14-38.

Popper, A. N., and Fay, R. R. (1999). The auditory periphery in fishes. In: *Comparative hearing: fish and amphibians* (ed. Fay, R.R. and Popper, A.N.). Pp. 43-100. New York: Springer, Berlin Heidelberg.

Popper, A. N., Ramcharitar, J., and Campana, S. E. (2005). Why otoliths? Insights from inner ear physiology and fisheries biology. *Mar. Fresh. Res.* **56**, 497-504.

Ramcharitar, J. (2003). Sciaenids: model species for investigating structure-function relation in the teleost inner ear. Doctoral dissertation. University of Maryland, College Park.

Ramcharitar, J., Gannon, D. P., and Popper, A. N. (2006a). Bioacoustics of the fishes of the Family Sciaenidae (croakers and drums). *Trans. Am. Fish. Soc.* **135**, 1409-1431.

Ramcharitar, J. U., Higgs, D. M., and Popper, A. N. (2006b). Audition in sciaenid fishes with different swim bladder-inner ear configurations. *J. Acoust. Soc. Am.* **119(1)**, 439-443.

Ramcharitar, J. U. and Popper, A. N. (2004a). Masked auditory thresholds in sciaenid fishes: a comparative study. *J. Acoust. Soc. Am.* **166(3)**, 1687-1694.

Ramcharitar, J. U., Deng, X., Ketten, D., and Popper, A. N. (2004b). Form and

function in the unique inner ear of a teleost: the silver perch (*Bairdiella chrysoura*). *J. Compar. Neurol.* **475**, 531-539.

Ramcharitar, J. U., Higgs, D.M., and Popper, A. N. (2001). Sciaenid inner ears: a study in diversity. *Brain. Behav. Evol.* **58**, 152-162.

Ripley, J. L., Lobel, P. S., and Yan, H. Y. (2002). Correlation of sound sproduction with hearing sensitivity in the Lake Malawi cichlid *Tramitichromis intermedius*. *Bioacoustics*. **12**, 238-240.

Rogers, P., and Cox, M. (1988). Underwater sound as a biological stimulus. In: *Sensory Biology of Aquatic Animals* (Atema, J., Fay, R. R., Popper, A. N., Tavolga, W. N., eds.) pp. 131–149. Springer-Verlag, New York,

Roundtree, R. A., Gilmore, R. G., Goudey, C. A., Hawkins, A. D., Luczkovitch, J. J., and Mann, D.A. (2006). Listening to fish: applications of passive acoustics to fisheries science. *Fisheries.* **31(9)**, 433-446.

Sand, O. and Karlsen, H. E. (2000). Detection of infrasound and linear acceleration in fishes. *Phil. Trans. Royal Soc. Lond. Ser. B*. **355**: 1295–1298.

Saucier, M. H. and Baltz, D. M. (1993). Spawning site selection by spotted seatrout, *Cynoscion nebulosus*, and black drum, *Pogonias cromis*, in Louisiana. *Env. Biol. Fish*. **36(3)**, 257-272.

Sprague, M. W. and Luczkovitch, J. J. (2004). Measurement of an individual silver perch *Bairdiella chrysoura* sound pressure level in a field recording. *J. Acoust. Soc. Am.* **116(5)**, 3186-3191.

Underwood, A. J. (2002). *Experiments in ecology: their logical design and*

interpretation using analysis of variance. P. 385-418. New York, NY: Cambridge University Press,

van den Berg, A. V. (1985). Analysis of the phase difference between particle motion components of sound by teleosts. *J. Exp. Biol.* **119**, 183-197.

Vasconcelos, R. O., Amorim, M. C. P., and F. Ladich. (2007). Effects of ship noise on the detectability of communication signals in the Lusitanian toadfish. *J. Exp. Biol.* **210**, 2104-2112.

Wahlberg, M. and Westerberg, H. (2005). Hearing in fish and their reactions to sounds from offshore wind farms. *Mar. Ecol. Prog. Ser.* **288**, 295-309.

Weeg, M. S., Fay, R. R., and Bass, A. H. (2002). Directionality and frequency tuning of primary saccular afferents of a vocal fish, the plainfin midshipman (*Porichthys notatus*). *J. Comp. Physiol. A.* **188**, 631-641.

Wysocki, L. E. and Ladich, F. (2003). The representation of conspecific sound sin the auditory brainstem of teleost fishes. *J. Exp. Biol.* **206**, 2229-2240.

Yan, H. Y. (1998). Auditory role of the suprabranchial chamber in gourami fish. *J. Comp. Physiol. A* **183**, 325–333.

Yan, H. Y. and Curtsinger, W. S. (2000). The otic gasbladder as an ancillary auditory structure in a mormyrid fish. *J. Comp. Physiol. A* **186**, 595–602.

Yan, H. Y., Fine, M. L., Horn, N. S., and Colon, W. E. (2000). Variability in the role of the gasbladder in fish audition. *J. Comp. Physiol. A.* **186**, 435-445.

Table 1 – Species, sample size, standard length (SL), and mass of the six sciaenid fishes investigated in this study.

Species	*n*	SL (mm)	Mass (g)
Cynoscion nebulosus	6	225 – 515	165 – 730
Cynoscion regalis	6	230 – 315	190 – 460
Micropogonias undulatus	6	230 – 485	185 – 790
Sciaenops ocellatus	6	305 – 555	585 – 955
Leiostomus xanthurus	6	115 – 381	65 – 405
Menticirrhus saxatilis	6	200 – 305	140 – 325

Table 2 – Particle accelerations in three orthogonal Cartesian directions and for the magnitude of the three directions combined, following Casper and Mann (2006). Sound pressure level was measured by hydrophone, and mean sound pressure levels of these recordings (in dB re: 1 μPa) were: x-axis (116.7 dB), y axis (116.3 dB), z-axis (119.7 dB). The x-axis was considered to be anterior-posterior along each subject's body while the y-axis was considered to be lateral (right-left) relative to the subject. Particle acceleration was calculated from the particle velocity measured by the geophone for stimulus acoustic sound pressures. The speaker was mounted in air 1.5 m directly above each test subject. Most of the acoustic energy was along the vertical (z) axis coming from directly above test subjects. The magnitude of particle acceleration ($m\ s^{-2}$) was calculated as $\sqrt{(x^2+y^2+z^2)}$.

Frequency (Hz)	x-axis acceleration ($m\ s^{-2}$)	y-axis acceleration ($m\ s^{-2}$)	z-axis acceleration ($m\ s^{-2}$)	Magnitude of particle acceleration ($m\ s^{-2}$)
100	0.015	0.010	0.182	0.033
200	0.018	0.061	0.578	0.370
300	0.064	0.082	1.17	1.38
400	0.080	0.096	1.01	1.04
500	0.084	0.129	0.428	0.206
600	0.113	0.109	0.670	0.473
700	0.141	0.114	0.482	0.266
800	0.168	0.125	0.510	0.304
900	0.184	0.115	0.305	0.140
1000	0.219	0.124	0.362	0.194
1100	0.218	0.206	0.413	0.260
1200	0.168	0.249	0.339	0.205

Table 3 – Models of pressure and particle motion data with three candidate covariance structures: first order autoregressive (AR(1)), compound symmetry (CS), and unstructured (UN). The AR(1) model consistently had the lowest values of the small sample adjusted Akaike's Information Criterion (AIC_c). This covariance structure was therefore used in the two way repeated measures ANOVAs for pressure, velocity, and acceleration thresholds. The unstructured covariance model failed to converge for velocity and acceleration analyses (n/a = not applicable).

Analysis	Model	Number of parameters	-ln(likelihood)	AIC_c
(A) Pressure	AR(1)	2	2362	2366
	CS	2	2474	2478
	UN	78	2220	2420
(B) Velocity	AR(1)	2	-6878	-6874
	CS	2	-6758	-6754
	UN	78	n/a	n/a
(C) Acceleration	AR(1)	2	-584	-580
	CS	2	-470	-466
	UN	78	n/a	n/a

Table 4 – Approximate propagation distances presuming spherical spreading of sciaenid vocalizations under idealized conditions. Sound pressure levels (SPL) and auditory thresholds are given in dB re: 1μPa. These calculations assume: spherical spreading (decrease of 6 dB for each distance doubled, in m), uniform water of sufficient depth to not preclude sound propagation, no additional scattering or attenuating objects, and background noise below each species' auditory threshold. Vocalization SPLs are for single individuals except C, which recorded the SPL of an aggregation.

Common name	Vocalization frequency (Hz)	Vocalization SPL	Mean auditory pressure threshold	Spherical spreading distance (m)
Weakfish	400-500[a]	127[b]	96.4	32
Spotted seatrout	400-500[a]	139.6[c]	97.3	128
Atlantic croaker	300[a]	114[d]	94.9	8
Red drum	200[a]	128[e]	99.6	32

[a] – Ramcharitar et al. (2006a); Connaughton et al. (1997); Fine et al. (2004)
[b] – Sprague and Luczkovich (2004)
[c] – Baltz (2002)
[d] – Barimo and Fine (1998)
[e] - Luczkovich , pers. comm.

Figure 1 – Sample 500 Hz waveforms: (A) a pure tone 500 Hz stimulus waveform, (B) an echo-canceled 500 Hz stimulus, and (C) a 500 Hz signal that was not echo-canceled. B and C were recorded in our experimental chamber by the submersed, omnidirectional hydrophone.

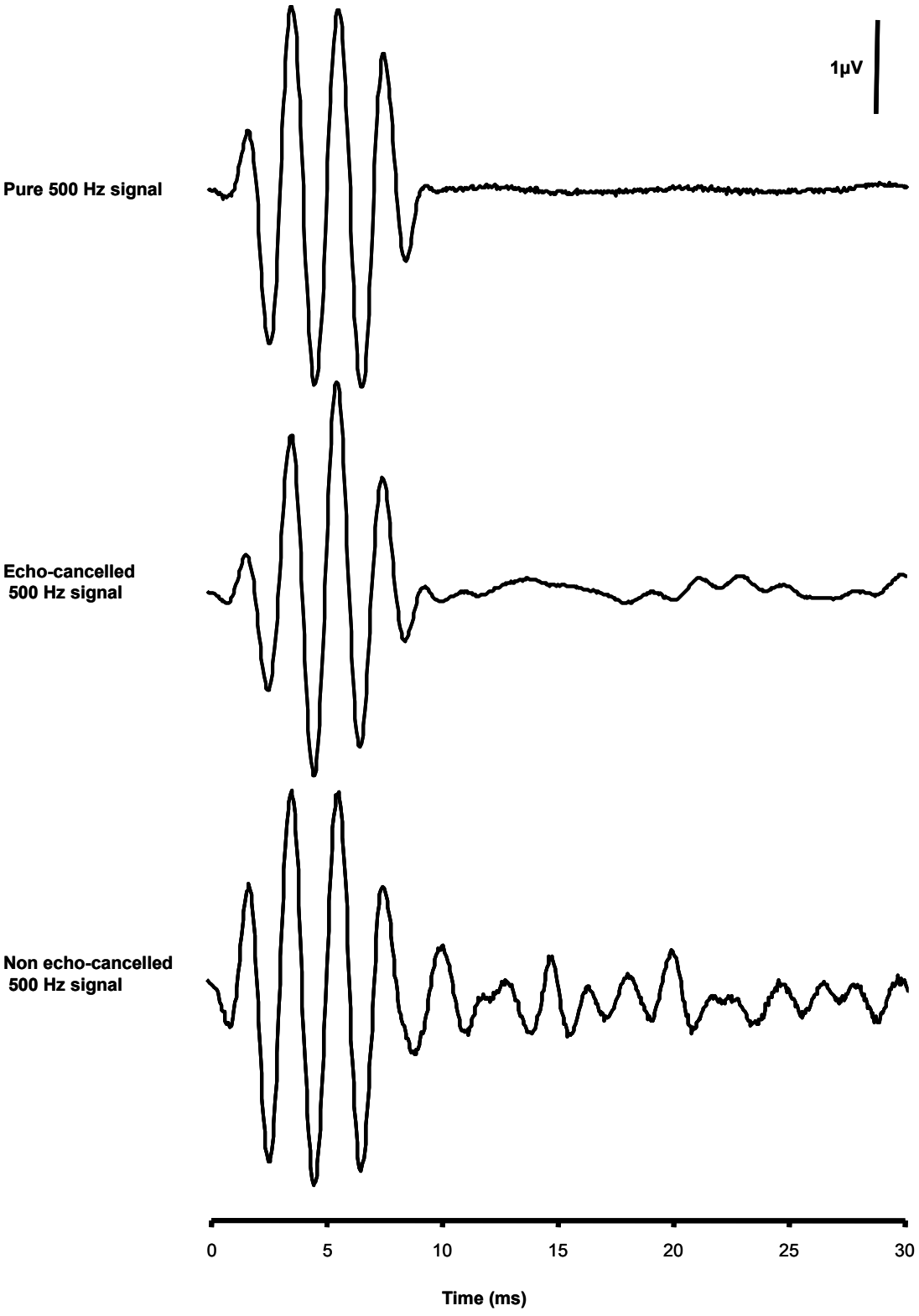
1µV
Pure 500 Hz signal
Echo-cancelled
500 Hz signal
Non echo-cancelled
500 Hz signal
0
5
10
15
20
25
30
Time (ms)

Figure 2 – Sample ABR waveforms from each species, obtained in response to echo-canceled 500 Hz pure tone bursts: spotted seatrout, weakfish, Atlantic croaker, red drum, spot, and northern kingfish. Black and grey lines are replicate ABR responses at a given attenuation that each result from the addition of two ABR recordings of opposite polarities. Vertical labels are the sound pressure levels (SPL, dB re: 1μPa at 1m).

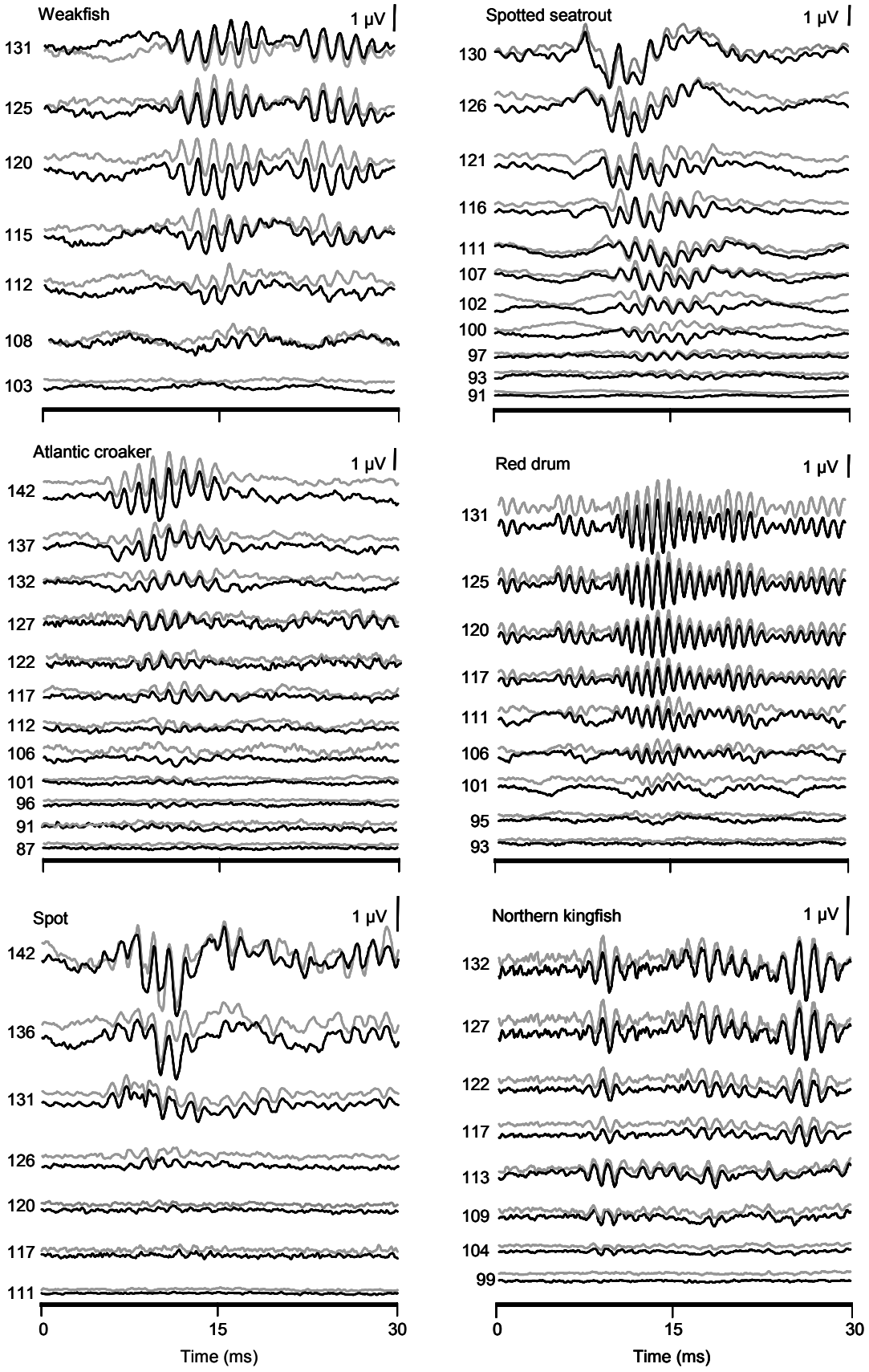
Weakfish
1 μV
131
125
120
115
112
108
103
Spotted seatrout
1 μV
130
126
121
116
111
107
102
100
97
93
91
Atlantic croaker
1 μV
142
137
132
127
122
117
112
106
101
96
91
87
Red drum
1 μV
131
125
120
117
111
106
101
95
93
Spot
1 μV
142
136
131
126
120
117
111
0
15
30
Time (ms)
Northern kingfish
1 μV
132
127
122
117
113
109
104
99
0
15
30
Time (ms)

Figure 3 – Audiograms of (A) mean sound pressure in dB re: 1µPa, (B) mean velocity in cm s^{-1}, and (C) mean acceleration in cm s^{-2} for six sciaenid species: spotted seatrout (solid blue circles), weakfish (open grey circles), Atlantic croaker (solid green triangles), red drum (open red triangles), spot (solid black squares), and northern kingfish (open brown squares).

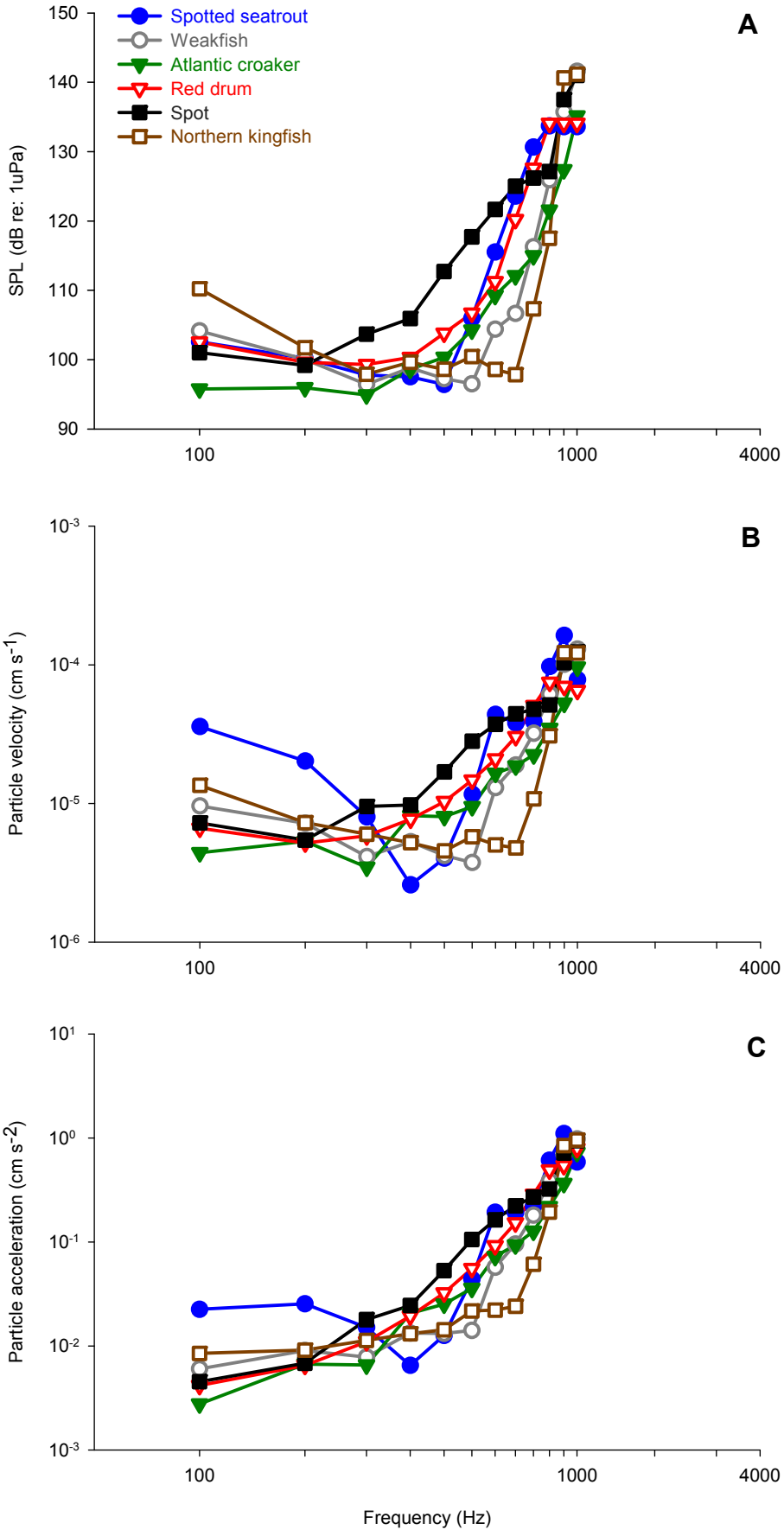
A
Spotted seatrout
Weakfish
Atlantic croaker
Red drum
Spot
Northern kingfish
SPL (dB re: 1uPa)
150
140
130
120
110
100
90
100
1000
4000
B
Particle velocity (cm s-1)
10-3
10-4
10-5
10-6
100
1000
4000
C
Particle acceleration (cm s-2)
101
100
10-1
10-2
10-3
100
1000
4000
Frequency (Hz)

CHAPTER 2:

Comparative Visual Function in Five Sciaenid Fishes Inhabiting Chesapeake Bay

INTRODUCTION

Daily irradiance in near-surface waters can vary over an intensity range of nine orders of magnitude; scatter and absorption further restrict the spectral bandwidth (color) and intensity (brightness) of downwelling light with depth (Lythgoe, 1979; McFarland, 1986). In its simplest form, maximal transmission occurs at short wavelengths (blue) in pure natural waters and clear pelagic seas, at intermediate (green) wavelengths in coastal waters, and at longer (yellow-red) wavelengths in estuarine and fresh waters (Jerlov, 1968). Closer to shore, the increasing concentrations of phytoplankton, yellow products of vegetative decay (*Gelbstoffe*), and suspended particulates scatter, absorb, and more rapidly attenuate light (Lythgoe, 1975; Lythgoe, 1988). The spectral distribution in these waters shifts to longer wavelengths (Jerlov, 1968).

Fishes have radiated into a broad range of aquatic habitats possessing complex photic properties, resulting in a myriad of selective pressures on their visual systems (Munz, 1977; Levine and MacNichol, 1979; Collin, 1997). The characteristics of aquatic light fields are generally reflected in the visual systems of fishes inhabiting them (Guthrie and Muntz, 1993). However, maintaining optimal visual performance over the full range of possible light intensities is near-impossible, thus unavoidable tradeoffs exist between visual sensitivity and resolution. For example, at the cost of acuity, luminous sensitivity can be extended under dim conditions by widening pupils, increasing spatial and temporal summation, and reradiating light through retinal media to maximize photon capture (Warrant, 1999). Luminous and chromatic sensitivities as well as temporal and

spatial properties of fish visual systems vary depending on ecological and phylogenetic constraints, and are thus useful metrics to describe the functions and tasks of visual systems (Lythgoe, 1979; Warrant, 1999; Marshall et *al*., 2003).

The range of light from which visual information can be obtained is further extended in species with duplex retinae that use cone cells under photopic (bright) conditions, and rod cells during scotopic (dim/dark) conditions (Lythgoe, 1979; Crescitelli, 1991). Much discussion has centered on the properties of these cells, their pigments, and correlations to the photic properties of habitats (McFarland and Munz, 1975; Dartnall, 1975; Levine and MacNichol, 1979; Bowmaker, 1990, Jokela et *al.*, 2003; Jokela-Määtä et *al.*, 2007), leading to two hypotheses that relate the spectral properties of pigments to those of light fields. The 'Sensitivity Hypothesis' suggests that pigment absorption spectra should match the ambient background to maximize photon capture in scotopic (rod-based) vision (Bayliss et *al.*, 1936; Clark, 1936). The 'Contrast Hypothesis' suggests that maximal contrast between an object and the background is provided by a combination of matched and offset visual pigments (Lythgoe 1968). Fishes that possess multiple spectrally-distinct visual pigments likely use both mechanisms (McFarland and Munz, 1975).

There has been considerable research on the properties of visual systems in closely-related taxa inhabiting similar environments. Comparative methods have provided novel insights into the form-function-environment relationships of the fish eye (Walls, 1942; Levine and MacNichol, 1979; Parkyn and Hawryshyn, 2000; Jokela-Määtä et *al.*, 2007), the distributions and movements of fishes (McFarland, 1986), communication (Hart *et al.*, 2006; Siebeck et *al.*, 2006), predator-prey interactions

(Browman *et al.*, 1994; De Robertis et *al.*, 2003), and even vulnerability to capture (Buijse et *al.*, 1992; Weissburg, 2005). Few such comparisons exist for the commercially and recreationally important fauna that use mid-Atlantic coastal and estuarine waters as key juvenile nurseries (Levine and MacNichol, 1979; Beck et *al.*, 2001).

Teleosts of the family Sciaenidae support valuable fisheries along the US East coast and are good candidate organisms for comparative sensory study by virtue of their taxonomic, morphological, and microhabitat diversity (Chao and Musick, 1977; Horodysky et *al.*, 2008). Sciaenids occupy a myriad of habitats in freshwater, estuarine, coastal neritic, and reef-associated marine systems, but are most speciose in coastal and estuarine waters (Myers, 1960). Species-specific ecomorphologies and microhabitats result in niche separation in sympatry among piscivorous, midwater zooplanktivorous, and benthivorous sciaenids in Chesapeake Bay, eastern USA (Chao and Musick, 1977; Fig 1). Light fields in such microhabitats may differ widely in chromatic and luminous properties, and have changed rapidly over the past century of anthropogenic degradation of coastal waters (Levine and MacNichol, 1979; McFarland, 1991; Kemp et *al.*, 2005). Unfortunately, photic form:function:environment relationships for sciaenids have been precluded by the lack of information on their visual systems. We therefore used corneal electroretinography (ERG) to assess the absolute sensitivities, temporal properties, and spectral sensitivities of the visual systems of five sciaenid species.

MATERIALS AND METHODS

Hook and line gear was used to capture study animals including: weakfish *(Cynoscion regalis* Bloch and Schneider, 1801), spotted seatrout (*Cynoscion nebulosus* Cuvier, 1830), red drum (*Sciaenops ocellatus* Linnaeus, 1766), Atlantic croaker (*Micropogonias undulatus* Linnaeus, 1766), and spot (*Leiostomus xanthurus* Lacepede, 1802) (Table 1). Animals were maintained in recirculating 1855 L aquaria at 20°C ± 1°C (winter) or 25°C ± 2°C (summer) and fed a combination of frozen Atlantic menhaden (*Brevoortia tyrannus*), squid (*Loligo* sp.), and commercially-prepared food (AquaTox flakes; Zeigler, Gardners, PA, USA). Indirect sunlight passing through standard window glass in the animal holding facility allowed us to maintain all subjects on natural ambient photoperiods.

Experimental and animal care protocols were approved by the College of William and Mary's Institutional Animal Care and Use Committee, protocol no. 0423, and followed all relevant laws of the United States. ERG experiments were conducted on six animals of each species. Subjects were removed from holding tanks during daylight hours, sedated with an intramuscular (IM) dose of ketamine hydrochloride (Butler Animal Health, Middletown, PA, USA; 30 mg kg^{-1}), and immobilized with an IM injection of the neuromuscular blocking drug gallamine triethiodide (Flaxedil; Sigma, St. Louis, MO., USA; 10 mg kg^{-1}). Recording of vertebrate neural waveforms in anaesthetized and/or immobile subjects is a common practice to minimize the obscuring effect of muscular noise (Hall, 1992; Parkyn and Hawryshyn, 2000; Horodysky et *al.*,

2008). Following drug injections, fish were moved into a light-tight enclosure and placed on a chamois sling submerged in a rectangular 800 x 325 x 180 mm plexiglass tank such that only a small portion of the head and the eye receiving the light stimulus remained above the water surface. Subjects were ventilated (1 L min^{-1}) with filtered and oxygenated sea water that was temperature-controlled (20 ± 2°C) to minimize the potential confounding effects of temperature on ERG recordings (Saszik and Bilotta, 1999; Fritsches et *al.*, 2005)

Experiments were conducted during both day and night to account for any circadian rhythms in visual response (McMahon and Barlow 1992; Cahill and Hasegawa 1997; Mangel 2001). We defined "day" and "night" following ambient photoperiods: experiments conducted during the hours the fish holding tanks were sun-lit are hereafter referred to as "day", while those repeated following sunset when the fish holding tanks were in darkness are referred to as "night". At the conclusion of each experiment, fishes were euthanized via a massive overdose (~300 mg kg^{-1}) of sodium pentobarbital (Beuthanasia-D, Schering-Plough Animal Health Corp., Union, N.J, USA).

Electroretinography (ERG)

Whole-animal corneal ERGs were conducted to assess the absolute sensitivities, temporal properties, and spectral sensitivities of scaienid visual systems. Corneal ERG is a comprehensive method to measure summed retinal potentials that account for any optical filtering of light by ocular media (Brown, 1968; Ali and Muntz, 1975). This technique is well-suited for comparative investigations of vision and form:function relationships in fishes (Ali and Muntz, 1975; Pankhurst and Montgomery, 1989; Makhankov et *al*., 2004).

Teflon-coated, chlorided 0.5 mm silver wire (Ag-$AgCl_2$) electrodes were used to measure and record ERG potentials: the active electrode was placed on the corneal surface and a reference electrode was placed subdermally in the dorsal musculature. The system was grounded to the water of the experimental tank via a 6 cm by 26 cm stainless steel plate. ERG signals were amplified with a DAM50 amplifier (World Precision Instruments, Sarasota, FL, USA) using a 10,000 gain passed through a 1 Hz high pass and 1 kHz low pass filter. Amplified ERG signals were further filtered with a HumBug ® active electronic filter (Quest Scientific, N. Vancouver, B.C., Canada) to remove periodic electrical noise, and were digitized at 1kHz sampling frequency with a 6024E multifunction DAQ card (National Instruments, Austin, TX, USA). ERG recordings and stimulus presentations were controlled using software written in LabVIEW (National Instruments, Austin, TX, USA). All subjects were dark-adapted for a minimum for 30 min prior to stimulus exposure. Light intensities for all experiments were calibrated using an International Light IL1700 radiometer.

Absolute (luminous) sensitivity

Absolute sensitivity of sciaenid visual systems was assessed by intensity-response (V/logI) experiments. A uniform circular source, 3.8 cm in diameter, consisted of an array of 20 bright white light emitting diodes (LEDs, Advanced Illumination, Rochester, VT, U.S.A.) that were diffused and collimated (see Fritsches *et al.*, 2005). The LED output was driven by an intensity controller (Advanced Illumination, Rochester, VT, U.S.A). A sinusoidal voltage, variable between 0V and 5V, could be sent to the intensity controller from the analog output of the DAQ card, thus allowing a sinusoidally-modulated light intensity from the LEDs. Our LED light source had a working range of

roughly 3 $\log_{10}$ units, and a maximum output intensity of 1585 cd m^{-2}. Six orders of magnitude of stimulus intensity were therefore presented to subjects by using appropriate combinations of Kodak Wratten 1.0 and 2.0 neutral density filters (Eastman Kodak Co., Rochester, N.Y., U.S.A.). V/logI experiments progressed from subthreshold to saturation intensity levels in 0.2 log unit steps. At each intensity step, ERG b-waves were recorded from a train of five 200 ms flashes, each separated by 200 ms rest periods. This process was repeated three times. ERG responses of the final averaged flashes ($V_{response}$) were recorded at each intensity step and subsequently normalized to the maximum voltage response (V_{max}). Mean V/logI curves for each species were created by averaging the V/logI curves of six individuals of that species. Interspecific comparisons of relative sensitivity were made at stimulus irradiances eliciting 50% of V_{max} (referred to as K_{50}). Dynamic ranges, defined as the log irradiance range between the limits of 5-95% V_{max}, were also calculated for each species (*sensu* Frank, 2003).

Temporal resolution

The temporal resolution of sciaenid visual systems was assessed via flicker fusion frequency (FFF) experiments with the white light LED setup described above using methods developed elsewhere (Fritsches et *al.*, 2005). FFF experiments monitored a visual system's ability to track light flickering in logarithmically increasing frequencies. Sinusoidally-modulated white light stimuli ranging in frequency from 1 Hz (0 log units) to 100 Hz (2.0 log units) were presented to subjects in 0.2 log unit frequency steps. The voltage offset and the amplitude of the sinusoidal light stimulus signal were always equal (contrast = 1). At each frequency step, light stimuli were presented for 5 s, followed by 5 s of darkness (i.e., rest). This stimulus train was repeated three times at each frequency,

and b-wave responses were averaged for each subject. For each subject, seven total FFF experiments were conducted: one at 25% (I_{25}) of maximum stimulus intensity (I_{max}) from the V/logI curve, and one in each of $\log_{10}$ step intervals over six orders of magnitude of light intensity.

A subject's FFF threshold at a given intensity increment was determined by analyzing the power spectrum of the averaged responses from 1-100 Hz and comparing the power of the subject's response frequency (signal) to the power of a neighboring range of frequencies (noise). FFF was therefore defined as the frequency at which the power of the response signal fell below the power of the noise, as determined by graphical analysis of normalized power amplitudes as a function of frequency. Diel and interspecific comparisons were conducted on the FFF data at I_{max} and I_{25}. We considered the FFF at I_{max} as the probable maximum flicker fusion frequency attainable by the visual system of a given species, and FFF at I_{25} to be a proxy for ambient environmental light intensity.

Spectral (chromatic) sensitivity

Spectral sensitivity experiments were conducted to assess the ability of sciaenid visual systems to respond to colored light stimuli. The output of a Cermax Xenon fiberoptic light source (ILC Technology, Sunnydale, C.A., U.S.A.) was controlled by a CM110 monochromator, collimated, and passed through each of two AB301 filter wheels containing quartz neutral density filters (CVI Laser Spectral Products, Albuquerque, NM, USA). The first wheel allowed light attenuation from 0 to 1 log units of light intensity in 0.2 log unit steps, the second from 0 to 4 log units in 1 log unit steps. In concert, the two wheels allowed the attenuation of light from 0 to 5 log units in 0.2 log unit steps. Stimuli

were delivered by a LabVIEW program that controlled a Uniblitz LS6 electronic shutter (Vincent Associates, Rochester, NY, USA) using the analog and digital output of the DAQ card and the computer's serial RS232 interface. A cylindrical lens focused the attenuated light beam onto the entrance slit of the monochromator to produce colored light. The 1 cm diameter quartz light guide was placed within 10 mm of a subject's eye. Approximately isoquantal spectral stimuli were presented to subjects via the selective use of neutral density filters.

Light stimuli covering the spectral range from UV (300 nm) to the near infrared (800 nm) were presented sequentially in 10 nm steps during spectral response experiments. Subjects were presented with five single 40 ms stimulus flashes at each experimental wavelength, each followed by 6 s rest. The amplitudes of ERG b-wave responses were recorded and averaged to form raw spectral response curves for each individual. A spectral V/logI recording was subsequently conducted for each subject at the wavelength (λ_{max}) that generated its maximum ERG response (V_{max}). This allowed the subsequent calculation of the subject's spectral sensitivity curve. V/logI experiments exposed the subject to five individual monochromatic 200 ms flashes at each intensity. Intensities increased in 0.2 log unit increments over five orders of magnitude. The amplitudes of these flashes were recorded and averaged to create each subject's spectral V/logI curve. To transform spectral response voltages to spectral sensitivities for each subject, the former were converted to equivalent intensities through the V/LogI curve following the equation 1:

$$S = 100 * 10^{-|I_{\max} - I_n|}, \text{ where} \qquad \text{(Eq. 1)}$$

S=sensitivity

I_{max}= intensity at maximum response voltage

I_n= intensity at response voltage *n*

Spectral sensitivity curves for each individual were expressed on a percentage scale, with 100% indicating maximum sensitivity. To obtain the final spectral sensitivity curve for each species, we averaged the sensitivity curves of all subjects and normalized to the maximum resulting value such that maximum sensitivity equaled 100%.

Data Analyses

V/logI and FFF

Corneal recordings are non-independent within individual subjects (Underwood, 2002), and require that the nature of within-individual autocorrelation is explicitly understood (Littell et *al.*, 2006). To consider corneal recordings as independent within a subject is tantamount to pseudoreplication (Hurlbert, 1984). Sciaenid V/logI and FFF data were therefore analyzed separately using two-way repeated measures ANOVAs with Tukey's post hoc comparisons to assess whether ERG responses varied among the five sciaenid species and between photoperiods. All statistical analyses were conducted using SAS v 9.1 (SAS Institute, Cary, NC, U.S.A.). A general model for these analyses is given in equation 2:

$Y_{ijk} = \mu + \alpha_i + \beta_j + \delta_k + \varepsilon_{ijk}$, where, (Eq. 2)

Y_{ijk}= value of the response variable (response) for the i^{th} species, j^{th} diel period, and the k^{th} level of their interaction

μ=overall mean of threshold for all combinations of species and diel periods property

α_i=species (fixed factor)

β_j=diel period (fixed factor)

δ_k=species:diel interaction

ε_{ijk}=random error term associated with the observation at each combination of the i^{th} species, the j^{th} diel period, and k^{th} level of their interaction.

Spectral sensitivity

Intraspecific diel differences in sciaenid spectral sensitivity curves were assessed by subtracting the day and night curves and calculating confidence intervals (CI) of the resulting difference curve. In this analysis, positive values corresponded to increased day sensitivity, negative values indicated increased nocturnal sensitivity. Similarly, we subtracted the curves of weakfish and spotted seatrout within each diel period to assess potential interspecific differences in the spectral sensitivities of these congeners. Positive values indicated increased response by weakfish, negative values increased response by spotted seatrout. Significant differences in spectral sensitivity were defined where the mean ± CI of difference curves did not encompass zero.

To form hypotheses regarding the number and spectral distribution of pigments potentially contributing to sciaenid spectral ERG responses, we fitted the SSH (Stavenga *et al.*, 1993) and GFRKD (Govardovkii *et al.*, 2000) vitamin A1 rhodopsin absorbance templates separately to the photopic spectral sensitivity data. A range of possible conditions was considered: 1-3 α-band rhodopsins, 1-3 α-band rhodopsins with a single β-band on any pigment, and 1-3 α-band rhodopsins with multiple β-bands. For a given species, condition and template, models of summed curves were created by adding the products of pigment-specific templates and their respective weighting factors. Estimates of the unknown model parameters (λ_{max} values and their respective weighting

proportions) were derived by fitting the summed curves to the ERG data using maximum likelihood.

For each species, we objectively selected the appropriate template (SSH or GFRKD) and number of contributing pigments using an Information Theoretic approach (Burnham and Anderson, 2002) following Akaike's Information Criterion (AIC):

$\mathrm{AIC} = -2\ln(\hat{L}) + 2p$, where (Eq. 3)

AIC: Akaike's Information Criterion

$\hat{L}$: the estimated value of the likelihood function at its maximum

p: number of estimated parameters

AIC is a parsimonious measure that strikes a balance between model simplicity and complex overparameterization (Burnham and Anderson, 2002). Accordingly, AIC provided a quantitative metric to evaluate the simplest, most likely estimates of sciaenid rhodopsin parameters given our data (Stavenga *et al.*, 1993; Govardovskii *et al.*, 2000). All parameter optimization, template fitting, and model selection was conducted using the software package *R* version 2.7.1 (R Development Core Team, 2008).

Spectrophotometry of eye subcomponents

To assess whether sciaenid ocular media transmit or absorb ultraviolet wavelengths, we dissected and separately tested corneal tissue, vitreous humor, and lenses of 1-3 freshly euthanized specimens per species not used for ERG experiments. Dissected tissues were immersed in UV-transmitting cuvettes filled with 0.9% saline, placed in a Shimadzu BioSpec-1601 spectrophotometer such that the measuring beam passed through the tissue to be measured, and measured relative to a blank cuvette

containing saline alone. Transmission and absorbance were recorded over the spectral range from 250-750 nm.

RESULTS

White-light evoked ERG b-wave responses of the five sciaenids increased non-monotonically with stimulus intensity to maximum amplitudes (V_{max}) of 100-849 μV then decreased at intensities above those at V_{max} (Fig.2), presumably due to photoreceptor saturation and a lack of pigment regeneration. The K_{50} values of V/logI curves differed significantly among species ($F_{4,25}$=9.94, $p<0.0001$) but not between diel periods ($F_{4,25}$=0.74, $p>0.05$). Tukey's post-hoc comparisons revealed that the mean K_{50} values of Atlantic croaker were significantly left-shifted (0.5-0.7 log units, $p< 0.008$) relative to the other sciaenids, indicating higher sensitivity to dim light. Mean dynamic ranges, defined as 5-95% of V_{max}, varied between 3.15-3.43 log units among the species (Fig. 2) but were not significant with respect to species or diel periods ($p>0.05$). Slightly broader ranges were evident in benthic sciaenids (Atlantic croaker and spot; mean = 3.34) than in more pelagic species (weakfish, spotted seatrout, and red drum; mean = 3.19).

Sciaenid FFF values (Fig 3) varied significantly among the five species ($F_{4,25}$= 4.63, $p<0.007$) (Fig 3) and increased with increasing light intensity ($F_{1, 84}$=148.27, $p< 0.001$), but not between diel periods ($p>0.05$). Likewise, no differences were observed among FFF at I_{25}, but weakfish had significantly lower FFF values at I_{max} than the other sciaenids ($p<0.004$). In contrast, spotted seatrout, a congener of weakfish, had the highest mean FFF values at I_{max} in this study (60 Hz).

Sciaenid spectral sensitivities spanned 400-610 nm in most fishes (Fig 4, 5). Weakfish were a clear exception, exhibiting short wavelength sensitivity (350-400 nm) that was not evident in other sciaenids including a congener, spotted seatrout (Fig 4, 5). The UV-A sensitivity of weakfish was the significant interspecific difference (Fig 6). Weakfish and Atlantic croaker demonstrated a significant nocturnal short wavelength shift, while red drum and spot did not exhibit any significant nocturnal spectral shifts (Fig 4, 5).

Given our data, maximum likelihood estimation using published SSH and GFRKD rhodopsin templates suggested that sciaenid fishes may have multiple pigment mechanisms. Spotted seatrout (λ_{max}= 450, 542 nm) and spot (λ_{max}= 450, 546 nm) photopic spectral sensitivities were most consistent with the presence of two α-band vitamin A1 pigments and were optimally fitted with the GFRKD template (Table 2). The trichromatic condition was most likely for Atlantic croaker (SSH λ_{max}= 430, 484, 562 nm) and red drum (GFRKD λ_{max}= 444, 489, 564), but estimates were quite variable among templates (Table 2, Fig 7). The weakfish photopic spectral sensitivity curve was optimally fitted with the SSH template featuring a short wavelength α-band pigment (λ_{max}= 459 nm) and a longer wavelength pigment (λ_{max}= 532 nm) that possessed a β-band (λ_{max}= 366 nm).

Spectrophotometric examination of the transmission of sciaenid ocular media revealed that wavelengths in the UV-A range (350-380) were transmitted through the cornea, vitreous humor, and lens of weakfish (n = 2, Fig 8). In Atlantic croaker (n = 3, Fig 8) and all other sciaenids examined, ultraviolet wavelengths were transmitted by corneal tissue and vitreous humor, but were absorbed by the lens.

DISCUSSION

The complexity of aquatic photohabitats has resulted in a diverse assemblage of visual adaptations in fishes that are generally well-matched to habitat (Guthrie and Muntz, 1993). While the light environment of deep pelagic seas are fairly stable and homogenous, fresh waters and estuaries tend to be more labile and heterogeneous photohabitats (Loew and Lythgoe, 1978; Loew and McFarland, 1990). In the latter, spectral bandwidths and downwelling intensities can vary greatly over a range of temporal and spatial scales. The estuarine light field, for example, varies temporally due to passing surface waves (milliseconds), clouds and weather (seconds to hours), tides (multihour), sunrise and sunset (daily), and seasonal solar irradiance and phytoplankton dynamics (McFarland and Loew, 1983; Bowers and Brubaker, 2004; Gallegos *et al.*, 2005). Spatial variations include vertical mixing and wave effects (cm-m) as well as tidal and freshwater inputs (m-km) along salinity gradients (Harding, 1994; Schubert *et al.*, 2001). Fish movements within and among habitats are further superimposed on these complex temporal and spatial variations. Given the dynamic nature of estuarine photohabitats, the visual systems of near-coastal fishes such as sciaenids should balance sensitivity, acuity, contrast perception, and rapid adaptation to dynamic light conditions depending on evolutionary pressures and phylogenetic constraints (Dartnall, 1975; Levine and MacNichol, 1979).

Sciaenid light sensitivities, evidenced by the K_{50} points and dynamic ranges of V/logI curves, are comparable to other freshwater and marine teleosts (Naka and Rushton, 1966; Kaneko and Tachibana, 1985; McMahon and Barlow, 1992; Wang and Mangel, 1996; Brill *et al.*, in press) but demonstrate lower sensitivity than deep sea fishes (Warrant, 2000) and arthropods (Frank, 2003). The K_{50} points of Chesapeake Bay sciaenid fishes (Fig. 2) were similar in magnitude and relative diel invariance to demersal Pacific halibut (*Hippoglossus stenolepis*) measured with the same experimental setup (halibut day: 0.15, night: 0.14 log cd m^{-2}; Brill *et al.*, in press). Benthic Atlantic croaker and spot (Fig 1, 2) have left-shifted K_{50} values (i.e. more light sensitivity) relative to halibut, while pelagic sciaenids were right-shifted (i.e. less sensitivity). All Chesapeake Bay sciaenids had substantially left-shifted K_{50} values relative those of black rockfish (*Sebastes melanops*), a fairly shallow-dwelling coastal Pacific sebastid (2.0 log cd m^{-2}, Brill *et al.*, in press). Increased luminous sensitivity in sciaenids is facilitated by non-guanine tapeta lucida that backscatter high proportions of the incident light similar to those of haemulid grunts, ophidiid cusk eels, and ephippid spadefishes (Arnott *et al.*, 1970), Sciaenids also undertake retinomotor movements at intensities ~10 lux to improve sensitivity to dim light (Arnott *et al.*, 1972). Collectively, these results suggest that the light sensitivities of sciaenids from Chesapeake Bay tend toward the lower (more sensitive) end of an emerging continuum for coastal fishes, consistent with their use of frequently light-variable photic habitats.

Temporal properties of sciaenid visual systems are also comparable to a range of diurnal freshwater and marine fishes. As FFF typically increases with light intensity (Crozier *et al.*, 1938), sciaenid FFFs were significantly lower at $I_{25\%}$, than at I_{max} during

both day and night. If $I_{25\%}$, approximates average estuarine intensity, the *in situ* temporal properties of sciaenids may converge on similar function at lower light intensities. Similarly, maximum FFF values reveal the scope of the visual system when light is not limiting. Predators that exploit rapidly swimming prey in clear, bright conditions tend towards high FFFs and low spatial summation of photoreceptors (Bullock *et al.*, 1991). Maximum day FFFs for most sciaenids were 50-60 Hz, similar to photopic maxima of coastal thornback rays (*Platyrhinoidis triserata*: 30-60Hz), grunion (*Leutesthes tenuis*: > 60 Hz), sand bass (*Paralabrax nebulifier*: > 60Hz) (Bullock *et al.*, 1991), and freshwater centrarchid sunfishes (51-53 Hz, Crozier *et al.* 1936, 1938) that inhabit less turbid environments than sciaenids. Since FFF varies with temperature (Saszik and Bilotta, 1999; Fritsches *et al.*, 2005), sciaenids at 20°C predictably had higher FFFs than Antarctic nototheniid fishes at 0°C (< 15 Hz, Pankhurst and Montgomery, 1989). Sciaenid FFF data were also lower than those of yellowfin tuna (*Thunnus albacares*: 60-100 Hz,) that inhabit warm, clear nearsurface waters and forage on rapidly swimming prey (Bullock et al, 1991), and higher than those of the broadbill swordfish (*Xiphias gladius*: 32 Hz) that are predators of the organisms in the deep scattering layer (Fritsches *et al.*, 2005). We caution that experimental and analytical differences among studies may limit inferences in the broad qualitative comparisons above, but consider the collective generalizations to be consistent with ecologies and life histories of the species discussed.

The temporal and spatial properties of sciaenid visual systems are consistent with inferences based on ecology and lifestyle. Weakfish, a coastal pelagic crepuscular/ nocturnal predator of small translucent crustaceans and planktivorous fishes (Fig 1), exhibited the lowest maximum FFFs, and thus the highest degree of temporal summation

(FFF_{day} = 40.8 Hz; FFF_{night} = 43 Hz). Not surprisingly, weakfish also have low ganglion cell densities, suggesting high spatial summation of photoreceptors and low acuities relative to other sciaenids (K. Fritsches, pers. comm.; Poling and Fuiman; 1998). The slow, light sensitive eyes of weakfish have thus evolved to maximize photon capture at the expense of acuity, as would be expected of dim-dwelling species (Warrant, 1999). In contrast, maximum diel FFFs of spotted seatrout were the highest measured during day and night, indicating the lowest temporal summation. Ganglion cell densities of spotted seatrout also demonstrate less summation of individual photoreceptors and substantially higher acuity than their congener weakfish (K. Fritsches, pers. comm.). The greater image sampling via temporal and spatial mechanisms of spotted seatrout eyes are likely more advantageous than dim light sensitivity for prey location in the shallow, structurally-complex seagrass meadows they inhabit (Fig 1). Ecology and lifestyle thus appear to influence visual function more than phylogeny in the genus *Cynoscion*. Finally, maximum FFF of the three benthic-foraging sciaenids, Atlantic croaker, red drum, and spot (Fig 1), were intermediate between those of the *Cynoscion* endmembers, with generally lower values at night than during the day. Benthic-foraging sciaenids likely possess generalist eyes that balance luminous sensitivity, speed, and resolution without excelling at any one task.

Spectral properties of sciaenid visual systems can likewise be placed in context of other fishes. Near-coastal fishes are typically sensitive to longer wavelengths than coral reef, deep sea and pelagic species and a shorter subset of wavelengths than many freshwater fishes (Levine and McNichol, 1979; Marshall *et al.*, 2003). All sciaenids demonstrated broad spectral responses to wavelengths from 400-610 nm that blue-shifted

nocturnally in weakfish and Atlantic croaker. Whether these results are the byproduct of retinomotor movements that increase rod contributions in night recordings, occur as a result of mesopic conditions due to our methodology, or some combination of both is unclear. Under photopic conditions, previous work has demonstrated that coastal and estuarine fishes are commonly dichromats possessing short wavelength visual pigments with λ_{max} values ranging from 440-460 nm and intermediate wavelength pigments with λ_{max} values of 520-540 nm (Lythgoe and Partridge, 1991; Lythgoe, 1994; Jokela-Määttä *et al.*, 2007). Yellow-orange light of 515-600 nm penetrates maximally in Chesapeake Bay (Champ *et al.* 1980), thus intermediate wavelength rhodopsins of coastal dichromats may be matched to ambient optical conditions consistent with the 'Sensitivity Hypothesis' (Bayliss *et al.*, 1936; Clark, 1936), while the short wavelength rhodopsins may conform to the 'Contrast Hypothesis' (Lythgoe, 1968).

Given the lack of published data on sciaenid photopigments, we fitted SSH and GFRKD rhodopsin templates to our spectral ERG data as a descriptive exercise to generate hypotheses that may be subsequently examined using other techniques. Dichromatic visual systems were most likely in weakfish, spotted seatrout, and spot while trichromatic visual systems were most likely in red drum and Atlantic croaker. Whether the exact values of our λ_{max} estimates represent meaningful interspecific differences in pigment locations or result from the expression of variance due to our methodology remains unknown. We therefore strongly emphasize caution in their interpretation. Corneal recordings can contain the summed responses of multiple retinal cells and pigments after filtering of light by pre-retinal optical media (Brown, 1968; Ali and Muntz, 1975), and the interpretation of pigment absorbance maxima without selective

isolation of individual mechanisms is tenuous. These preliminary hypotheses should be critically evaluated with more sensitive techniques such as microspectrophotometry (MSP), behavioral experiments, and/or ERG chromatic adaptation before any valid conclusions regarding potentially contributory photopigment mechanisms can be drawn (Barry and Hawryshyn, 1999; Parkyn and Hawryshyn, 2000). Unfortunately, explicit morphological assessment of cone types, the pigments they contain, and their distributions in sciaenid retinae were beyond the scope of our study. However, our suggestion of the possibility of multiple chromatic mechanisms in sciaenids is potentially supported by the presence of different photoreceptor morphotypes in at least some study species. Atlantic croaker and weakfish retinas contain both single and paired cones (Poling and Fuiman, 1997; A. Horodysky, pers. obs). The latter cone type is frequently sensitive to longer wavelengths than the former in many fishes (Boehlert, 1978), and the presence of both single and paired cones in a species suggests that multiple pigment mechanisms are likely (Bowmaker, 1990). Finally, the ambient light field and background spectral properties, the reflectance of conspecifics, prey, and competitors, and the manner in which these change in space and time should be understood in order to synoptically summarize the utility of visual system and tasks for a species (Levine and MacNichol, 1979; Johnsen, 2002).

Spectral responses in the ultraviolet were observed in weakfish but not in any of the other sciaenids. Whether a species is able to see in the ultraviolet spectrum depends on the transmission of the ocular media, the retinal density of UV-sensitive photoreceptors, and the concentrations of attenuating particulate and dissolved organic matter in the photohabitat (Leech and Johnsen, 2003, 2006). The general lack of ERG

responses in the ultraviolet is not surprising for most sciaenids because of strong absorption of these wavelengths in lenses (50% transmission points greater than 380 nm, Fig 8). Vision in the ultraviolet is considered unlikely if much of the adjoining spectrum is absorbed by preretinal ocular media (Losey *et al.*, 2003). In contrast, the corneas, humors, and lenses of weakfish transmit UV (50% at 356 nm, Fig 8) consistent with a class II response (*sensu* Losey et al, 2003). It is thus possible that weakfish may achieve at least some ability to form images in the UV via an independent cone mechanism or the secondary β-band absorption peak (<400 nm) characteristic of visual pigments (Dartnall and Lythgoe, 1965; Douglas and McGuigan, 1989; Losey et al, 2003; Siebeck *et al.*, 2006). Although the causal mechanism has not been formally demonstrated, AIC values of fitted pigment templates suggested that weakfish UV responses are more likely due to a β-band of the longer wavelength pigment than a separate UV cone. Whether UV-responding pigments occur in sufficient density to contribute to contrast enhancement and image formation (*sensu* Leech and Johnsen, 2003) is likewise unknown.

The potential utility of UV sensitivity to the species also remains unclear, since little is known about the UV reflectance of weakfish predators, conspecifics, and prey. Any potential benefit of increased visual contrast in the ultraviolet channel would presumably be limited by seasonal turbidity that rapidly attenuates UV in the upper 1-3 m of Chesapeake Bay in warmer months (Banaszak and Neale, 2001). However, like most species in this study, weakfish did not evolve under present day Chesapeake Bay optical conditions and are only seasonal inhabitants of this estuary (Murdy *et al.*, 1997). Most overwinter in coastal Mid-Atlantic waters where downwelling UV-A wavelengths may reach 10-15 m (Cohen and Forward, 2002) in sufficient intensity for vision (Losey *et al.*,

1999). Fruitful questions remain on the topics of ultraviolet attenuation in coastal photohabitats, potential mechanism(s) mitigating UV response and its potential utility for weakfish, and the possibility of similar UV responses in other *Cynoscion*.

Combined, our results suggest that the visual systems of these five coastal and estuarine sciaenids appear fairly well-suited to the typical photic conditions of the turbid coastal and estuarine habitats they utilize throughout their range. Turbidity in estuarine systems scatters light, reducing ambient light intensity and degrading contrast, ultimately reducing the distances over which conspecifics, predators, and prey interact (De Robertis *et al.*, 2003; Mazur and Beauchamp, 2003). Paradoxically, many fishes that inhabit productive, turbid ecosystems, such as estuaries, rely on vision to detect their predators, prey, and mates (Abrahams and Kattenfield, 1997; Engström-Östa and Candolin, 2007). Interspecific differences in sensory integration have been demonstrated in sympatric sciaenids (Poling and Fuiman, 1998; Liao and Chang, 2003), suggesting that turbidity may affect species differently. For example, increasing turbidity can force predators to modify their behavior from visual-based foraging strategies to less efficient encounter rate approaches (Grecay and Targett, 1996). Further, human-induced turbidity can also affect mate choice, relax sexual selection, and reduce reproductive isolation in sympatric species (Lake Victoria cichlids: Seehausen *et al.*, 1997).

Optical conditions in Chesapeake Bay have changed dramatically over the past century of industrialization, population expansion, and eutrophication (Kemp *et al.*, 2005), at a pace faster than the evolution of the visual systems of its fauna. Similar anthropogenic changes are likely to be occurring in many coastal ecosystems that serve as key habitats for managed aquatic organisms, where the consequences for predation,

mating, and other activities involving vision have received little attention (McFarland, 1986; Beck *et al.*, 2001; Evans, 2004). In light of increasing anthropogenic degradation, comparative studies that examine the relationships between sensory physiology and behavioral ecology are thus important to mechanistically link processes from the cellular to the individual to the population level to support the management of aquatic resources.

REFERENCES

Abrahams, M. and Kattenfeld, M. (1997). The role of turbidity as a constraint on predator-prey interactions in aquatic environments. *Behav. Ecol. Sociobiol*. **40**, 169-174.

Ali, M. A., and Muntz, W. R. A. (1975). Electroretinography as a tool for studying fish vision. In *Vision in Fishes* (ed M. A. Ali), pp 159-170. New York, NY: Plenum Press.

Arnott, H. J., Maciolek, N. J., and Nichol, J. A. C. (1970). Retinal tapetum lucidum: a novel reflecting system in the eye of teleosts. *Science* **169(3944)**, 478-480.

Arnott, H. J. Nichol. J. A. C., and Querfeld, C. W. (1972). Tapeta lucida in the eyes of the Seatrout (Sciaenidae). *Proc. R. Soc. Lond. B.* **180**, 247-271.

Barry, K. L., and Hawryshyn, C. W. (1999). Spectral sensitivity of the Hawaiian saddle wrasse, *Thallassoma duperrey*, and implications for visually mediated behavior on coral reefs. *Env. Biol. Fishes*. **56**, 429-442.

Banaszak, A. T., and Neale, P. J. (2001). Ultraviolet radiation sensitivity of

photosynthesis in plankton from an estuarine environment. *Limnol. Oceanogr.* **46(3)**, 592-603.

Bayliss, L. E., Lythgoe, J. N., and Tansley, K. (1936). Some forms of visual purple in sea fishes with a note on the visual cells of origin. *Proc. Royal Soc. B.* **120**, 95-114.

Beck, M. W., Heck, K. L., Able, K. W., Childers, D. L., Eggleston, D. B., Gillanders, B. M., Halpern, B., Hays, C. G., Hoshino, K., Minello, T. J., Orth, R. J., Sheridan, P. F., and Weinstein, M. P. (2001). The identification, conservation, and management of estuarine and marine nurseries for fish and invertebrates. *BioSci*. **51(8)**, 633-641.

Boehlert, G. W. (1978). Intraspecific evidence for the function of single and double cones in the teleost retina. *Science* **202**, 309–311.

Bowers, D.G. and Brubaker, J. M. (2004). Underwater sunlight maxima in the Menai Strait. *J. Opt. A: Pure Appl. Opt.* **6 (2004)**, 684–689.

Bowmaker, J. K. (1990). Visual pigments of fishes. In *The visual system of fish* (eds R. H. Douglas and M. B. A.Djamgoz), pp. 82-107. London: Chapman and Hall Ltd.

Brill, R., Magel, C., Davis, M., Hannah, B., and Rankin, P. (2008). Effects of rapid decompression and exposure to bright light on visual function in black rockfish (*Sebastes melanops*) and Pacific halibut (*Hippoglossus stenolepis*). *Fish Bull*. **106**, 427–437.

Browman, H. I. (2005). Applications of sensory biology in marine ecology and

aquaculture. In *Sensory biology: linking the internal and external ecologies of marine organisms*. (eds M. J. Weismann and H. I. Browman) *Mar. Ecol. Prog. Ser.* **287**, 263-307.

Browman, H. I., Novales-Flamarique, I., and Hawryshyn, C. W. (1994). Ultraviolet photoreception contributes to prey search behavior in two species of zooplanktivorous fishes. *J. Exp. Biol.* **186**, 187-198.

Brown, K. T. (1968). The electroretinogram: its components and origins. *Vis. Res*. **8**, 633-677.

Buijse, A. D., Schaap, L. A., Bult, T. P. (1992). Influence of water clarity on the catchability of six freshwater fish species in bottom trawls. *Can. J. Fish. Aquat. Sci*. **49(5)**, 885-893.

Bullock, T. H., Hoffmann, M. H., New, J. G., and Nahm, F. K. (1991). Dynamic properties of visual evoked potentials in the tectum of cartilaginous and bony fishes, with neuroethological implications. *J. Exp. Zool. Suppl*. **5**, 142-255.

Burnham, K.P. and D.R. Anderson. (2002). *Model selection and multimodel inference: a practical information-theoretic approach*. Springer: NY. 488 pp.

Cahill, G. M., and Hasegawa, M. (1997). Circadian oscillators in vertebrate retina photoreceptor cells. *Biol. Signals*. **6**, 191-200.

Champ, M. A., Gould, G. A., Bozzo, W. A., Ackleson, S G., and Vierra, K. C. (1980). Characterization of light extinction and attenuation in Chesapeake Bay, August, 1977. In: Kennedy. V. S. (ed.) *Estuarine perspectives*. Academic Press. New York, p. 262-277.

Chao, L.N., and J. A. Musick, J. A. (1977). Life history, feeding habits, and

functional morphology of juvenile sciaenid fishes in the York River estuary, Virginia. *Fish Bull.* **75(4)**, 657-702.

Clark, R. L. (1936). On the depths at which fishes can see. *Ecology*. **17**, 452-456.

Cohen, J. H. and Forward, R. B. (2002). Spectral sensitivity of vertically migrating marine copepods. *Biol. Bull*. **203**, 307-314.

Collin, S. P. (1997). Specialisations of the teleost visual system: adaptive diversity from shallow-water to deep-sea. *Acta Physio. Scand.* **161(Suppl. 638)**, 5–24.

Crescitelli, F. (1991). The scotopic photoreceptors and their visual pigments of fishes: Functions and adaptations. *Vis. Res*. **31**, 339–348.

Crozier, W. J., Wolf, E. and Zerrahn-Wolf, G. (1936). On critical frequency and critical illumination for response to flickered light. *J. Gen Physiol.* **20**, 211-228.

Crozier, W. J., Wolf, E. and Zerrahn-Wolf, G. (1938). Critical illumination and flicker requency as a function of flash duration: for the sunfish. *J. Gen Physiol.* **21**, 313-334.

Dartnall, H. J. A. (1975). Assessing the fitness of visual pigments for their photic environments. In *Vision in fishes: new approaches in research* (ed M. A. Ali), pp. 159-170. New York, NY: Plenum Press.

Dartnall, H. J. A. and Lythgoe, J. N. (1965). The spectral clustering of visual pigments. *Vis. Res.* **5**, 81-100.

De Robertis, A., Ryer, C. H., Veloza, A., and Brodeur, R. D. (2003). Differential effects of turbidity on prey consumption of piscivorous and planktivorous fish. *Can. J. Fish. Aquat. Sci.* **60**, 1517-1526.

Douglas, R. H., & McGuigan, C. M. (1989). The spectral transmission of freshwater teleost ocular media — an interspecific comparison and a guide to potential ultraviolet sensitivity. *Vision Research*. **29**, 871–879.

Engström-Östa, J. and Candolin, U. (2007). Human-induced water turbidity alters selection on sexual displays in sticklebacks. *Behav. Ecol.* **18(2)**, 393-398.

Evans, B. I. (2004). A fish's eye view of habitat change. In *The senses of fish: adaptations for the reception of natural stimuli*. (eds. G. van der Emde, J. Mogdans, and B. G. Kapoor), pp. 1-30. Boston, MA: Klewer Academic Publishers.

Frank, T. M. (2003). Effects of light adaptation on the temporal resolution of deep-sea crustaceans. *Integr. Comp. Biol.* **43**, 559-570.

Fritsches, K.A., Brill, R. W., and Warrant, E. J. (2005). Warm eyes provide superior vision in swordfishes. *Curr. Biol.* **15**, 55–58.

Gallegos, C. L., Jordan, T. E., Hines, A. H., and Weller, D. E. (2005). Temporal variability of optical propertes in a shallow, eutrophic estuary: seasonal and interannual variability. *Est. Coast. Shelf Sci.* **64**, 156-170.

Govardovskii, V.I., N. Fyhrquist, T. Reuter, D.G. Kuzmin, and K. Donner. (2000). In search of the visual pigment template. *Vis. Neurosci*. **17**, 509–528.

Grecay, P.A., and Targett, T.E. (1996). Spatial patterns in condition and feeding of juvenile weakfish in Delaware Bay. *Trans. Am. Fish. Soc*. **125 (5)**, 803–808.

Guthrie, D. M. and Muntz, W. R. A. (1993). Role of vision in fish behavior. In

Behavior of teleost fishes (ed T. J. Pitcher), 2nd Edition, pp. 89-128. London: Chapman & Hall.

Hall, J. W. (1992). *Handbook of auditory evoked responses*. Allyn and Bacon, Boston MA, U.S.A.

Harding L.W., Jr. (1994). Long-term trends in the distribution of phytoplankton in Chesapeake Bay: roles of light, nutrients and streamflow. *Mar. Ecol. Prog. Ser.* **104**, 267-291.

Hart, N. S., Lisney, T. J., and Collin, S. P. (2006). Visual communication in elasmobranches. In *Communication in fishes* (ed F. Ladich, S. P. Collin, P. Moller, and B. G. Kapoor), pp. 337-392. Enfield, N. H.: Science Publishers,

Horodysky, A.Z., Brill, R. W., Fine, M. L., Musick, J. A., and Latour, R. J. (2008). Acoustic pressure and particle motion thresholds in six sciaenid fishes. *J. Exp. Biol*. **211(9)**, 1504-1511.

Hurlbert, S H. (1984). Pseudoreplication and the design of ecological field experiments. *Ecol Monogr*. **54**, 187-211.

Jerlov, N.G. (1968). *Optical Oceanography*. Pp. 4-9, Elsevier, New York.

Johnsen, S. (2002). Cryptic and conspicuous coloration in the pelagic environment. *Proc. R Soc Lond B* **269**, 243–56.

Jokela, M. Vartio, A., Paulin, L., Fyhrquist-Vanni, N., and Donner, K. (2003). Polymorphism of the rod visual pigment between allopatric populations of the sand goby (*Pomatoschistus minutus*): a microspectrophotometric study. *J. Exp. Biol.* **206**, 2611-2617.

Jokela-Määttä, M., Smura, T. Aaltonen, A., and Ala-Laurila, P. (2007) Visual pigments of Baltic Sea fishes of marine and limnic origin. *Vis. Neurosci.* **24**, 389-398.

Johnson, M. L., Gaten, E., and Shelton, P. M. J. (2002). Spectral sensitivities of five marine decapods and a review of spectral sensitivity variation in relation to habitat. *J. Mar. Biol. Ass. U. K*. **82**, 835-842.

Kaneko, A. and Tachibana, M. (1985). Electrophysiological measurements of the spectral sensitivity of three types of cones in the carp retina. *Jap. J. Physiol.* **35**, 355-365.

Kemp, W. M., Boynton, W. R., Adolf, J. E., Boesch, D. F., Boicourt, W. C., Brush, G., Cornwell, J. C., Fisher, T. R., Glibert, P. M., Hagy, J. D., Harding, L. W., Houde, E. D., Kimmel, D. G., Miller, W. D., Newell, R. I. E., Roman, M. R., Smith, E. M., and Stevenseon, J. C. (2005). Eutrophication of Chesapeake Bay: historical trends and ecological interactions. *Mar. Ecol. Progr. Ser.* **303**, 1-29.

Leech, D. and Johnsen, S. (2003). Avoidance and UV vision. Pp. 455-484 In *UV Effects in Aquatic Organisms and Ecosystems*, (W. Helbling, H. Zagarese eds.), Royal Society of Chemistry, London.

Leech, D. M. and Johnsen, S. (2006). Ultraviolet vision and foraging in juvenile bluegill (*Lepomis macrochirus*). *Can. J. Fish. Aquat. Sci*. **63**: 2183-2190.

Levine, J. S. and MacNichol, E. F. (1979). Visual pigments in teleost fishes: effects of habitat, microhabitat, and behavior on visual system evolution. *Sens. Proc*. **3**, 95-131.

Liao, I. C., and Chang, E. Y. (2003). Role of sensory mechanisms in predatory feeding behavior of juvenile red drum *Sciaenops ocellatus*. *Fish. Sci*. **69(2)**, 317-322.

Littell, R.C., G. A. Milliken, W. W. Stroup, R.D. Wolfinger, and O. Schabenberger. (2006). *SAS for mixed models, 2nd Edition*. 814 Pp. Cary, N.C., U.S.A.: SAS Institute.

Loew, E. R. and Lythgoe, J. N. (1978). The ecology of cone pigments in teleost fishes. *Vis. Res*. **18**, 715-722.

Loew, E.R. and W.N. McFarland. (1990). The underwater visual environment. In: *The visual system of fish* (eds. R. H. Douglas and M. B. A. Djamgoz), pp. 3-43. London: Chapman and Hall Ltd.

Losey, G. S., Cronin, T. W., Goldsmith, T. H., Hyde, D., Marshall, N. J., and McFarland, W. N. (1999). The UV visual world of fishes: a review. *J. Fish Biol.* **54**, 921-943.

Losey, G. S., McFarland, W. N., Loew, E. R., Zamzow, J. P., Nelson, P. A., and Marshall, N. J. (2003). Visual biology of Hawaiian coral reef fishes. I. Ocular transmission and visual pigments. *Copeia* **2003(3)**, 433-454.

Murdy, E.O., R.S. Birdsong, and J.A. Musick. (1997). *Fishes of Chesapeake Bay*. Smithsonian Institution Press, Washington, D.C. 324 pp.

Lythgoe, J. N. (1968). Visual pigments and visual range underwater. *Vis. Res*. **8**, 997–1012.

Lythgoe, J. N. (1975) Problems of seeing colours under water. In, *Vision in fishes: new approaches in research*. (ed M. A. Ali), pp. 619–634. New York, NY: Plenum Press.

Lythgoe, J. N. (1979). *Ecology of Vision*. Clarendon Press, Oxford.

Lythgoe, J. N. (1984). Visual pigments and environmental light. *Vis. Res.* **24**, 1539-1550.

Lythgoe, J. N. (1988) Light and vision in the aquatic environment. In: *Sensory biology of aquatic animals* (ed J. Atema, R. R. Fay, A. N. Popper, W. N. Tavolga), pp. 131–149. New York,NY: Springer-Verlag.

Lythgoe, J. N. and Partridge, J. C. (1991). The modeling of optimal visual pigments of dichromatic teleosts in green coastal waters. *Vis. Res.* **31(3)**, 361-371.

Lythgoe, J. N., Muntz, W. R. A., Partridge, J. C., Shand, J., and Williams, D. M. (1994). The ecology of the visual pigments of snappers (Lutjanidae) on the Great Barrier reef. *J. Comp. Physiol.* **174**, 461-467.

Makhankov, Y. V., Rinner, O., and Neuhauss, S. C. F. (2004). An inexpensive device for non-invasive electroretinography in small aquatic vertebrates. *J. Neurosci. Meth*. **153**, 205-210.

Mangel, S. C. (2001). Circadian clock regulation of neuronal light responses in the vertebrate retina. *Prog. Brain Res*. **131**, 505-518.

Marshall, N.J., Jennings, K., McFarland, W. N., Loew, E. R., and Losey, G. S. (2003). Visual biology of Hawaiian coral reef fishes. III. Environmental light and an integrated approach to the ecology of reef fish vision. *Copeia*. **2003(3)**: 467-480.

Mazur, M. M, and Beauchamp, D. A. (2003). A comparison of visual prey detection among species of piscivorous salmonids: effects of light and low turbidities. *Env. Biol. Fish.* **67(4)**, 397-405.

McFarland, W. N. (1986). Light in the sea – correlations with behaviors of fishes and invertebrates. *Amer. Zool.* **26(2)**, 389-401.

McFarland, W. (1991). Light in the sea: the optical world of elasmobranchs. *J. Exp. Zool. Suppl.* **5**, 3-12.

McFarland, W. N. and Loew, E. R. (1983). Wave produced changes in underwater light and their relations to vision. Env. Biol. Fish. **8(3-4)**,173-184.

McFarland, W. N. and Munz, F. W. (1975). Part III: The evolution of photopic visual pigments in fishes. *Vis. Res*. **15**, 1071-1080.

McMahon, D. G., and Barlow, R. B. (1992). Electroretinograms, eye movements, and circadian rhythms. *J. Gen. Physiol*. **100**, 155-169.

Munz, F.W. (1977). Evolutionary adaptations of fishes to the photic environment. In *Handbook of sensory physiology.* Vol. VII/5 (ed F. Crescitelli) Berlin: Springer-Verlag.

Murdy, E. O., Birdsong, R. S., and Musick, J. A. (1997). *Fishes of Chesapeake Bay*, pp. 324. Washington, DC: Smithsonian Institution Press.

Myers, G.S. (1960). Restriction of the croakers (Sciaenidae) and anchovies (Engraulidae) to continental waters. *Copeia*, 1960(1), 67-68.

Naka, K. I., and Rushton, W. A. H. (1966). S-potentials from colour units in the retina of fish (Cyprinidae). *J. Physiol*. **185**, 536-555.

Pankhurst, N. W. and Mongomery, J. C. (1989). Visual function in four Antarctic nototheniid fishes. *J. Exp. Biol.* **142**, 311-324.

Parkyn, D. C. and Hawryshyn, C. W. (2000). Spectral and ultraviolet-polarization

sensitivity in juvenile salmonids: a comparative analysis using electrophysiology. *J. Exp. Biol.* **203**: 1173-1191.

Poling, K. R. and Fuiman, L. A. (1997). Sensory development and concurrent behavioural changes in Atlantic croaker larvae. *J. Fish. Biol.*. **51(6)**, 402-421.

Poling, K. R. and Fuiman, L. A. (1998). Sensory development and its relation to habitat change in three species of sciaenids. *Brain, Behav. Evol.* **52(6)**, 270-284.

R development core team. (2008). R: a language and environment for statistical computing. R Foundation for Statistical Computing, Vienna, Austria.

Saszik, S. and Bilotta, J. (1999). The effects of temperature on the dark-adapted spectral sensitivity function of the adult zebrafish. *Vis. Res.* **39**, 1051-1058.

Schubert, H., Sagert, S., and Forster, R. M. (2001). Evaluation of the different levels of variability in the underwater light field of a shallow estuary. *Helgol. Mar. Res.* **55(1)**, 12-22.

Seehausen, O., van Alphen, J. J. M., and Witte, F. (1997). Cichlid fish diversity threatened by eutrophication that curbs sexual selection. *Science* **277**, 1808-1811.

Siebeck, U. E., Losey, G. S., and Marshall, J. (2006). UV communication in fish. In *Communication in fishes* (eds, F. Ladich, S. P. Collin, P. Moller and B. G. Kapoor), pp. 337-392. Enfield, N. H.: Science Publishers,

Stavenga, D.G., Smits, R.P., and Hoenders, B. J. (1993). Simple exponential functions describing the absorbance bands of visual pigment spectra. *Vis. Res.* **33(8)**, 1011-1017.

Underwood, A. J. (2002). *Experiments in ecology: their logical design and interpretation using analysis of variance*. P. 385-418. New York, NY: Cambridge University Press.

Walls, G. L. (1942). *The vertebrate eye and its adaptive radiation*. Hafner Publishing Co, NY.

Wang, Y. and Mangel, S. C. (1996). A circadian clock regulates rod and cone input to fish retinal cone horizontal cells. *Proc. Nat. Acad. Sci. USA* **93**, 4655-4660.

Warrant, E. J. (1999). Seeing better at night: life style, eye design, and the optimum strategy of spatial and temporal summation. *Vis. Res.* **39**, 1611-1630.

Warrant, E. J. (2000). The eyes of deep-sea fishes and the changing nature of visual scenes with depth. *Proc. Royal Soc. B.* **355(1401)**, 1155-1159.

Weissburg, M. J. (2005). Introduction. In *Sensory Biology: Linking the internal and external ecologies of marine organisms* (eds. M. J. Weissburg and H. I. Browman), *Mar. Ecol. Progr. Ser.* **287**, 263-265.

Table 1 – Species, sample size, standard length (SL), and mass of the five sciaenid fishes investigated in this study.

Species	*n*	SL (mm)	Mass (g)
Cynoscion regalis	6	190-289	100-280
Cynoscion nebulosus	6	278-560	220-755
Sciaenops ocellatus	6	291-378	460-1020
Micropogonias undulatus	6	223-393	140-890
Leiostomus xanthurus	6	70-270	60-215

Table 2 – Parameter estimates and model rankings of SSH (Stavenga *et al.*, 1993) and GFRKD (Govardovskii *et al.*, 2000) vitamin A1 rhodopsin templates fitted to sciaenid photopic spectral ERG data via maximum likelihood. The character "p" refers to the number of parameters in a model, "Di" = dichromatic, "Tri" = trichromatic. The character "α" indicates scenarios where only alpha bands were considered. The letters "S", "L", and "B" following the character "β" illustrate the modeled position of β-band(s) on short, long, or both pigments. The number following $\lambda_{max,1}$ refers to pigment 1, etc. Monochromatic conditions were very unlikely, demonstrating extremely poor fits given our data (ΔAIC values > 110), and were thus omitted from this table.

Species	Condition	Template	$\lambda_{max,1}$	$\lambda_{max,2}$	$\lambda_{max,3}$	-log(L)	p	AIC	ΔAIC
Weakfish	Di, α	GFRKD	428	524	-	-62.2	5	-114	72
		SSH	445	530	-	-56.0	5	-102	84
	Di, β, S	GFRKD	443	529	-	-59.3	6	-107	79
		SSH	456	532	-	-91.8	6	-172	14
	Di, β, L	GFRKD	454	530	-	-94.7	6	-177	9
		SSH	**459**	**532**	**-**	**-98.9**	**6**	**-186**	**0**
	Di, β, B	GFRKD	459	531	-	-72.1	7	-130	56
		SSH	472	532	-	-91.4	7	-169	17
	Tri, α	GFRKD	453	531	368	-91.2	7	-168	17
		SSH	456	532	369	-93.5	7	-173	13
Spotted seatrout	Di, α	**GFRKD**	**450**	**542**	**-**	**-69.8**	**5**	**-130**	**0**
		SSH	451	542	-	-64.7	5	-119	10
	Tri, α	GFRKD	450	542	502	-69.8	7	-126	4
		SSH	455	540	468	-64.9	7	-116	14
Red drum	Di, α	GFRKD	457	555	-	-65.0	5	-120	8
		SSH	459	556	-	-61.2	5	-112	16
	Tri, α	**GFRKD**	**444**	**564**	**489**	**-71.1**	**7**	**-128**	**0**
		SSH	448	564	493	-66.0	7	-118	10
Atlantic croaker	Di, α	GFRKD	454	545	-	-67.4	5	-125	45
		SSH	457	546	-	-66.3	5	-123	47
	Tri, α	GFRKD	**430**	**562**	**484**	**-92.0**	**7**	**-170**	**0**
		SSH	437	562	486	-87.9	7	-162	8
Spot	**Di, α**	**GFRKD**	**450**	**546**	**-**	**-86.1**	**5**	**-162**	**0**
		SSH	451	547	-	-82.4	5	-155	7
	Tri, α	GFRKD	450	547	499	-86.1	7	-158	4
		SSH	445	548	466	-83.0	7	-152	10

Figure 1. Conceptual diagram of the microhabitat specialization of the five sciaenid fishes examined in this study (*sensu* Chao and Music, 1977; Murdy *et al.*, 1997). Weakfish (A) are crepuscular/nocturnal predators of small pelagic crustaceans and fishes in the Chesapeake Bay mainstem and deeper waters. Spotted seatrout (B) are predators of small crustaceans and fishes in shallow seagrass habitats. Red drum (C) prey on invertebrates and fishes in marsh, seagrass, and oyster reef habitats. Atlantic croaker (D) and spot (E) forage on a suite of small crustacean, polychaete, and bivalve prey in sand and mud bottoms throughout the Chesapeake Bay mainstem and tributaries. All are seasonal residents of Chesapeake Bay.

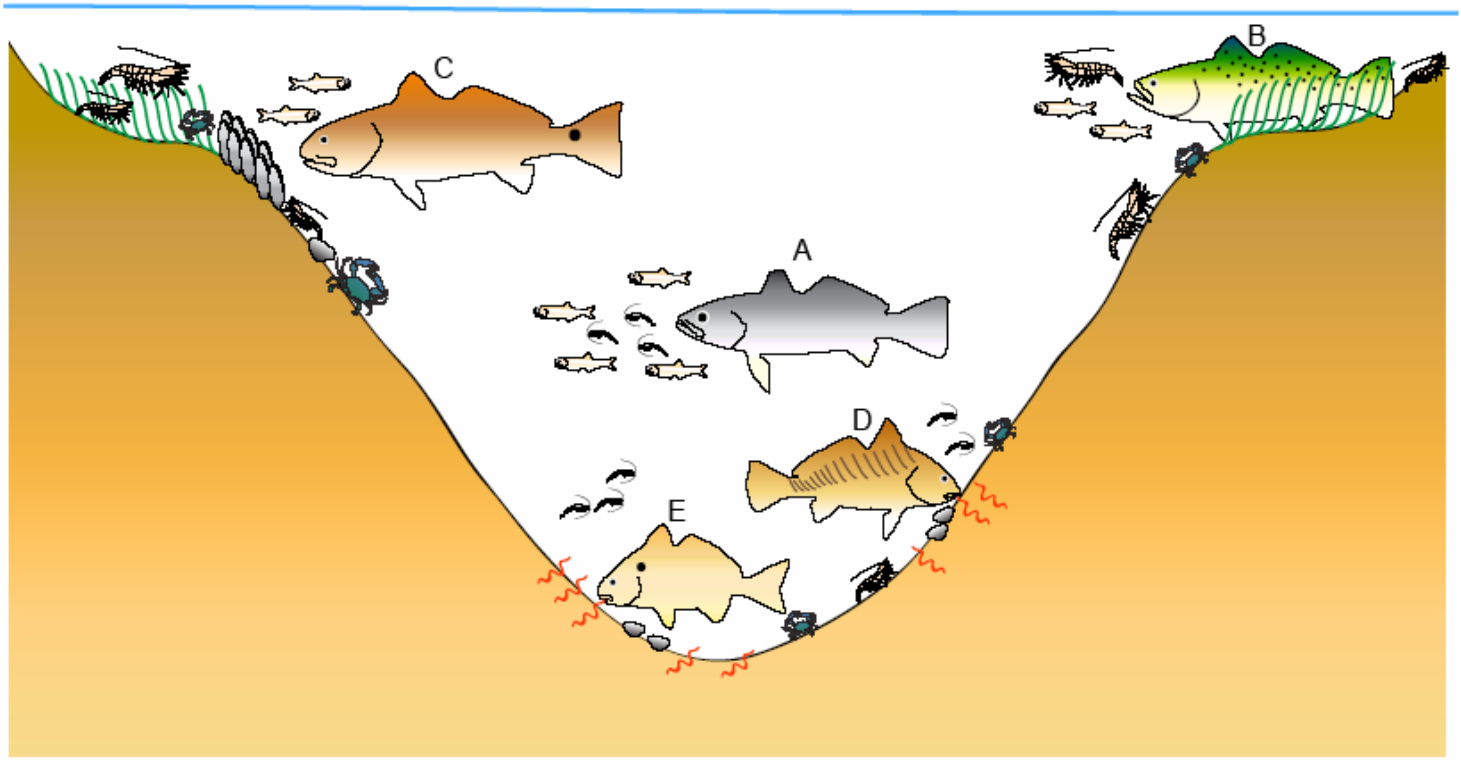
C
B
A
D
E

Figure 2. Intensity-response electroretinograms (ERGs) of weakfish, spotted seatrout, red drum, Atlantic croaker, and spot. Each species' intensity response curve is an average of six individuals. Responses were normalized to the maximal response voltage (V_{max}) for each individual. Shaded boxes represent each species' dynamic range (5-95% V_{max}), numbers at the top indicate its breadth (in log units). Dashed drop lines and adjacent numbers indicate K_{50} points (illumination at 50% V_{max}). Open symbols and white text represent day experiments, filled symbols and black text represent night experiments. Light intensities are in log candela m^{-2}. Error bars are ± 1 SE.

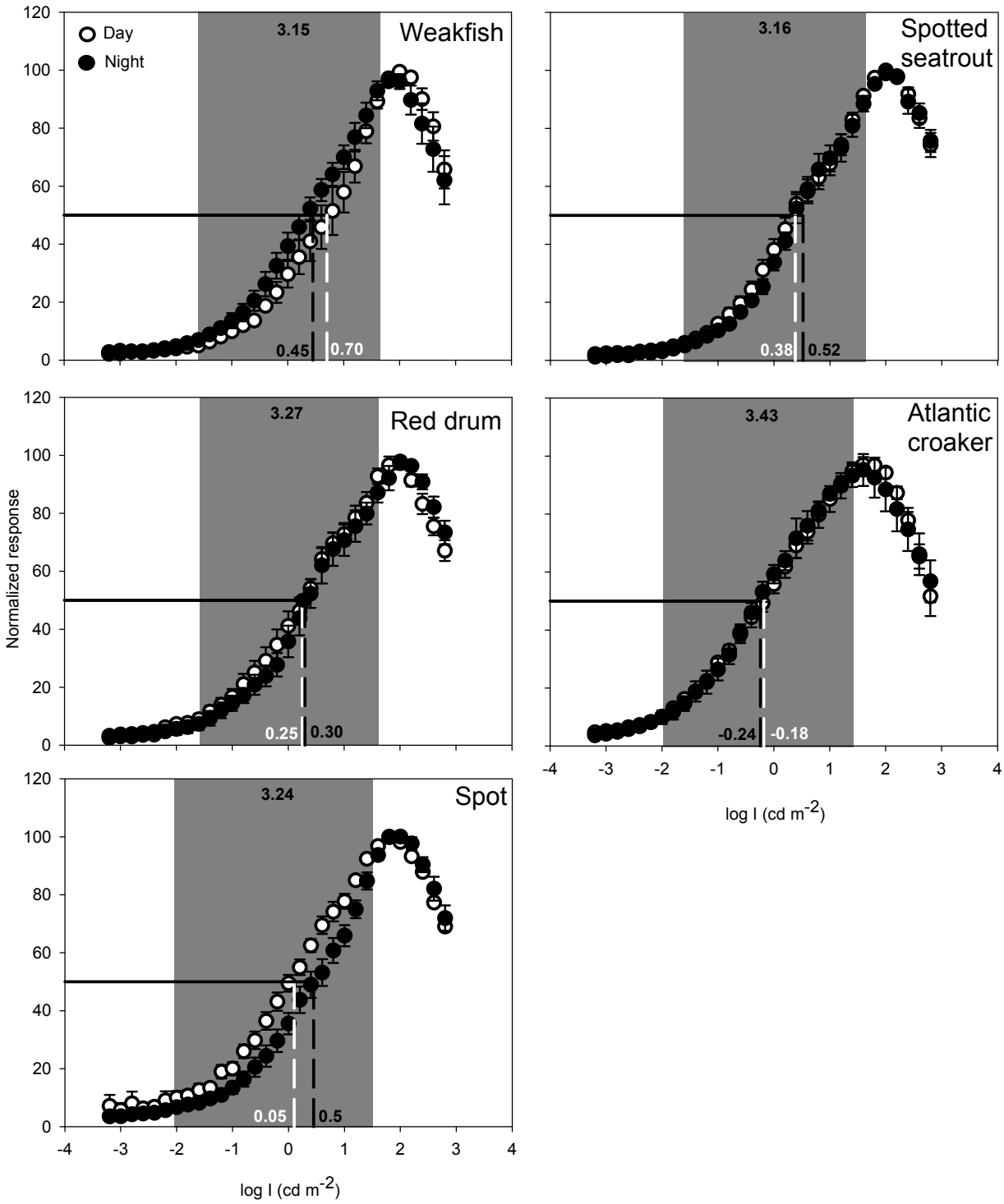
Day
Night
Weakfish
3.15
0.45
0.70
Spotted seatrout
3.16
0.38
0.52
Red drum
3.27
0.25
0.30
Atlantic croaker
3.43
-0.24
-0.18
Spot
3.24
0.05
0.5
Normalized response
log I (cd m-2)
log I (cd m-2)

Figure 3. Mean flicker fusion frequency (FFF) values for five sciaenid fishes. Open symbols represent day experiments, filled symbols represent night experiments. Error bars are ± 1 SE. Triangles represent the FFF at maximum stimulus intensity (I_{max}). Circles represent FFF at I_{25} (light levels 25% of I_{max}). We considered I_{25} to be a proxy for ambient environmental light intensity.

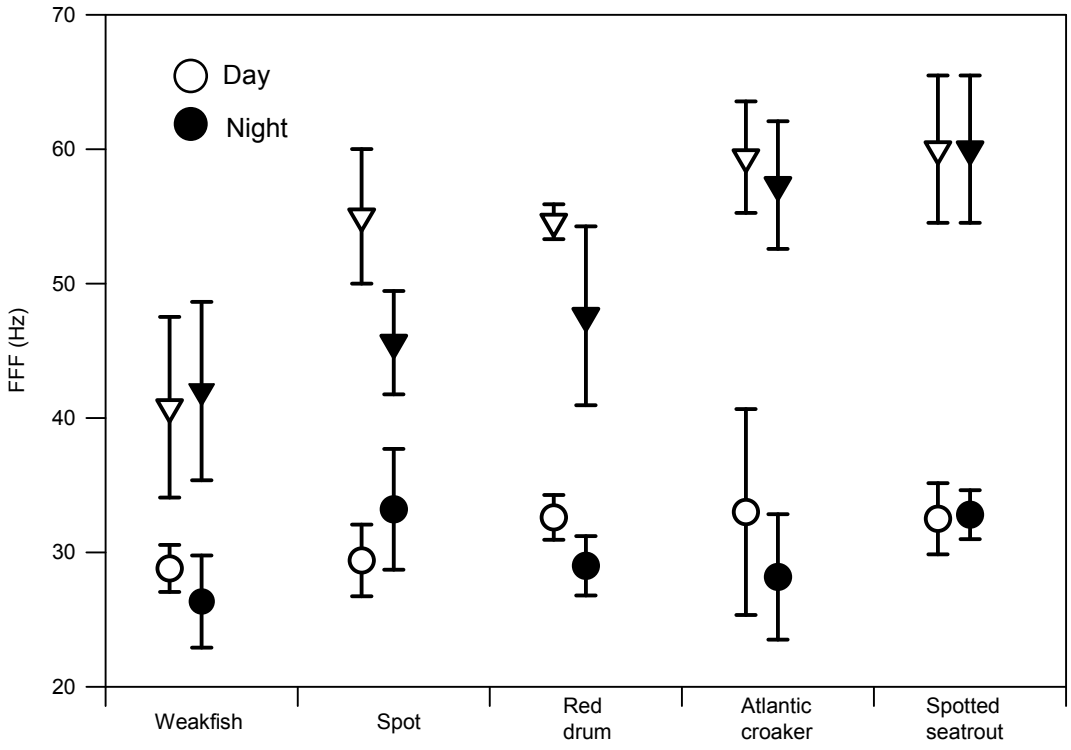
70
60
50
40
30
20
FFF (Hz)
Day
Night
Weakfish
Spot
Red drum
Atlantic croaker
Spotted seatrout

Figure 4. Spectral sensitivity curves calculated from the electroretinograms (ERGs) of weakfish, spotted seatrout, red drum, Atlantic croaker, and spot for wavelengths of 300-800 nm. Each species' curve is an average of six individuals. Responses at each wavelength were normalised to the wavelength of maximal voltage response (V_{max}) for each individual. Open symbols represent day experiments, filled symbols represent night experiments. Error bars are ± 1 SE.

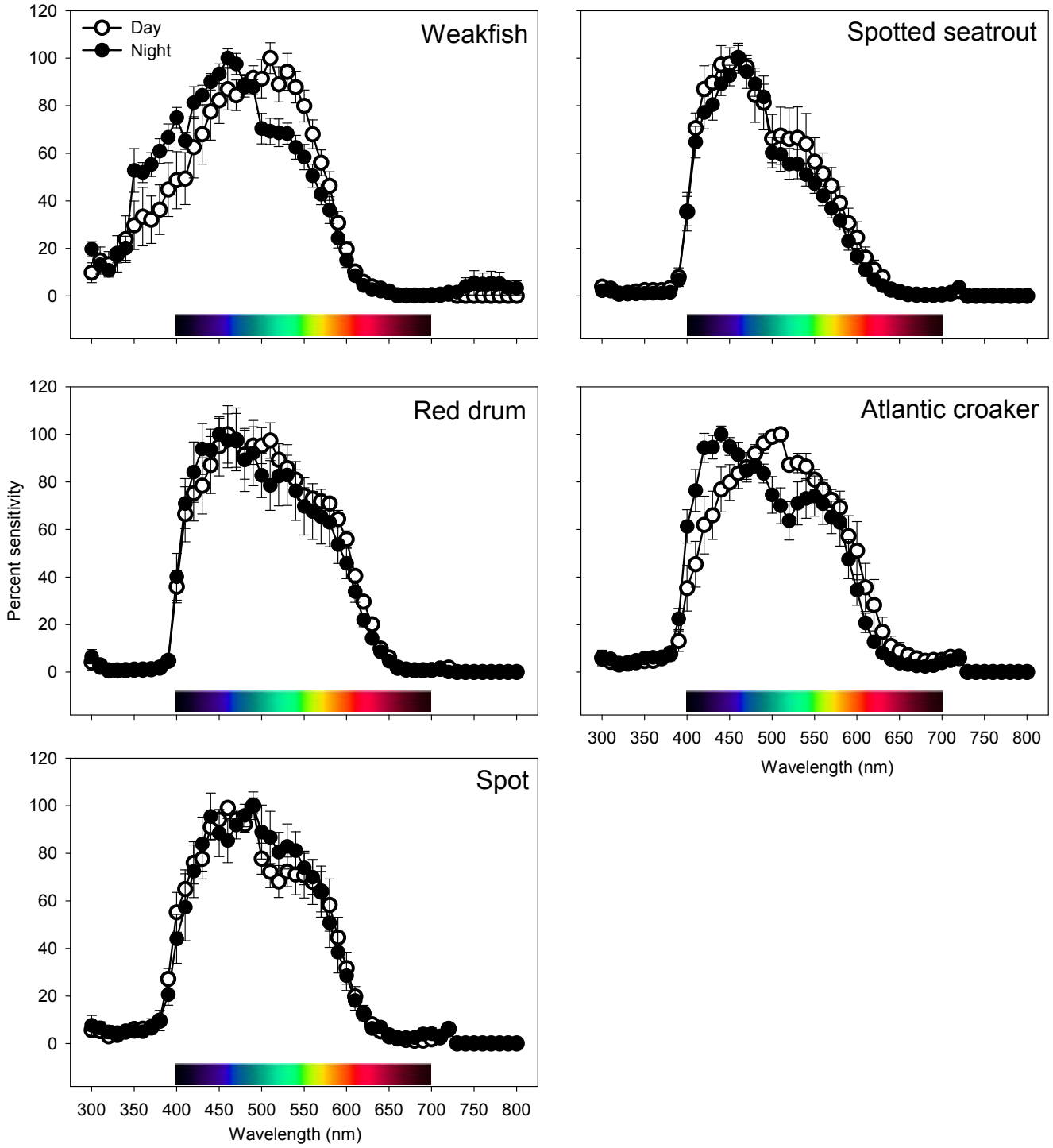
Day
Night
Weakfish
Spotted seatrout
Red drum
Atlantic croaker
Spot
Percent sensitivity
Wavelength (nm)
0
20
40
60
80
100
120
300
350
400
450
500
550
600
650
700
750
800

Figure 5. Diel differences in spectral electroretinograms (ERGs) of weakfish, spotted seatrout, red drum, Atlantic croaker, and spot. Differences were calculated by subtracting the day spectral responses (R_{day}) from night responses (R_{night}). Thin grey lines are ± 95% CI, calculated as 1.96 (s.e.m). Values above the horizontal zero line (i.e. positive) indicate wavelengths of greater response during daylight, those below the zero line (i.e. negative) indicate wavelengths of greater nocturnal response. Significant differences occurred when CI did not encompass zero.

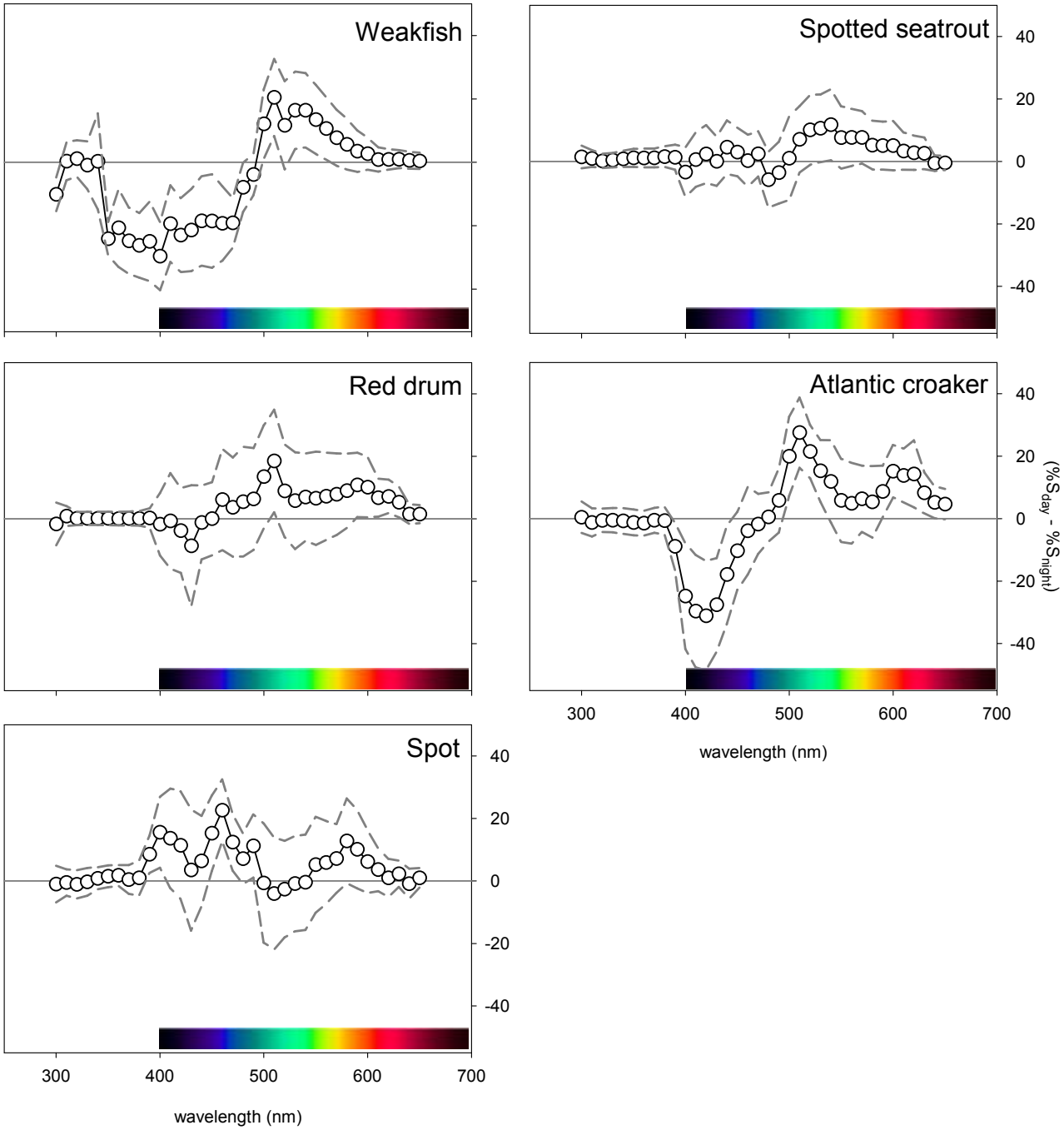
Weakfish
Spotted seatrout
Red drum
Atlantic croaker
Spot
40
20
0
-20
-40
300
400
500
600
700
wavelength (nm)
(%S_day - %S_night)

Figure 6. Differences in spectral electroretinograms of weakfish and spotted seatrout, calculated by subtracting the weakfish spectral responses ($R_{weakfish}$) from those of spotted seatrout ($R_{spotted\ seatrout}$). Open symbols represent day values, filled symbols represent night values. Thin grey lines are ± 95% CI, calculated as 1.96*SE. Significant differences occurred when CI did not encompass zero.

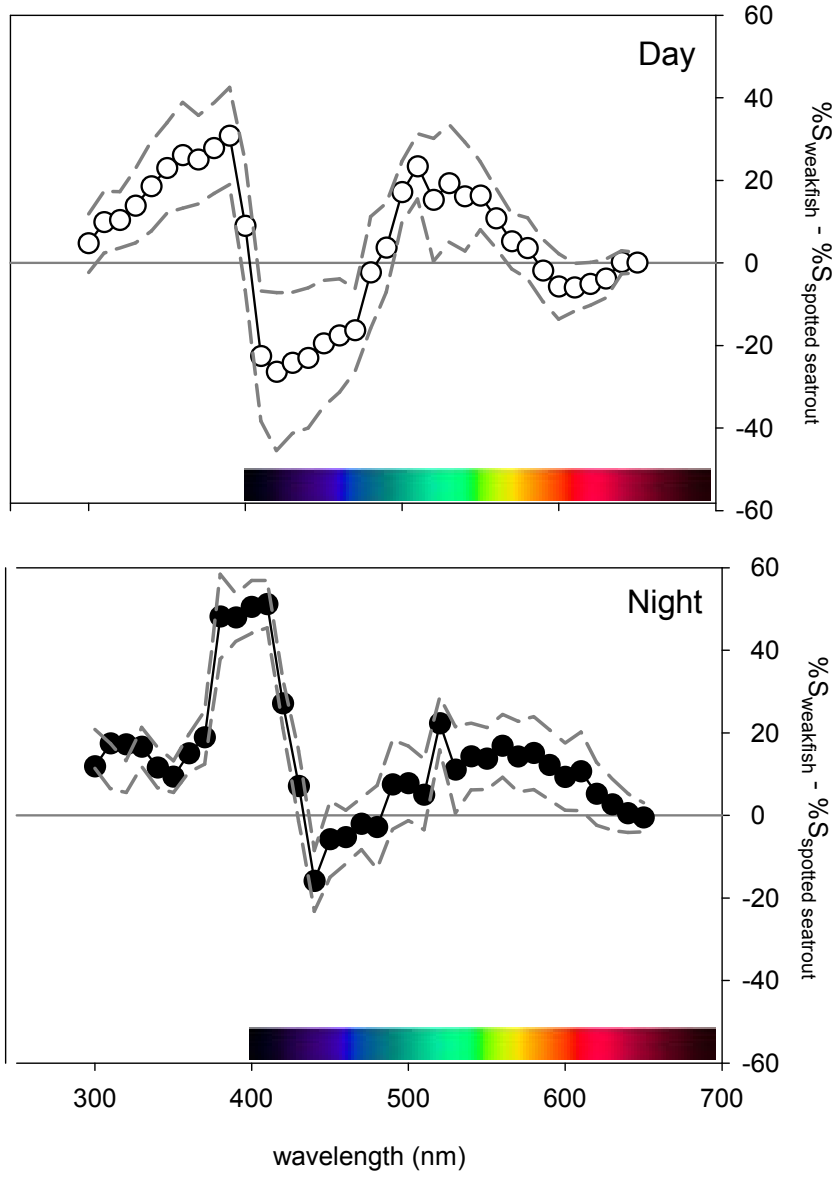
Day
Night
60
40
20
0
-20
-40
-60
%S weakfish - %S spotted seatrout
300
400
500
600
700
wavelength (nm)

Figure 7. SSH (Stavenga *et al.*, 1993) and GFRKD (Govardovskii *et al.*, 2000) vitamin A1 templates fitted to sciaenid spectral ERD data by maximum likelihood. Only estimates from best fitting models from Table 2 were plotted for each species. Values to the right of each pigment label are estimated λ_{max} and pigment specific weight as estimated by the model. P1 (blue) is the short wavelength pigment, P2 (yellow) is the long wavelength pigment, and P3 (where applicable) is the intermediate pigment. Black lines represent additive curves developed by summing the product of each curve weighted by the estimated weighting factor. For weakfish, β refers to the estimated peak of the P2 β-band.

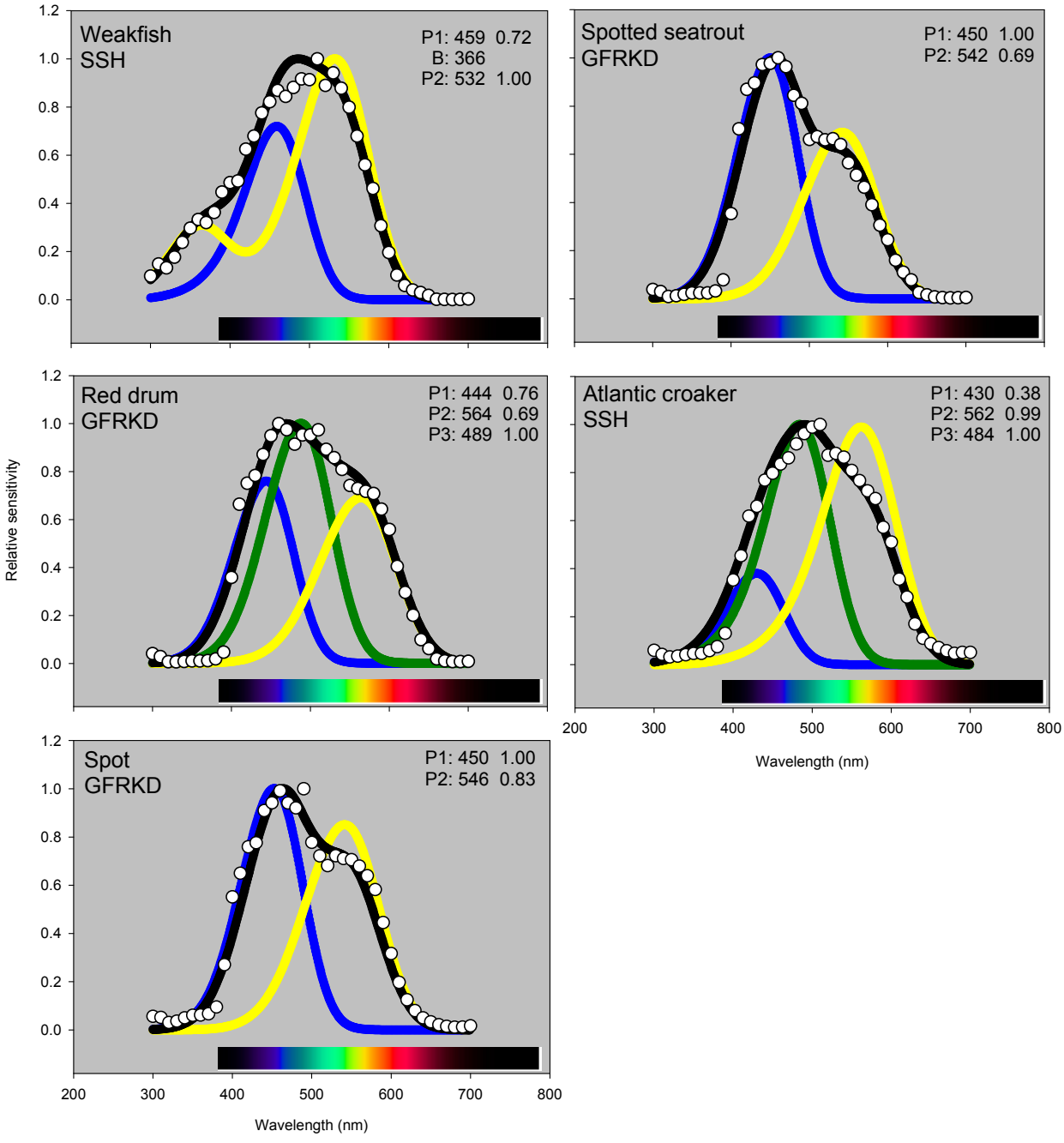
Weakfish
SSH
P1: 459 0.72
B: 366
P2: 532 1.00
Spotted seatrout
GFRKD
P1: 450 1.00
P2: 542 0.69
Red drum
GFRKD
P1: 444 0.76
P2: 564 0.69
P3: 489 1.00
Atlantic croaker
SSH
P1: 430 0.38
P2: 562 0.99
P3: 484 1.00
Spot
GFRKD
P1: 450 1.00
P2: 546 0.83
Relative sensitivity
Wavelength (nm)
0.0
0.2
0.4
0.6
0.8
1.0
1.2
200
300
400
500
600
700
800

Figure 8. Relative spectral transmission of the cornea, vitreous humor, and lens of weakfish (*n*=2) and Atlantic croaker (*n*=3) demonstrating that UV-A wavelengths (350-380 nm) are transmitted by all three optical tissues in weakfish, but appear to be absorbed by the lens of croaker. Optical tissues of spotted seatrout, red drum, and spot followed the croaker pattern, absorbing strongly below 380 nm.

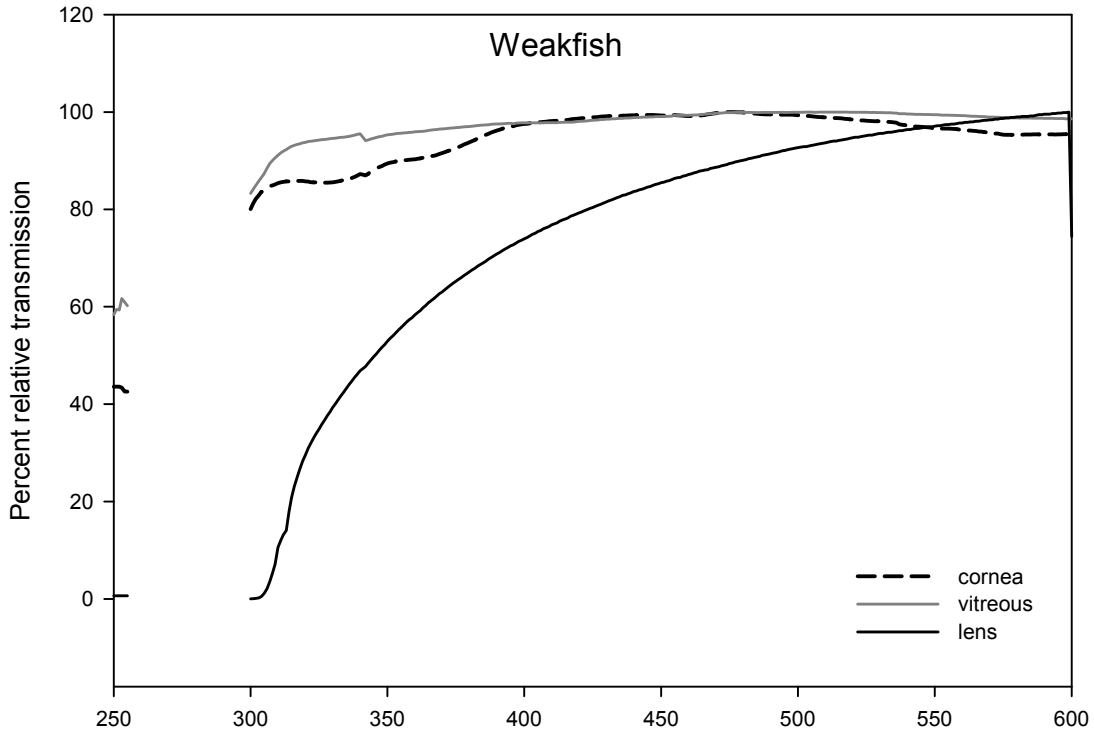
Weakfish
Percent relative transmission
120
100
80
60
40
20
0
250
300
350
400
450
500
550
600
cornea
vitreous
lens

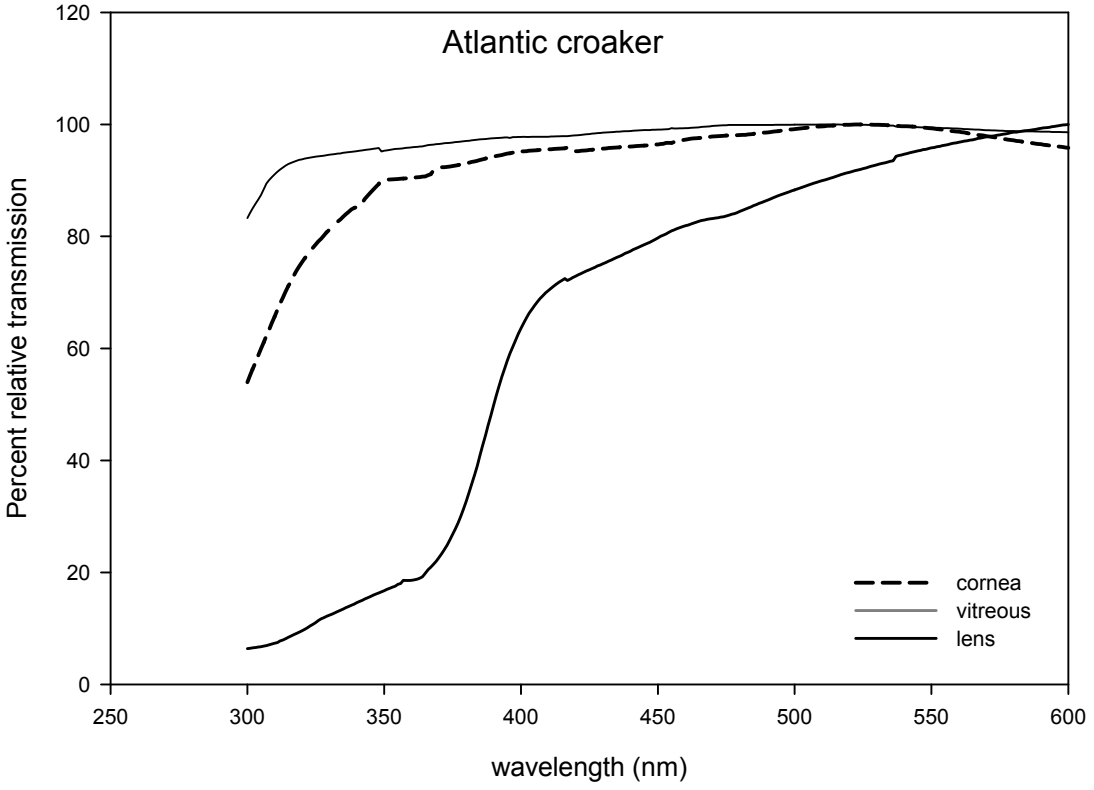
Atlantic croaker
Percent relative transmission
120
100
80
60
40
20
0
250
300
350
400
450
500
550
600
wavelength (nm)
cornea
vitreous
lens

CHAPTER 3: COMPARATIVE VISUAL FUNCTION IN FOUR PISCIVOROUS FISHES INHABITING CHESAPEAKE BAY

INTRODUCTION

Waters of different properties differentially scatter and absorb downwelling light, affecting its spectral bandwidth (color) and intensity (brightness). Pure natural waters and clear pelagic seas maximally transmit short wavelength (blue) light, whereas coastal waters are most deeply penetrated by intermediate (green) wavelengths. Estuarine and many fresh waters maximally transmit longer (yellow-red) wavelengths due to increasing concentrations of phytoplankton, yellow products of vegetative decay (*Gelbstoffe*), and suspended particulates that scatter, absorb, and more rapidly attenuate light (Lythgoe, 1975; Lythgoe, 1988; Jerlov, 1968). Fishes radiated into a wide range of aquatic photohabitats possessing complex photic properties, exposing their visual systems to a myriad of selective pressures (Levine and MacNichol, 1979; Collin, 1997). The visual systems of fishes have thus evolved to generally reflect the characteristics of aquatic light fields in their specific micro- and macrohabitats (Guthrie and Muntz, 1993).

Estuarine and nearcoastal waters represent some of the most dynamic aquatic photohabitats on Earth. Luminous and chromatic properties of these waters vary on temporal and spatial scales ranging from milliseconds to decades and millimeters to kilometers (McFarland and Loew, 1983; Gallegos *et al.*, 2005; Kemp et al., 2005). This extensive variability is due to vertical mixing, stratification, wave activity, clouds and weather, sunrise and sunset, seasonal solar irradiance, phytoplankton dynamics, as well

as anthropogenically-induced processes such as eutrophication and sedimentation (Harding, 1994; Schubert *et al.*, 2001). Finally, at midday, a fixed point in an estuary can range widely in luminous and chromatic properties due to tidal and freshwater inputs along salinity gradients. Flood tides push relatively well-lit green coastal waters into estuaries, while falling ebb tides draw highly-attenuating, turbid riverine waters through the estuary and out to sea (Bowers and Brubaker, 2004).

The visual systems of fishes inhabiting highly productive and frequently turbid neritic waters must balance sensitivity, resolution, contrast perception, and rapid adaptation to dynamic light conditions depending on evolutionary pressures and phylogenetic constraints (Dartnall, 1975; Levine and MacNichol, 1979). The eyes of diurnal predatory fishes typically use rod photoreceptors during scotopic (dim/dark) conditions and cone photoreceptors under photopic (bright) conditions, the latter potentially differing in their number, the pigments they contain, and their spectral position depending on phylogeny, species' lifestyle, and optical microhabitat (Lythgoe, 1979; Crescitelli, 1991; Levine and MacNichol, 1979). At the cost of acuity, luminous sensitivity can be extended under dim conditions by widening pupils, increasing spatial and temporal summation, and even reradiating light through retinal media to maximize photon capture (Warrant, 1999). However, unavoidable tradeoffs between sensitivity and resolution limit the plasticity of optical responses to widely-ranging photic conditions (Warrant, 1999).

Many shallow-dwelling piscivores have large, broadly-tuned, and highly resolute eyes, foraging visually when light is not limiting because a wider breadth of information is rapidly available through this sensory channel relative to other modalities (Hobson et

al., 1981; Guthrie and Muntz, 1993; Rowland, 1999). Paradoxically, many fishes that inhabit productive, but turbid estuaries rely on vision to detect their predators, prey, and mates (Abrahams and Kattenfield, 1997; Engström-Östa and Candolin, 2007). The visual range of fishes is constrained when the luminous and chromatic properties of light are limiting due to changing diel light conditions or via scattering and absorption by suspended materials. Degradation of optical conditions affects predators and prey asymmetrically. Mild turbidity may enhance prey contrast, but piscivory is inhibited under adverse optical conditions via the reduction of ambient light intensity and contrast degradation, with the ultimate effect of decreasing effective visual fields and increasing search time (Vogel and Beauchamp, 1999; Utne-Palm, 2002). Simultaneously, turbidity enhances cover and foraging opportunities for planktivorous species that are released from predation by piscivores (i.e., 'Turbidity as Cover Hypothesis'; Gregory and Northcote, 1993). Piscivores may therefore be forced to abandon visual foraging for less-efficient encounter-rate feeding and to shift from pelagic to benthic prey when optical conditions are greatly degraded (Grecay and Targett, 1996; De Robertis et al., 2003). Such foraging shifts may tip the competitive predatory balance in an ecosystem from visually-feeding piscivores to tactile and chemoreceptive foragers, with potentially cascading effects (Carpenter and Kitchell, 1993; Asknes and Utne, 1997). Additionally, degradation of the chromatic and luminous properties of light fields can affect the distribution and movements of predatory fishes (McFarland, 1986), inter- and intraspecific communication (Siebeck et al., 2006), reproductive habits and speciation (Seehausen et al., 1997), as well as vulnerability to fishing gear (Loesch et al., 1982; Walsh, 1991; Buijse et al., 1992).

In summary, because predation by visually-foraging piscivorous fishes can affect the structure and function of aquatic communities (Paine, 1966; Northcote, 1988), changes in the visual environment may thus have far reaching effects on coastal ecosystems and their management through light-induced changes in picscivore behavior (Asknes, 2007). However, visual function of coastal piscivorous fishes has received fairly little attention despite their importance to both commercial and recreational fisheries. We therefore used corneal electroretinography (ERG) to assess the absolute sensitivities, temporal properties, and chromatic sensitivities of four piscivores common to coastal waters of the western North Atlantic. Optical conditions in key mid-Atlantic estuaries such as Chesapeake Bay have changed dramatically over the past century due to industrialization, population expansion, eutrophication, and sedimentation (Jackson, 2001; Kemp et al., 2005), with unknown consequences for predation, mating, and other activities involving vision because so little is known of the visual function of this estuary's diverse fish fauna. A previous investigation of fish visual ecophysiology (Horodysky et al., 2008) applied comparative methods to assess the visual function in five phylogenetically-related fishes that use different optical microhabitats in Chesapeake Bay. Using the same experimental setup and methods, we investigate the converse question, assessing the visual systems of four coastal western North Atlantic piscivores with different phylogenies that use similar microhabitats, bear similar trophic ecologies, or both (Fig. 1). We seek mechanistic insights into how biotic and abiotic processes influence relationships between form, function, and the environment in the visual systems of coastal marine fishes.

METHODS

Striped bass (*Morone saxatilis* Walbaum, 1792), bluefish (*Pomatomus saltatrix* Linnaeus, 1766), summer flounder (*Paralichthys dentatus* Linnaeus, 1766), and cobia (*Rachycentron canadum* Linnaeus, 1766) were all captured by standard hook and line fishing gear. Animals were maintained in recirculating 1855 L aquaria on natural ambient photoperiods at 20°C ± 1°C (winter) or 25°C ± 2°C (summer). Fish were fed a combination of frozen Atlantic menhaden (*Brevoortia tyrannus*), squid (*Loligo* sp.), and commercially-prepared food (AquaTox flakes; Zeigler, Gardners, PA, USA).

Experimental and animal care protocols were approved by the College of William and Mary's Institutional Animal Care and Use Committee (protocol no. 0423) and followed all relevant laws of the United States. Fish were removed from holding tanks, sedated with an intramuscular (IM) dose of ketamine hydrochloride (Butler Animal Health, Middletown, PA, USA; 30 mg kg^{-1}), and immobilized with an IM injection of the neuromuscular blocking drug gallamine triethiodide (Flaxedil; Sigma, St. Louis, MO., USA; 10 mg kg^{-1}). Drugs were readministered during the course of experiments as required. Following initial drug injections, fish were moved into a light-tight enclosure and placed in a rectangular 800 x 325 x 180 mm Plexiglas tank with only a small portion of the head and eye receiving the light stimulus remaining above the water. Subjects were ventilated with filtered and oxygenated sea water (1 L min^{-1}) that was temperature-controlled (20 ± 2°C) to minimize the potential confounding effects of temperature on

ERG recordings (Saszik and Bilotta, 1999; Fritsches *et al.*, 2005). Fish were dark adapted for at least 30 min prior to any measurements.

Experiments were conducted during both day and night to account for any circadian rhythms in visual response (McMahon and Barlow 1992; Cahill and Hasegawa 1997; Mangel 2001). We defined "day" and "night" following ambient photoperiods. At the conclusion of each experiment, fishes were euthanized via a massive overdose (~300 mg kg^{-1}) of sodium pentobarbital (Beuthanasia-D, Schering-Plough Animal Health Corp., Union, N.J, USA).

Electroretinography (ERG)

Whole-animal corneal ERGs were conducted to assess the absolute sensitivities, temporal properties, and spectral sensitivities. Teflon-coated silver-silver chloride electrodes were used for recording ERGs. The active electrode was placed on the corneal surface and a reference electrode was placed subdermally in the dorsal musculature. ERG recordings and stimulus presentations were controlled using software developed within the LabVIEW system (National Instruments, Austin, TX, USA).

Absolute sensitivities were assessed via intensity-response (V/logI) experiments described in Horodysky et al. (2008). Briefly, six orders of magnitude of stimulus intensity were presented to subjects using appropriate combinations of Kodak Wratten 1.0 and 2.0 neutral density filters (Eastman Kodak Co., Rochester, N.Y., USA) with a white LED light source that had a working range of roughly three $\log_{10}$ units, and a maximum output intensity of 1585 cd m^{-2}. V/logI experiments progressed from subthreshold to saturation intensity levels in 0.2 log unit steps. At each intensity step, ERG b-waves were recorded from a train of five 200 ms flashes, each separated by 200

ms rest periods. This process was repeated three times, recorded, and normalized to the maximum voltage response (V_{max}). Mean V/logI curves for each species were created by averaging the V/logI curves of individuals of that species. Interspecific comparisons of relative sensitivity were made at stimulus irradiances eliciting 50% of V_{max} (referred to as K_{50}). Dynamic ranges, defined as the log irradiance range between the limits of 5-95% V_{max} (*sensu* Frank, 2003), were calculated separately for day and night experiments.

The temporal resolution of sciaenid visual systems was assessed via flicker fusion frequency (FFF) experiments using the white light LED source and methods developed by Fritsches et al. (2005). Sinusoidally-modulated white light stimuli ranging in frequency from 1 Hz (0 log units) to 100 Hz (2.0 log units) were presented to subjects in 0.2 log unit frequency steps, repeated three times at each frequency, and averaged for each subject. Light stimuli were presented for 5 s, followed by 5 s of darkness. Seven total FFF experiments were conducted for each subject: one at 25% (I_{25}) of maximum stimulus intensity (I_{max}) from the V/logI curve, and one in each in $\log_{10}$ step intervals over of six orders of magnitude of light intensity. A subject's FFF threshold at a given intensity was determined by analyzing the power spectrum of the averaged responses from 1-100 Hz and comparing the power of the subject's response frequency (signal) to the power of a neighboring range of frequencies (noise). Diel and interspecific comparisons were conducted on the FFF data at I_{max} and I_{25}. The FFF at I_{max} was considered to be the probable maximum flicker fusion frequency attainable by the visual system of a given species, and FFF at I_{25} to be a proxy for ambient environmental light intensity (Horodysky et al., 2008).

Spectral sensitivity experiments were conducted to assess the ability of piscivore visual systems to respond to colored light stimuli that covered the spectral range from UV (300 nm) to the near infrared (800 nm) in 10 nm steps. Stimuli were presented as five single 40 ms stimulus flashes at each experimental wavelength, each followed by 6 s of darkness. The amplitudes of ERG responses were recorded and averaged to form raw spectral response curves for each individual. A spectral V/logI recording was subsequently conducted for each subject at the wavelength (λ_{max}) that generated its maximum ERG response (V_{max}), which allowed the subsequent calculation of the subject's spectral sensitivity curve. Spectral V/logI experiments exposed the subject to five individual monochromatic 200 ms flashes at each intensity, increasing in 0.2 log unit increments over five orders of magnitude. To transform spectral response voltages to spectral sensitivities for each subject, the former were converted to equivalent intensities and were expressed on a percentage scale, with 100% indicating maximum sensitivity. Final spectral sensitivity curves for each species were obtained by averaging the sensitivity curves of all subjects and normalizing to the maximum resulting value so that maximum sensitivity equaled 100%.

Data Analyses

V/logI and FFF

Piscivore V/logI and FFF data were analyzed separately using two-way repeated measures ANOVAs with Tukey's post hoc comparisons to assess whether ERG responses varied among the four species and between photoperiods. All statistical analyses were conducted using SAS v 9.1 (SAS Institute, Cary, NC, USA). A general

model for these analyses is given in equation 1:

$Y_{ijk} = \mu + \alpha_i + \beta_j + \delta_k + \varepsilon_{ijk}$, where, (Eq. 1)

Y_{ijk}= value of the response variable (response) for the i^{th} species, j^{th} diel period, and the k^{th} level of their interaction

μ=overall mean of threshold for all combinations of species and diel periods

α_i=species (fixed factor)

β_j=diel period (fixed factor)

δ_k=species:diel interaction

ε_{ijk}=random error term associated with the observation at each combination of the i^{th} species, the j^{th} diel period, and k^{th} level of their interaction.

Spectral sensitivity

Intraspecific diel differences in spectral sensitivity curves were assessed by subtracting the day and night curves and calculating confidence intervals (CI) of the resulting difference curve. In this analysis, positive values corresponded to increased day sensitivity; negative values indicated increased nocturnal sensitivity. Significant differences in spectral sensitivity were defined where the mean ± CI of difference curves did not encompass zero.

To form hypotheses regarding the number and spectral distribution of pigments potentially contributing to piscivore spectral ERG responses, we fitted the SSH (Stavenga *et al.*, 1993) and GFRKD (Govardovkii *et al.*, 2000) vitamin A1 rhodopsin absorbance templates separately to the photopic spectral sensitivity data (Horodysky et al., 2008). A range of possible conditions was considered: 1-3 α-band rhodopsins, 1-3 α-band rhodopsins with a single β-band on any pigment, and 1-3 α-band rhodopsins with

multiple β-bands. For a given species, condition and template, models of summed curves were created by adding the products of pigment-specific templates and their respective weighting factors. Estimates of the unknown model parameters (λ_{max} values and their respective weighting proportions) were derived by fitting the summed curves to the ERG data using maximum likelihood.

For each species, we objectively selected the appropriate template (SSH or GFRKD) and number of contributing pigments using an Information Theoretic approach (Burnham and Anderson, 2002) following Akaike's Information Criterion (AIC):

$$\mathrm{AIC} = -2\ln(\hat{L}) + 2p, \text{ where} \qquad \text{(Eq. 2)}$$

AIC: Akaike's Information Criterion

$\hat{L}$: the estimated value of the likelihood function at its maximum

p: number of estimated parameters

All parameter optimization, template fitting, and model selection was conducted using the software package *R* version 2.7.1 (R Development Core Team, 2008).

RESULTS

White-light evoked ERG b-wave responses of the four piscivores increased non-monotonically with stimulus intensity to maximum amplitudes (V_{max}) of 30-400 μV, then decreased at intensities above those at V_{max} (Fig.2), presumably due to photoreceptor saturation and a lack of pigment regeneration. The K_{50} values of V/logI curves differed significantly among species ($F_{3,16} = 18.83$, $p < 0.0001$) and between diel periods ($F_{1,16} = 44.23$, $p < 0.0001$). The interaction between species and diel period was also significant due to diel differences in K_{50} values of pelagic piscivores but not for benthic summer

flounder ($F_{1,16}$=11.18, p<0.0003). Tukey's post-hoc comparisons revealed that the mean photopic K_{50} values of summer flounder were significantly left-shifted (0.5-1.8 log units, p< 0.05) relative to the other piscivores, indicating higher sensitivity to dim light. Mean photopic dynamic ranges of the four species, defined as 5-95% of V_{max}, varied between 1.84-3.35 log units and scotopic dynamic ranges between 2.3-3.3 log units. Dynamic ranges varied significantly among the species ($F_{3,16}$=11.18, p<0.0003) and diel periods ($F_{3,16}$=36.43, p<0.0001), however, the significant interaction term ($F_{3,16}$=6.57, p<0.005) compromised interpretation. Pelagic piscivores generally had narrower photopic dynamic ranges with varying degrees of diel differences, contrasting the broader, diel-invariant dynamic range of benthic summer flounder.

Piscivore FFF values (Fig 3) varied significantly among the four species ($F_{3,20}$= 9.82, p<0.003), with benthic summer flounder having significantly lower values than pelagic piscivores. FFF increased with increasing intensity (i.e., greater at I_{max} than I_{25}; $F_{1, 67}$=75.46.27, p< 0.001). Likewise, FFF values were significantly higher during the day rather than at night ($F_{1, 67}$=75.46.27,p>0.001). This difference was most pronounced in cobia and striped bass. Interaction terms were not significant.

Piscivore photopic spectral sensitivities generally spanned 400-600 nm, with cobia having the narrowest spectral range (Fig 4). Striped bass were a clear exception, exhibiting the high sensitivity to longer wavelengths (650 nm and above). Striped bass and bluefish demonstrated a significant nocturnal short wavelength shift, while cobia and summer flounder exhibited no such shifts (Fig 5).

Given our data, maximum likelihood estimation using published SSH and GFRKD rhodopsin templates suggested that most of the Chesapeake Bay piscivores may

have multiple pigment mechanisms (Fig. 6). Striped bass (SSH; λ_{max}= 542, 612 nm), and summer flounder (SSH; λ_{max}= 449, 524 nm) photopic spectral sensitivities were consistent with the presence of two α-band vitamin A1 pigments (Table 2). By contrast, bluefish were fitted with four rhodopsins (GFRKD; λ_{max}= 433, 438, 507, 547), and the cobia spectral sensitivity curve was fitted by a single rhodopsin centered at 501 nm.

DISCUSSION

The number, properties, and distribution of photoreceptor cells in fish visual systems, their luminous sensitivities, chromatic sensitivities and photopigments, and correlations to the photic properties of habitats have received rigorous attention in the literature (McFarland and Munz, 1977; Dartnall, 1975; Levine and MacNichol, 1979; Bowmaker, 1990, Parkyn and Hawryshyn, 2000). The functional characteristics of the visual systems of fishes generally reflect the aquatic light fields they inhabit, within ecological and phylogenetic constraints (Guthrie and Muntz, 1993). Luminous and chromatic sensitivities as well as temporal and spatial properties of fish visual systems are therefore useful metrics to describe the functions and tasks of aquatic visual systems (Lythgoe, 1979; Warrant, 1999; Marshall et al., 2003).

The range of light from which visual information can be obtained is extended in fishes with duplex retinae that use cone cells under photopic (bright) conditions and rod cells during scotopic (dim/dark) conditions (Lythgoe, 1979; Crescitelli, 1991). Piscivore luminous sensitivities, evidenced by the K_{50} points and dynamic ranges of V/logI curves, are comparable to other Chesapeake Bay fishes (Horodysky et al., 2008) and a range of

freshwater and marine teleosts (Naka and Rushton, 1966; Kaneko and Tachibana, 1985; Wang and Mangel, 1996; Brill et al., 2008). Predictably, neritic piscivores demonstrated less sensitivity than deep sea fishes (Warrant, 2000) and mesopelagic arthropods (Frank, 2003). In fact, striped bass, bluefish, and cobia, which frequently forage in well-lit, shallow coastal and estuarine waters, had fairly high K_{50} values (~1-2 log cd m^{-2}) and very narrow dynamic ranges, similar to those observed in black rockfish (*Sebastes melanops*), a shallow-dwelling coastal Pacific sebastid (2.0 log cd m^{-2}, Brill *et al.*, 2008). The three pelagic piscivores demonstrated significant diel shifts in luminous sensitivity, presumably as a result of retinomotor movements (Ali, 1975), to allow the fish to detect prey both during daytime and at night. In daylight, the luminous sensitivities of these three neritic piscivores were substantially more right-shifted (i.e., less sensitive), with narrower dynamic ranges and larger diel shifts, than those of pelagic-foraging sciaenid fishes from the same estuary (Fig. 7; Horodysky et al., 2008). The K_{50} values of benthic summer flounder (0.14-0.17 log cd m^{-2}), were similar in magnitude and relative diel invariance to demersal Pacific halibut (*Hippoglossus stenolepis*: 0.14-0.15 log cd m^{-2}; Brill *et al.*, 2008) and benthic foraging sciaenids (-0.24-0.30 log cd m^{-2}; Horodysky et al., 2008) (Fig. 8). These results collectively suggest that the luminous sensitivities of coastal flatfishes, and of phylogenetically-dissimilar benthic foragers, tend toward the more sensitive end of an emerging continuum for coastal fishes, consistent with their use of low light habitats. By contrast, the eyes of shallow-dwelling diurnal piscivores tend to be less sensitive but more plastic (i.e., less sensitive during the day, but with increasing sensitivity at night), consistent with their need to hunt effectively in extensively variable photic habitats.

The temporal properties of the eyes of predators closely match species-specific visual requirements and tasks (Warrant, 2004). Temporal properties of piscivore visual systems are also comparable to a range of diurnal freshwater and marine fishes. The FFF of the four piscivores predictably increased with light intensity (*sensu* Crozier *et al.*, 1938), as was observed in neritic sciaenid fishes (Horodysky et al. 2008). The benthic summer flounder, however, had significantly lower FFF at $I_{25\%}$ than the three pelagic piscivores, consistent with the use of comparatively deeper and dimmer waters by this flatfish. Maximum FFFs of the four piscivores, which reveal the scope of the visual system when light is not limiting, were lowest for flounder, intermediate for bluefish, and highest for cobia and striped bass. Predators that forage on rapidly swimming prey in clear and bright conditions, such as yellowfin and bigeye tunas (*Thunnus albacares* and *T. obesus*, respectively), have high FFFs and low spatial summation of photoreceptors (60-100 Hz; Bullock *et al.*, 1991; Brill et al., 2005). By contrast, nocturnal species and those that forage in dim light, such as broadbill swordfish and weakfish (*Xiphias gladius* and *Cynoscion regalis*, respectively), have low FFFs and high spatial summation of photoreceptors (Fritsches et al., 2005; Horodysky et al., 2008). Cobia and striped bass maximum FFF were therefore comparable to those of epipelagic scombrids, those of bluefish were similar to most sciaenids (~50-60 Hz) and freshwater centrarchid sunfishes (51-53 Hz), while those of flounder were analogous to crepuscular-foraging weakfish (42 Hz) (Crozier *et al.* 1936, 1938; Bullock *et al.*, 1991; Horodysky et al., 2008). Collectively, maximum FFFs of benthic and nocturnal species in neritic areas of the northwest Atlantic are lower than those of daytime foraging pelagic species (Fig. 7, 8). We caution that metanalysis in the broad qualitative comparisons above may be limited

by experimental, ecosystem, and analytical differences among these many studies, but consider the collective synthesis to be consistent with ecologies of the species discussed.

Chromatic properties of the visual systems of piscivores can likewise be placed in context of fishes from this and other ecosystems. Coastal fishes are generally sensitive to shorter subset of wavelengths than many freshwater fishes and a longer range of wavelengths than coral reef, deep sea, and oceanic species (Levine and McNichol, 1979; Marshall *et al.*, 2003). For maximum sensitivity in an organism's light microhabitat, scotopic (rod-based) pigment absorption spectra should match the ambient background to optimize photon capture ('Sensitivity Hypothesis': Bayliss *et al.*, 1936; Clark, 1936). Maximal contrast between an object and the visual background is provided by a combination of matched and offset visual pigments ('Contrast Hypothesis': Lythgoe 1968). Fishes that possess multiple spectrally-distinct visual pigments likely use both mechanisms, depending on the optical constraints of their specific light niches (McFarland and Munz, 1975). Western North Atlantic neritic piscivores demonstrated broad, species-specific responses to wavelengths ranging from the blue (~440 nm) to the yellow-orange (600-650 nm) end of the spectrum (Fig. 4). Responses blue-shifted nocturnally in striped bass and bluefish, whereas cobia and flounder showed no diel shifts. Coastal and estuarine fishes are commonly dichromats possessing short wavelength visual pigments with λ_{max} values ranging from 440-460 nm and intermediate wavelength pigments with λ_{max} values of 520-540 nm (Lythgoe and Partridge, 1991; Lythgoe, 1994; Jokela-Määttä *et al.*, 2007; Horodysky et al., 2008).

Comparing rhodopsin templates fitted to our ERG data and published MSP for the species, chromatic sensitivities of the four piscivores indicate species-specific pigment

mechanisms. The ERG data of juvenile cobia were consistent with a single rhodopsin pigment (λ_{max} 501 nm). Although it is unclear if this condition remains throughout ontogeny in the species, monochromacy occurs in other large aquatic predators such as cetaceans, phocids, and elasmobranchs such as the sandbar shark (Peichl et al., 2001, Litherland, 2009). For anadromous striped bass, a dichromatic visual system with an intermediate (λ_{max} 542 nm) and a long wavelength pigment (λ_{max} 612 nm) was the most likely condition, consistent with published MSP data for the species (533, 611 nm: Jordan and Howe, 2007; 542, 605 nm: Miller and Korenbrot, 1993). Similarly, our summer flounder ERG data were most likely the result of a dichromatic visual system with a shorter wavelength rhodopsin (λ_{max} 449 nm) and an intermediate wavelength rhodopsin (λ_{max} 524 nm), generally consistent with MSP data for this species (468, 527 nm; Levine and MacNichol, 1979). Similarly, MSP data for bluefish demonstrates the presence of four rhodospins (λ_{max} 423, 447, 526, 564 nm: Jordan and Howe, 2007), and pigment templates fitted to our ERG data suggested λ_{max} values of 433, 438, 507, and 547 nm. Template fitting procedures did not always extract the exact λ_{max} values from prior MSP studies conducted on the same species due to potential differences in habitat optics, experimental error in ERG and/or MSP experiments, the generally poor performance of rhodopsin templates at short wavelengths (Govardovskii et al., 2000), or a combination of these factors. ERG is well-suited for comparative investigations of vision and form:function relationships in fishes (Ali and Muntz, 1975; Pankhurst and Montgomery, 1989) and measures summed retinal potentials that account for any filtration by ocular media, which MSP does not (Brown, 1968; Ali and Muntz, 1975). Selective isolation of individual mechanisms and behavioral experiments may help determine the functions and

utility of multiple cone mechanisms (Barry and Hawryshyn, 1999; Parkyn and Hawryshyn, 2000); however, the morphological assessment of cone types, their photopigments, and distributions in piscivore retinae were beyond the scope of our study. Collectively, comparisons of MSP estimates to those resulting from the rhodopsin template fitting procedure (Horodysky et al., 2008) suggest that the latter provides useful comparative insights into possible chromatic mechanisms in visual systems with few, fairly widely spaced visual pigments. The procedure does, however, risk mischaracterizing pigment λ_{max} in species with many closely-spaced pigments and/or when underlying data are sparse and fitting procedures balance optimization and parsimony.

Collectively, the luminous, temporal, and chromatic properties of the visual systems of neritic western North Atlantic piscivores are consistent with inferences based on ecology and lifestyle. The eyes of daytime-active pelagic piscivores, such as striped bass, bluefish, and sciaenid spotted seatrout are typified by fast temporal resolution, limited photopic luminous sensitivity, and broadly-tuned chromatic sensitivity, consistent with foraging on fast moving planktivorous fishes in well-lit waters (Fig 7). Ganglion cell densities of striped bass and spotted seatrout predictably indicate low summation of individual photoreceptors and high acuity (K. Fritsches, pers. comm.). Daytime active pelagic piscivores therefore enhance resolution at the expense of luminous sensitivity during daylight hours, but increase nocturnal sensitivity, presumably at the expense of acuity, to match their diurnal light niches. By contrast, deeper-dwelling piscivores, such as summer flounder and weakfish, are typified by comparatively slower, more sensitive vision, higher spatial summation, and reduced acuity (K. Fritsches, pers. comm.; Warrant,

1999; Horodysky et al., 2008). These species exhibit few diurnal differences in visual properties (Fig. 7, 8), presumably because their light niches are consistently dim.

Increasing turbidity asymmetrically affects the distances over which conspecifics, predators, and prey interact. For encounter-rate feeders such as planktivorous prey fishes and the larvae/juveniles of eventual piscivores, turbidity resuspends nutrients and forage, and may serve as cover by decreasing sighted distances and increasing escape rates from predatory attacks. Benthic foraging fishes are typically well adapted to low light ambient conditions typical of turbid habitats, and many also feature enhancements of other sensory modalities that increase prey detection (Huber and Rylander, 1992). Conversely, reductions in ambient light intensity and degradations in contrast due to veiling effects adversely affect the ability of typically low-sensitivity, high-contrast piscivore visual systems to view fast moving planktivorous fish prey against strongly turbid backgrounds (De Robertis et al., 2003; Thetmeyer and Kils, 1995). Moderate levels of turbidity may actually improve the contrast of prey against estuarine backgrounds (Utne-Palm, 2002), but the fast, resolute, and low sensitivity visual systems of piscivores such as striped bass and weakfish require bright light for optimal function and should thus be frequently disadvantaged in the coastal optical habitat due to increasing turbidity resulting from a myriad of anthropogenic factors. Anthropogenic light pollution in coastal habitats may, however, extend the duration of photopic vision and thus visual foraging via general illumination of the night sky in urbanized areas (*sensu* Mazur and Beauchamp, 2006), and/or constrain nocturnal foraging arenas to small, highly illuminated point sources such as dock and bridge piling lights. Human impacts may thus both benefit and impede visual feeding piscivores systems in the same

habitats. Turbidity may exert contradictory and asymmetric effects on different trophic levels and life stages, serving as an important ecologically structuring factor in coastal ecosystems (Utne-Palm, 2002).

Optical conditions in coastal and estuarine waters (e.g., Chesapeake Bay) are complex and have changed dramatically over the past century from industrialization, population expansion, sedimentation, and eutrophication (Kemp *et al.*, 2005), with potentially large consequences for visually-foraging piscivores. Characterizing visual function of coastal and estuarine fishes is a first step, but many questions remain on topics such as luminous and chromatic properties of ambient light levels in specific light niches (Marshall et al., 2006) as well as light threshold effects on predator-prey intereactions (Mazur and Beauchamp, 2003; De Robertis et al., 2003), reproduction (Engström-Östa and Candolin, 2007**)**, and fishery gear interactions (Buijse et al., 1992). The ambient light field and background spectral properties, the reflectance of conspecifics, prey, and competitors, encounter and reaction distances, and the manner in which these change in space and time should be investigated to gain insights into the utility of visual system and tasks for a species (Levine and MacNichol, 1979; Johnsen, 2002), and to help quantify man's impact on the visual ecology of a species. Comparative approaches investigating the form-function-environment relationships between sensory ecophysiology, behavioral ecology, and ecosystem dynamics are thus important to mechanistically link processes from the cellular to the individual to the population level to support better management of aquatic resources.

REFERENCES

Abrahams, M. and Kattenfeld, M. (1997). The role of turbidity as a constraint on predator-prey interactions in aquatic environments. *Behav. Ecol. Sociobiol.* **40**, 169-174.

Ali, M. A. (1975). Retinomotor responses. In *Vision in Fishes: New Approaches in Research*. (ed. M. A. Ali). Pp 313-355. New York, NY: Plenum Press.

Ali, M. A. and Muntz, W. R. A. (1975). Electroretinography as a tool for studying fish vision. In *Vision in Fishes: New Approaches in Research* (ed. M. A. Ali), pp. 159-170. New York, NY: Plenum Press.

Asknes, D.L., and Utne, A.C.W. (1997). A revised model of visual range in fish. *Sarsia*, **82**, 137-147.

Barry, K. L. and Hawryshyn, C. W. (1999). Spectral sensitivity of the Hawaiian saddle wrasse, *Thallassoma duperrey*, and implications for visually mediated behavior on coral reefs. *Environ. Biol. Fishes* **56**, 429-442.

Bayliss, L. E., Lythgoe, J. N. and Tansley, K. (1936). Some forms of visual purple in sea fishes with a note on the visual cells of origin. *Proc. R. Soc. Lond., B, Biol. Sci.* **120**,9 5-114.

Beck, M. W., Heck, K. L., Able, K. W., Childers, D. L., Eggleston, D. B., Gillanders, B. M., Halpern, B., Hays, C. G., Hoshino, K., Minello, T. J. et al. (2001). The

identification, conservation, and management of estuarine and marine nurseries for fish and invertebrates. *BioScience* **51**, 633-641.

Bowers, D. G. and Brubaker, J. M. (2004). Underwater sunlight maxima in the Menai Strait. *J. Opt. A: Pure Appl. Opt.* **6 (2004)**, 684-689.

Bowmaker, J. K. (1990). Visual pigments of fishes. In *The Visual System of Fish* (ed. R. H. Douglas and M. B. A. Djamgoz), pp. 82-107. London: Chapman & Hall.

Brown, K. T. (1968). The electroretinogram: its components and origins. *Vision Res.* **8**, 633-677.

Brill, R.W., Bigelow, K.A., Musyl, M.K., Fritsches, K.A., and Warrant, E.J. (2005). Bigeye tuna (*Thunnus obesus*) behavior and physiology and their relevance to stock assessments and fishery biology. *Col. Vol. Sci. Pap. ICCAT*, **57(2)**, 142-161.

Brill, R. W., Magel, C., Davis, M. W., Hannah, R. W. and Rankin, P. S. (2008). Effects of events accompanying capture (rapid decompression and exposure to bright light) on visual function in black rockfish (*Sebastes melanops*) and Pacific halibut (*Hippoglossus stenolepis*). *Fish Bull (Wash. DC)* **106**, 427-437.

Buijse, A. D., Schaap, L. A. and Bult, T. P. (1992). Influence of water clarity on the catchability of six freshwater fish species in bottom trawls. *Can. J. Fish. Aquat. Sci.* **49**, 885-893.

Bullock, T. H., Hoffmann, M. H., New, J. G. and Nahm, F. K. (1991). Dynamic properties of visual evoked potentials in the tectum of cartilaginous and bony fishes, with neuroethological implications. *J. Exp. Zool.* **Suppl. 5**, 142-255.

Burnham, K. P. and Anderson, D. R. (2002). *Model selection and multimodel inference: a practical information-theoretic approach*. Springer: NY. p.488.

Cahill, G. M. and Hasegawa, M. (1997). Circadian oscillators in vertebrate retina photoreceptor cells. *Biol. Signals* **6**, 191-200.

Carpenter, S.R. and Kitchell, J.F. (1993). *The trophic cascade in lakes*. Cambridge University Press, New York.

Clark, R. L. (1936). On the depths at which fishes can see. *Ecology*, **17**,452 -456.

Collin, S. P. (1997). Specialisations of the teleost visual system: adaptive diversity from shallow-water to deep-sea. *Acta Physio. Scand.* **161**(Suppl. 638), 5–24.

Crescitelli F. (1991). The scotopic photoreceptors and their visual pigments of fishes: functions and adaptations. *Vis. Res.* **31**, 339-348.

Crozier, W. J., Wolf, E. and Zerrahn-Wolf, G. (1936). On critical frequency and critical illumination for response to flickered light. *J. Gen. Physiol.* **20**, 211-228.

Crozier, W. J., Wolf, E. and Zerrahn-Wolf, G. (1938). Critical illumination and flicker frequency as a function of flash duration: for the sunfish. *J. Gen. Physiol.* **21**, 313-334.

Dartnall, H. J. A. (1975). Assessing the fitness of visual pigments for their photic environments. In *Vision in Fishes: New Approaches in Research* (ed. M. A. Ali), pp.159 -170. New York, NY: Plenum Press.

De Robertis, A., Ryer, C., Veloza, A. and Brodeur, R.D. (2003). Differential effects of turbidity on prey consumption of piscivorous and planktivorous fish. *Can. J. Fish. Aquat. Sci.* 60, 1517-1526.

Engström-Östa, J. and Candolin, U. (2007). Human-induced water turbidity alters selection on sexual displays in sticklebacks. *Behav. Ecol.* **18**, 393-398.

Frank, T. M. (2003). Effects of light adaptation on the temporal resolution of deep-sea

crustaceans. *Integr. Comp. Biol.* **43**, 559-570.

Fritsches, K. A., Brill, R. W. and Warrant, E. J. (2005). Warm eyes provide superior vision in swordfishes. *Curr. Biol*. **15**, 55-58.

Gallegos, C. L., Jordan, T. E., Hines, A. H. and Weller, D. E. (2005). Temporal variability of optical propertes in a shallow, eutrophic estuary: seasonal and interannual variability. *Estuar. Coast. Shelf Sci.* **64**, 156-170.

Grecay, P.A. and Targett, T.A. (1996). Effects of turbidity, light level and prey concentration on feeding of juvenile weakfish *Cynoscion regalis*. *Mar. Ecol. Progr. Ser.* **131**, 11-16.

Gregory, R.S. and Northcote, T.G. (1993). Surface, planktonic, and benthic foraging by juvenile Chinook salmon (*Oncorhynchus tshawytscha*) in turbid laboratory conditionns. *Can. J. Fish. Aquat. Sci.* **50**, 233-240.

Grecay, P. A. and Targett, T. E. (1996). Spatial patterns in condition and feeding of juvenile weakfish in Delaware Bay. *Trans. Am. Fish. Soc.* **125 (5)**, 803-808.

Govardovskii, V. I., Fyhrquist, N., Reuter, T., Kuzmin, D. G. and Donner. K. (2000). In search of the visual pigment template. *Vis. Neurosci.* **17**, 509-528.

Guthrie, D.M., and Muntz, W.R.A. (1993). Role of vision in fish behavior. In: *Behavior of teleost fishes*. 2nd ed. (ed T.P. Pitcher.) , pp 89-121. London: Chapman and Hall.

Hall, J. W. (1992). *Handbook of Auditory Evoked Responses*. Boston, MA: Allyn and Bacon.

Harding L. W., Jr. (1994). Long-term trends in the distribution of phytoplankton in

Chesapeake Bay: roles of light, nutrients and streamflow. *Mar. Ecol. Prog. Ser.* **104**, 267-291.

Hart, N.S., Lisney, T.J., and Collin, S.P. (2006). Visual communication in elasmobranchs. In: *S Communication in fishes* (eds, F. Ladich, S. P. Collin, P. Moller and B. G. Kapoor), pp. 337-392. Enfield, N. H.: Science Publishers.

Hobson, E.S., McFarland, W.N., and Chess, J.R. (1981). Crepuscular and nocturnal activities of Californian nearshore fishes, with consideration of their scotopic visual pigments and the photic environment. *Fish Bull.* **79(1)**, 1-30.

Horodysky, A.Z., Brill, R.W., Warrant, E.J., Musick, J.A., and Latour, R.J. (2008). Comparative visual function in five sciaenid fishes inhabiting Chesapeake Bay. *J. Exp. Biol*. **211**, 3601-3612.

Huber, R., and Rylander, M.K. (1992). Brain morphology and turbidity preference in *Notropis* and related genera (Cyprinidae, Teleostei). *Env. Biol. Fishes*. **33(1-2)**, 153-165.

Jackson, J. B. C. (2001). What was natural in the coastal oceans. *Proc. Natl. Acad. Sci.* U.S. A. **98**, 5411-5418.

Jerlov, N.G. (1968). Optical Oceanography. Pp. 4-9, Elsevier, New York.

Johnsen, S. (2002). Cryptic and conspicuous coloration in the pelagic environment. *Proc. R. Soc. Lond., B, Biol. Sci.* **269**,243 -256.

Jokela, M., Vartio, A., Paulin, L., Fyhrquist-Vanni, N. and Donner, K. (2003). Polymorphism of the rod visual pigment between allopatric populations of the sand goby (*Pomatoschistus minutus*): a microspectrophotometric study. *J. Exp. Biol.* **206**, 2611-2617.

Jokela-Määttä, M., Smura, T., Aaltonen, A. and Ala-Laurila, P. (2007). Visual pigments of Baltic Sea fishes of marine and limnic origin. *Vis. Neurosci.* **24**, 389 - 398.

Kaneko, A. and Tachibana, M. (1985). Electrophysiological measurements of the spectral sensitivity of three types of cones in the carp retina. *Jpn. J. Physiol.* **35**, 355 -365.

Levine, J. S. and MacNichol, E. F. (1979). Visual pigments in teleost fishes: effects of habitat, microhabitat, and behavior of visual system evolution. *Sens. Proc*. **3**, 95-131.

Loesch, J.G., Kriete, W.H., and Foell, E.J. (1982). Effects of light intensity on the catchability of juvenile anadromous *Alosa* species. *Trans. Am. Fish. Soc.* **111**, 41-44.

Loew, E. R. and Lythgoe, J. N. (1978). The ecology of cone pigments in teleost fishes. *Vision Res.* **18**,715 -722.

Litherland, L.E. (2009). Neuroethological studies in shark vision. PhD dissertation, University of Queensland, Brisbane, Australia. 211 pages.

Lythgoe, J. N. (1975) Problems of seeing colours under water. In, *Vision in fishes: new approaches in research*. (ed M. A. Ali), pp. 619–634. New York, NY: Plenum Press.

Lythgoe, J. N. (1979). *Ecology of Vision*. Clarendon Press, Oxford

Lythgoe, J. N. (1988) Light and vision in the aquatic environment. In: *Sensory biology of aquatic animals* (ed J. Atema, R. R. Fay, A. N. Popper, W. N. Tavolga), pp. 131–149. New York,NY: Springer-Verlag.

Lythgoe, J. N. and Partridge, J. C. (1991). The modeling of optimal visual pigments of dichromatic teleosts in green coastal waters. *Vision Res.* **31**, 361-371.

Mangel, S. C. (2001). Circadian clock regulation of neuronal light responses in the vertebrate retina. *Prog. Brain Res.* **131**, 505 -518.

Marshall, J.M., Vorobyev, M., and Siebeck, U.E. (2006). What does a reef fish see when it sees reef fish? Finding Nemo. In: *S Communication in fishes* (eds, F. Ladich, S. P. Collin, P. Moller and B. G. Kapoor), pp. 393-422. Enfield, N. H.: Science Publishers.

Marshall, N. J., Jennings, K., McFarland, W. N., Loew, E. R. and Losey, G. S. (2003). Visual biology of Hawaiian coral reef fishes. III. Environmental light and an integrated approach to the ecology of reef fish vision. *Copeia*. **2003**, 467-480.

Mazur, M.M., and Beauchamp, D.A. (2003). A comparison of visual prey detection among species of piscivorous salmonids: effects of light and low turbidities. *Env. Biol. Fishes*. 67, 397-405.

Mazur, M.M. and Beauchamp, D.A. (2006). Linking piscivory to spatial–temporal distributions of pelagic prey fishes with a visual foraging model. *J. Fish. Biol.* **69(1)**, 151-175.

McFarland, W. N. (1986). Light in the sea: correlations with behaviors of fishes and invertebrates. *Am. Zool.* **26**, 389-401.

McFarland, W.N. and Loew, E.R. (1983). Wave produced changes in underwater light and their relations to vision. *Environ. Biol. Fishes*. **8**, 173-184.

McMahon, D. G. and Barlow, R. B. (1992). Electroretinograms, eye movements, and circadian rhythms. *J. Gen. Physiol.* **100**, 155-169.

Miller, J.L., and Korenbrot, J.I. (1993). Phototransduction and adaptation in rods, single cones, and twin cones of the striped bass retina: a comparative study. *Vis. Neurosci*. **10(4)**, 653-657.

Naka, K. I. and Rushton, W. A. H. (1966). S-potentials from colour units in the retina of fish (Cyprinidae). *J. Physiol.* **185**, 536-555.

Northcote, T.G. (1988). Fish in the structure and function of freshwater ecosystems: a "top down" view. *Can. J. Fish. Aquat. Sci.* **45**: 361–379.

Paine, R.T. (1966). Food web complexity and species diversity. *Am. Nat*. **100**, 65-75.

Pankhurst, N. W. and Mongomery, J. C. (1989). Visual function in four antacric nototheniid fishes. *J. Exp. Biol.* **142**, 311-324.

Parkyn, D. C. and Hawryshyn, C. W. (2000). Spectral and ultraviolet-polarization sensitivity in juvenile salmonids: a comparative analysis using electrophysiology. *J. Exp. Biol.* **203**,1173 -1191.

Peichl, L., Berhmann, G., and Kroger, R. (2001). For whales and seals the ocean is not blue: a visual pigment loss in marine mammals. *Eur. J. Neurosci*. **13(8)**, 1520-1528.

Rowland, W.J. (1999). Studying visual cues in fish behavior: a review of ethological techniques. *Environ. Biol. Fishes.* **56**, 285-305.

Saszik, S. and Bilotta, J. (1999). The effects of temperature on the dark-adapted spectral sensitivity function of the adult zebrafish. *Vision Res.* **39**, 1051-1058.

Schubert, H., Sagert, S. and Forster, R. M. (2001). Evaluation of the different levels of variability in the underwater light field of a shallow estuary. *Helgol. Mar. Res.* **55**, 12-22.

Seehausen, O., van Alphen, J. J. M. and Witte, F. (1997). Cichlid fish diversity threatened by eutrophication that curbs sexual selection. *Science* **277**, 1808-1811.

Siebeck, U. E., Losey, G. S. and Marshall, J. (2006). UV communication in fish. In *Communication in Fishes* (ed. F. Ladich, S. P. Collin, P. Moller and B. G. Kapoor), pp. 337-392. Enfield, NH: Science Publishers.

Stavenga, D. G., Smits, R. P. and Hoenders, B. J. (1993). Simple exponential functions describing the absorbance bands of visual pigment spectra. *Vision Res.* **33**, 1011 - 1017.

Thetmeyer, H. and Kils, U. (1995). To see and not be seen - the visibility of predator and prey with respect to feeding behavior. *Mar. Ecol. Prog. Ser.* **126**, 1-8.

Turesson, H. and Brönmark, C. (2007). Predator-prey encounter rates in freshwater piscivores: effects of prey density and water transparency. *Oecologia*. **152**, 281-290.

Utne-Palm, A. C. (2002). Visual feeding of fish in a turbid environment: physical and behavioural aspects. *Mar. Freshwater Behav. Physiol.* **35**,111 -128.

Walsh, S. J. (1991). Diel variation in availability and vulnerability of fish to a survey trawl. *J. Appl. Ichthyol.*, **7**, 147–159.

Wang, Y. and Mangel, S. C. (1996). A circadian clock regulates rod and cone input to fish retinal cone horizontal cells. *Proc. Nat. Acad. Sci. USA.* **93**, 4655-4660.

Warrant, E. J. (1999). Seeing better at night: life style, eye design, and the optimum strategy of spatial and temporal summation. *Vis. Res.* **39**, 1611-1630.

Warrant, E. J. (2000). The eyes of deep-sea fishes and the changing nature of visual scenes with depth. *Proc. R. Soc. Lond., B, Biol. Sci.* **355**,1155 -1159

Warrant, E.J. (2004). Vision in the dimmest habitats on Earth. *J Comp Physiol A* **190**, 765-789.

Table 1. Species, standard length (SL), and mass of the four piscivorous fishes investigated in this study.

Species	SL (mm)	Mass (g)
Morone saxatilis	183-358	320-670
Pomatomus saltatrix	183-260	55-95
Rachycentron canadum	91-388	40-820
Paralichthys dentatus	254-510	270-1045

Table 2. Parameter estimates and model rankings of SSH (Stavenga *et al.*, 1993) and GFRKD (Govardovskii *et al.*, 2000) vitamin A1 rhodopsin templates fitted to piscivore photopic spectral ERG data via maximum likelihood. The character "p" refers to the number of parameters in a model, "Mono" = monochromatic, "Di" = dichromatic, "Tetra" = tetrachromatic. Only alpha bands of pigments were considered. The number following $\lambda_{max,1}$ refers to pigment 1, etc. Bold type indicates the best supported pigment and template scenarios based on AIC values (lower is better).

Species	Condition	Template	$\lambda_{max,1}$	$\lambda_{max,2}$	$\lambda_{max,3}$	$\lambda_{max,3}$	-log(L)	p	AIC	ΔAIC
Striped bass	**Di**	GFRKD	**-**	521	611	-	-112	5	-214	**7**
		SSH	-	**542**	**612**	**-**	**-115**	**5**	**-221**	**0**
Bluefish	**Tetra**	**GFRKD**	**433**	**438**	**507**	**547**	**-152**	**7**	**-286**	**0**
		SSH	436	503	540	551	-148	7	-283	3
Cobia	**Mono**	GFRKD	-	501	-	-	-69	3	-134	11
		SSH	**-**	**501**	**-**	**-**	**-74**	**3**	**-145**	**0**
Summer	**Di**	**GFRKD**	**449**	**524**	**-**	**-**	**-88**	**5**	**-167**	**0**
Flounder		SSH	451	525	-	-	-82	5	-154	13

Figure 1. Conceptual diagram of the microhabitat specialization of the four Chesapeake Bay piscivores examined in this study. Striped bass (A) are schooling anadromous predators of a variety of fishes, crustaceans, and soft-bodied invertebrates. Bluefish (B) are voracious schooling pelagic predators of small fishes, decapods, and cephalopods. Cobia (C) are coastal migrant predators of a myriad of fishes and crustaceans, frequently associating with structure and following large marine vertebrates such as elasmobranchs, seaturtles, and marine mammals. Summer flounder (D) are benthic predators of small fishes, crustaceans, and soft-bodied invertebrates. Juveniles of these four species use Chesapeake Bay waters as nursery and foraging grounds; adults are seasonal inhabitants.

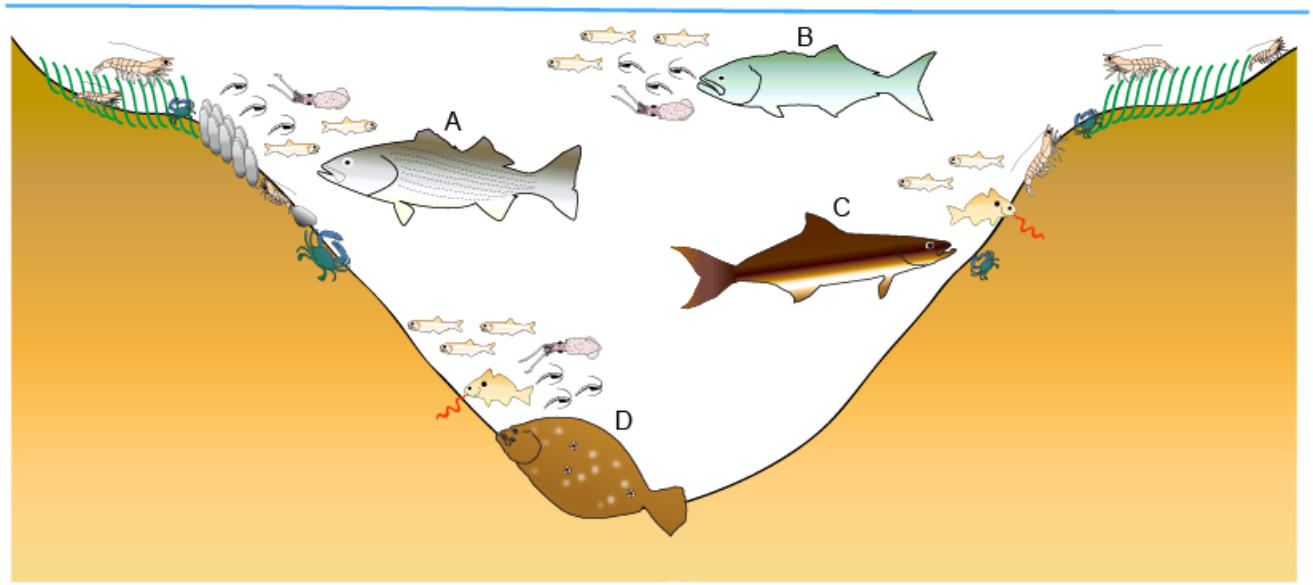
A
B
C
D

Figure 2. Intensity-response electroretinograms (ERGs) of striped bass, bluefish, cobia, and summer flounder. Each species' intensity response curve is an average of five individuals. Responses were normalized to the maximal response voltage (V_{max}) for each individual. Shaded boxes represent each species' dynamic range (5-95% V_{max}), numbers at the top indicate its breadth (in log units). Dashed drop lines and adjacent numbers indicate K_{50} points (illumination at 50% V_{max}). Open symbols and white text represent day experiments, filled symbols and black text represent night experiments. Light intensities are in log candela m^{-2}. Error bars are ± 1 SE.

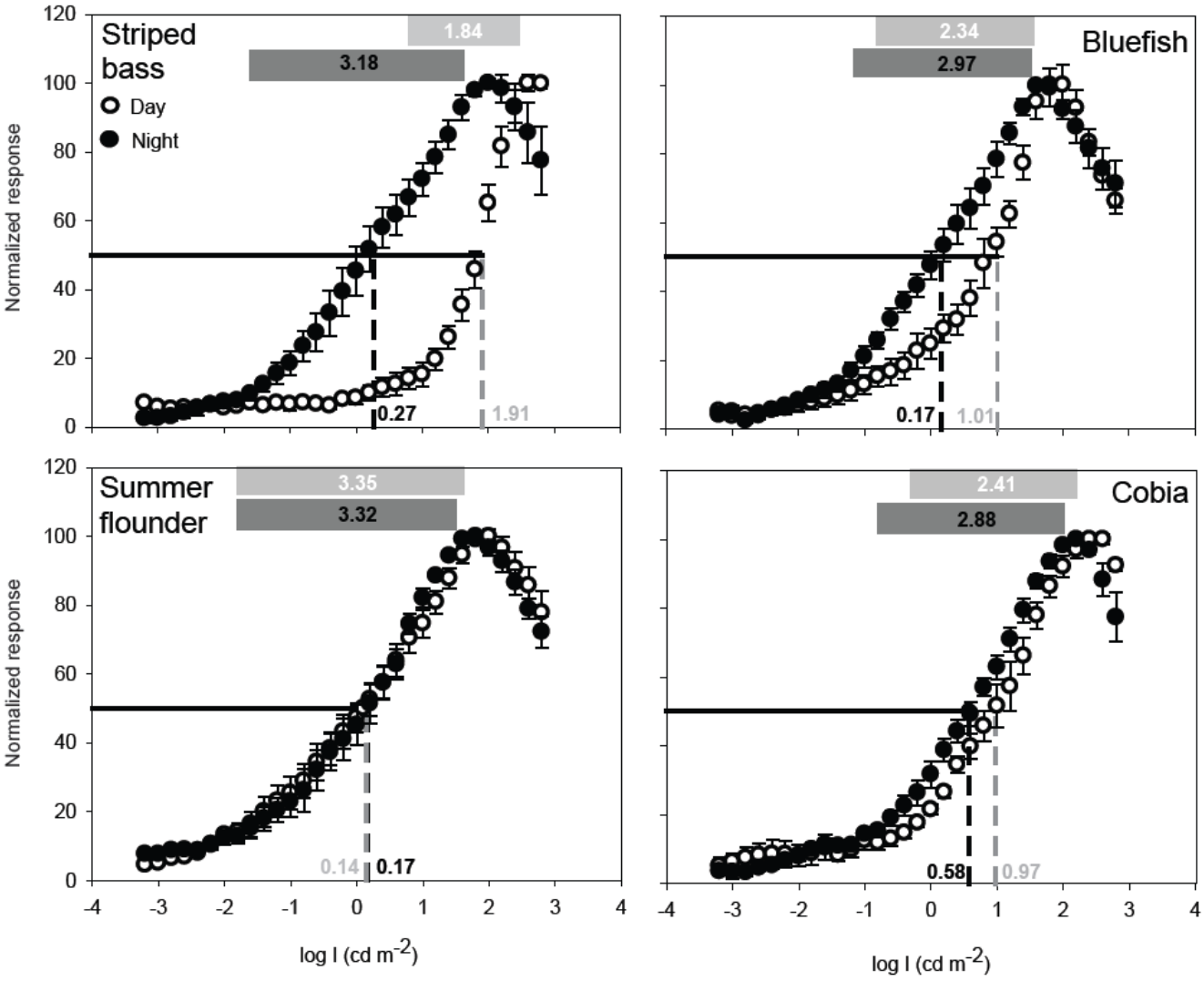
Striped bass
Day
Night
1.84
3.18
0.27
1.91
Bluefish
2.34
2.97
0.17
1.01
Summer flounder
3.35
3.32
0.14
0.17
Cobia
2.41
2.88
0.58
0.97
Normalized response
log I (cd m-2)

Figure 3. Mean flicker fusion frequency (FFF) values for the four Chesapeake Bay piscivores. Open symbols represent day experiments, filled symbols represent night experiments. Error bars are ± 1 SE. Triangles represent the FFF at maximum stimulus intensity (I_{max}). Circles represent FFF at I_{25} (light levels 25% of I_{max}). We considered I_{25} to be a proxy for ambient environmental light intensity (*sensu* Horodysky et al., 2008).

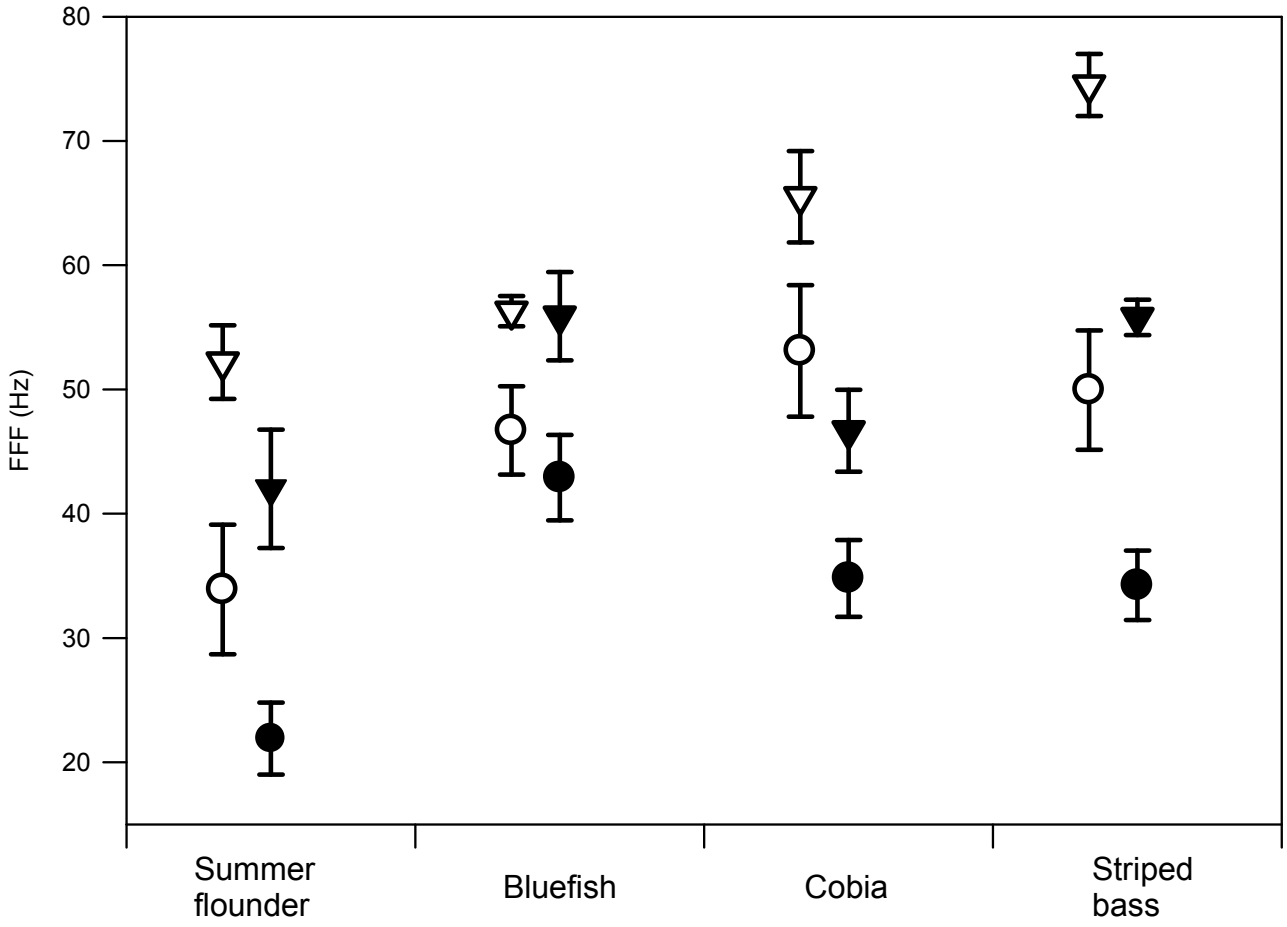
80
70
60
50
40
30
20
FFF (Hz)
Summer flounder
Bluefish
Cobia
Striped bass

Figure 4. Spectral sensitivity curves calculated from the electroretinograms (ERGs) of striped bass, bluefish, cobia, and summer flounder for wavelengths of 300-800 nm. Each species' curve is an average of five individuals. Responses at each wavelength were normalised to the wavelength of maximal voltage response (V_{max}) for each individual. Open symbols represent day experiments, filled symbols represent night experiments. Error bars are ± 1 SE.

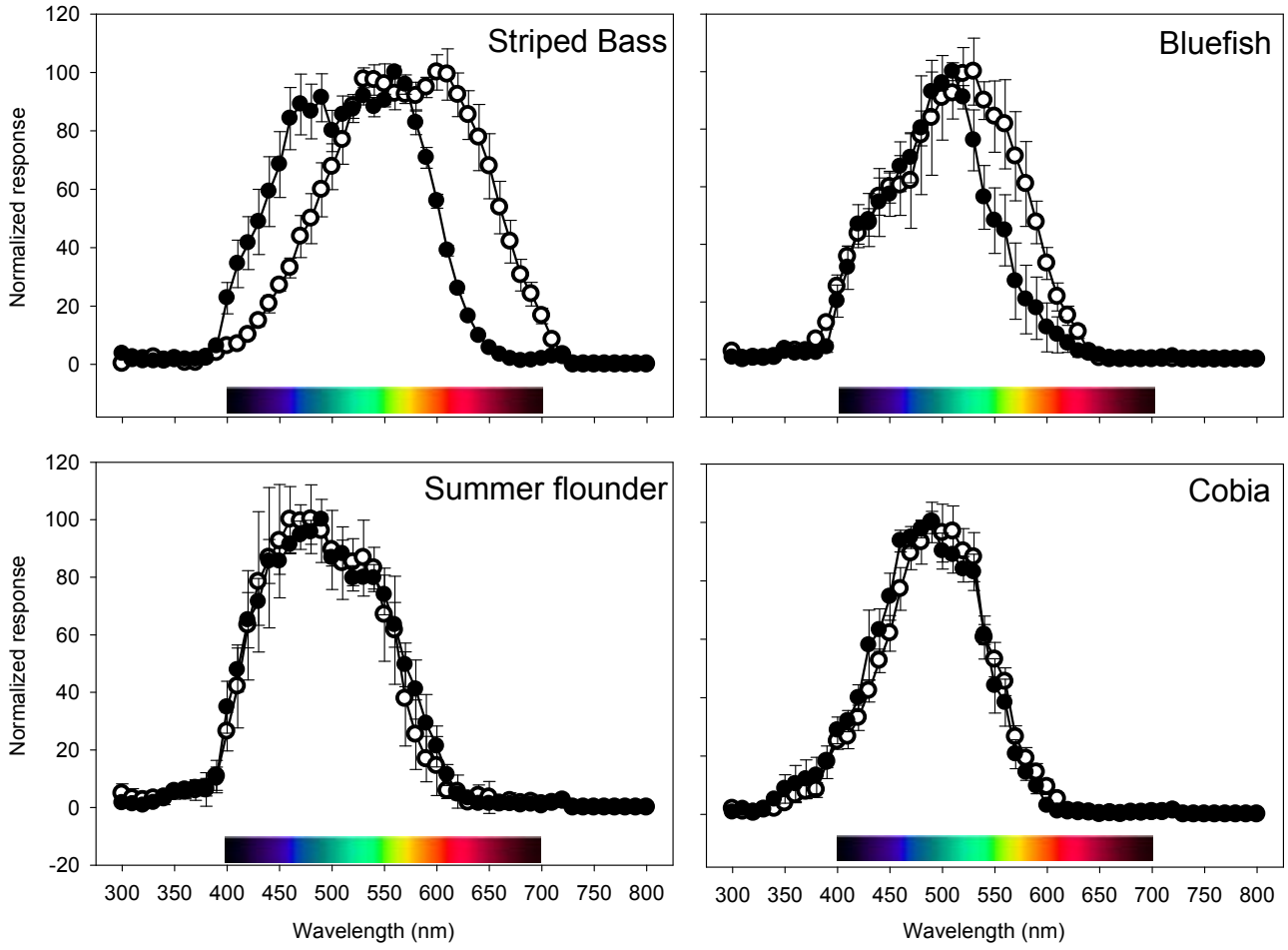
Striped Bass
Bluefish
Summer flounder
Cobia
Normalized response
Wavelength (nm)
120
100
80
60
40
20
0
-20
300 350 400 450 500 550 600 650 700 750 800

Figure 5. Diel differences in spectral electroretinograms (ERGs) of striped bass, bluefish, cobia, and summer flounder. Differences were calculated by subtracting the day spectral responses (R_{day}) from night responses (R_{night}). Thin grey lines are ± 95% CI, calculated as 1.96 (s.e.m). Values above the horizontal zero line (i.e. positive) indicate wavelengths of greater response during daylight, those below the zero line (i.e. negative) indicate wavelengths of greater nocturnal response. Significant differences occurred when CI did not encompass zero.

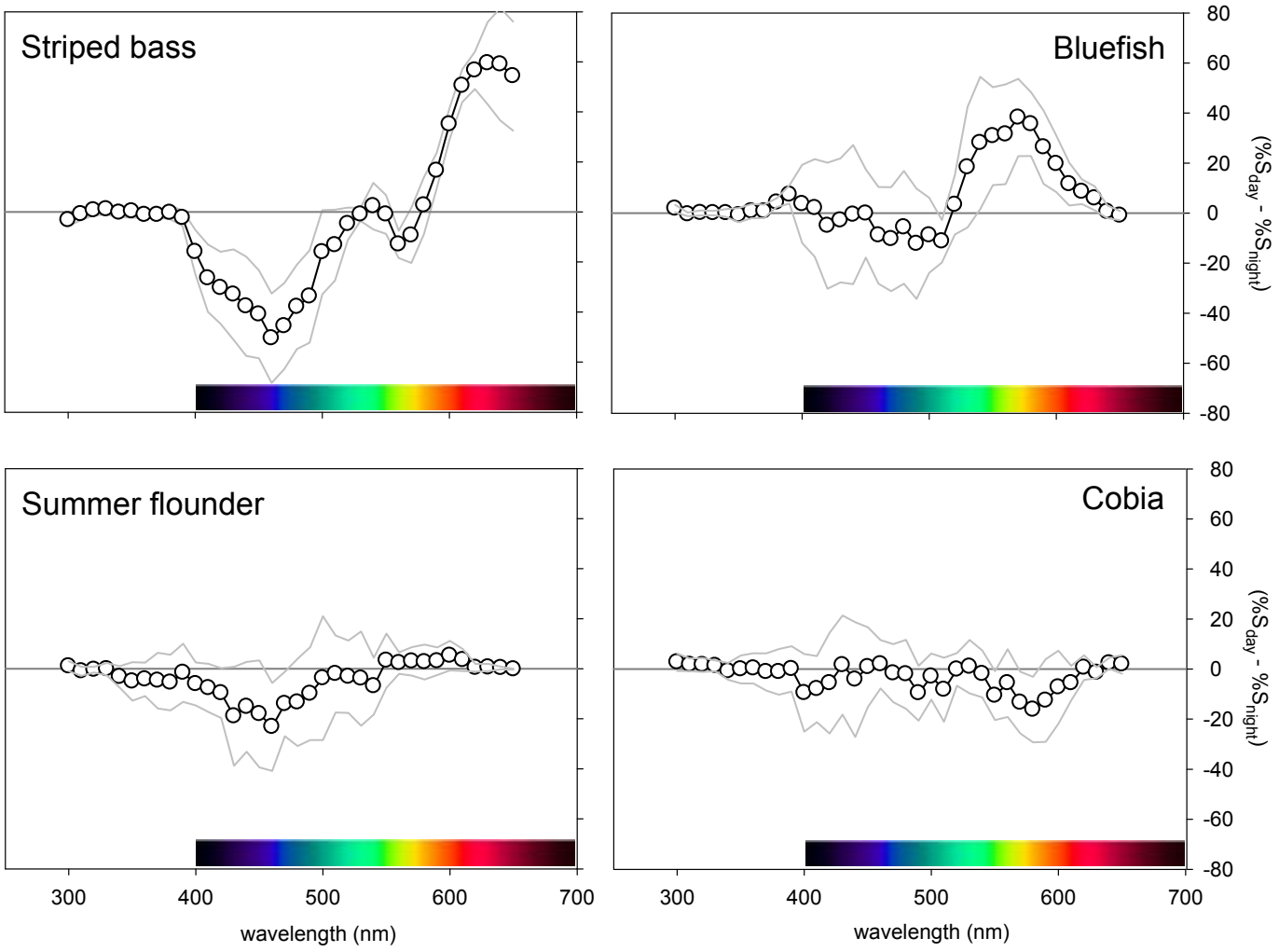
Striped bass
Bluefish
Summer flounder
Cobia
80
60
40
20
0
-20
-40
-60
-80
(%S day - %S night)
300
400
500
600
700
wavelength (nm)

Figure 6. SSH (Stavenga *et al.*, 1993) and GFRKD (Govardovskii *et al.*, 2000) vitamin A1 templates fitted to piscivore spectral ERG data by maximum likelihood (*sensu* Horodysky et al., 2008). Only estimates from best fitting models from Table 2 were plotted for each species. Values to the right of each pigment label are estimated λ_{max} and pigment specific weight as estimated by the model. P1 (blue or green) is the short wavelength pigment, P2 (yellow or red) is the intermediate or longer wavelength pigment. Black lines represent additive curves developed by summing the product of each curve weighted by the estimated weighting factor.

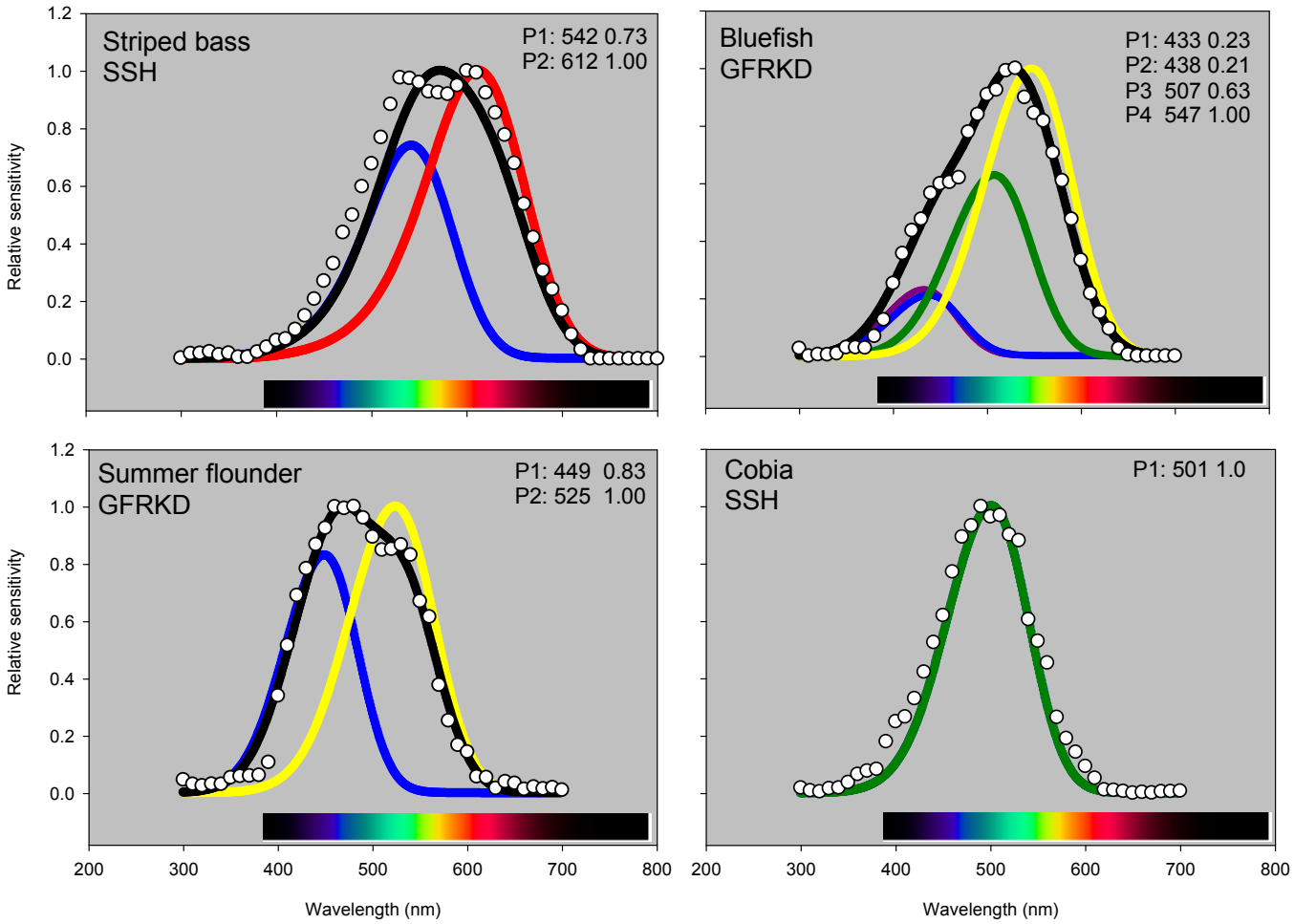
Striped bass
SSH
P1: 542 0.73
P2: 612 1.00
Bluefish
GFRKD
P1: 433 0.23
P2: 438 0.21
P3 507 0.63
P4 547 1.00
Summer flounder
GFRKD
P1: 449 0.83
P2: 525 1.00
Cobia
SSH
P1: 501 1.0
Relative sensitivity
Wavelength (nm)
0.0
0.2
0.4
0.6
0.8
1.0
1.2
200
300
400
500
600
700
800

Figure 7. Comparative visual function of five Chesapeake Bay pelagic predators. Data for striped bass (A), bluefish (B) , and cobia (E) are from the present study. Data for spotted seatrout (C) and weakfish (D) are from Horodysky et al. (2008). For all panels, open symbols and white or grey text are the result of day experiments, closed symbols and black text are the result of night experiments. All error bars indicate +/- 1 sem. i. Conceptual diagram of the microhabitat specialization of five pelagic piscivores. ii. Intensity-response electroretinograms (ERGs) of five pelagic predators. Each species' intensity-response curve is an average at least 5 individuals. Shaded boxes represent the dynamic range and breadth of each species in log candela m^{-2}: photopic (light grey, white text), scotopic (dark grey, black text). Dashed vertical lines and adjacent numbers indicate K_{50} points. iii. Mean flicker fusion frequency (FFF) values for the five pelagic predators. Triangles are the FFF at maximum stimulus intensity (I_{max}); circles are FFF at 25% of I_{max}, considered to be a proxy for ambient environmental light intensity. iv. Spectral sensitivity curves calculated from the ERGs of the five pelagic predators for wavelengths of 300-800 nm. Responses at each wavelength were normalized to the wavelength of maximum response (V_{max}) for each individual.

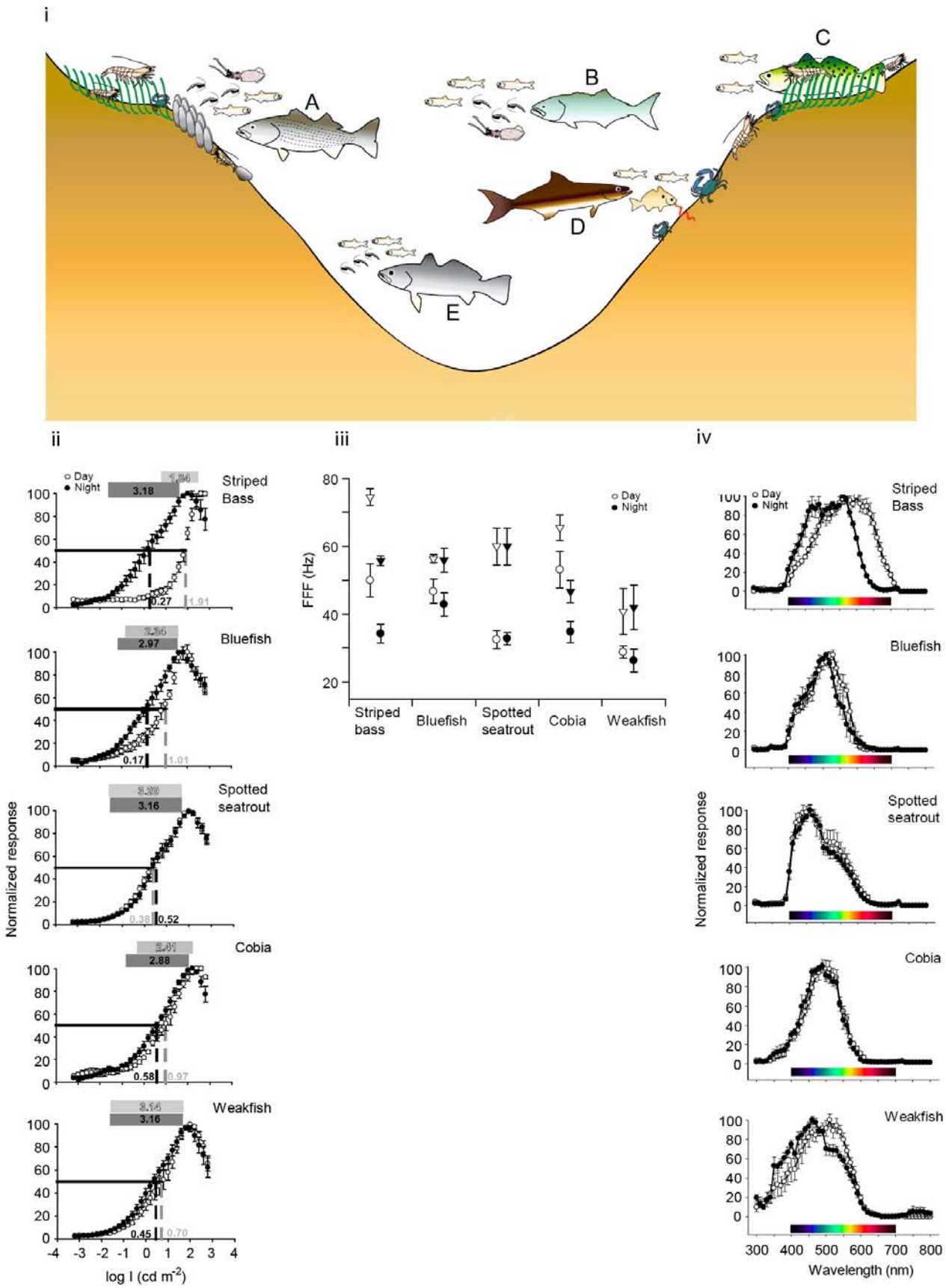
i
A
B
C
D
E
ii
iii
iv
Day
Night
Striped Bass
Bluefish
Spotted seatrout
Cobia
Weakfish
3.18
0.27
2.97
0.17
3.16
0.52
2.88
0.58
3.16
0.45
Normalized response
log I (cd m-2)
FFF (Hz)
Striped bass
Bluefish
Spotted seatrout
Cobia
Weakfish
Wavelength (nm)

Figure 8. Visual function of five benthic foragers from Chesapeake Bay. Data for red drum (A), Atlantic croaker (B) and spot (C) are from Horodysky et al. (2008). Data for summer flounder (D) are from the present study. For all panels, open symbols and white or grey text are the result of day experiments, closed symbols and black text are the result of night experiments. All error bars indicate +/- 1 sem. i. Conceptual diagram of the microhabitat specialization of the four benthic predators. ii. Intensity-response electroretinograms (ERGs) of the four predators. Shaded boxes represent the dynamic range of each species in log candela m^{-2}: photopic (light grey, white text), scotopic (dark grey, black text). Dashed vertical lines and adjacent numbers indicate K_{50} points. iii. Mean flicker fusion frequency (FFF) values for the four benthic predators. Triangles are the FFF at maximum stimulus intensity (I_{max}); circles are FFF at 25% of Imax, considered to be a proxy for ambient environmental light intensity. iv. Spectral sensitivity curves calculated from the ERGs of the four benthic predators for wavelengths of 300-800 nm. Responses at each wavelength were normalized to the wavelength of maximum response (V_{max}) or each individual.

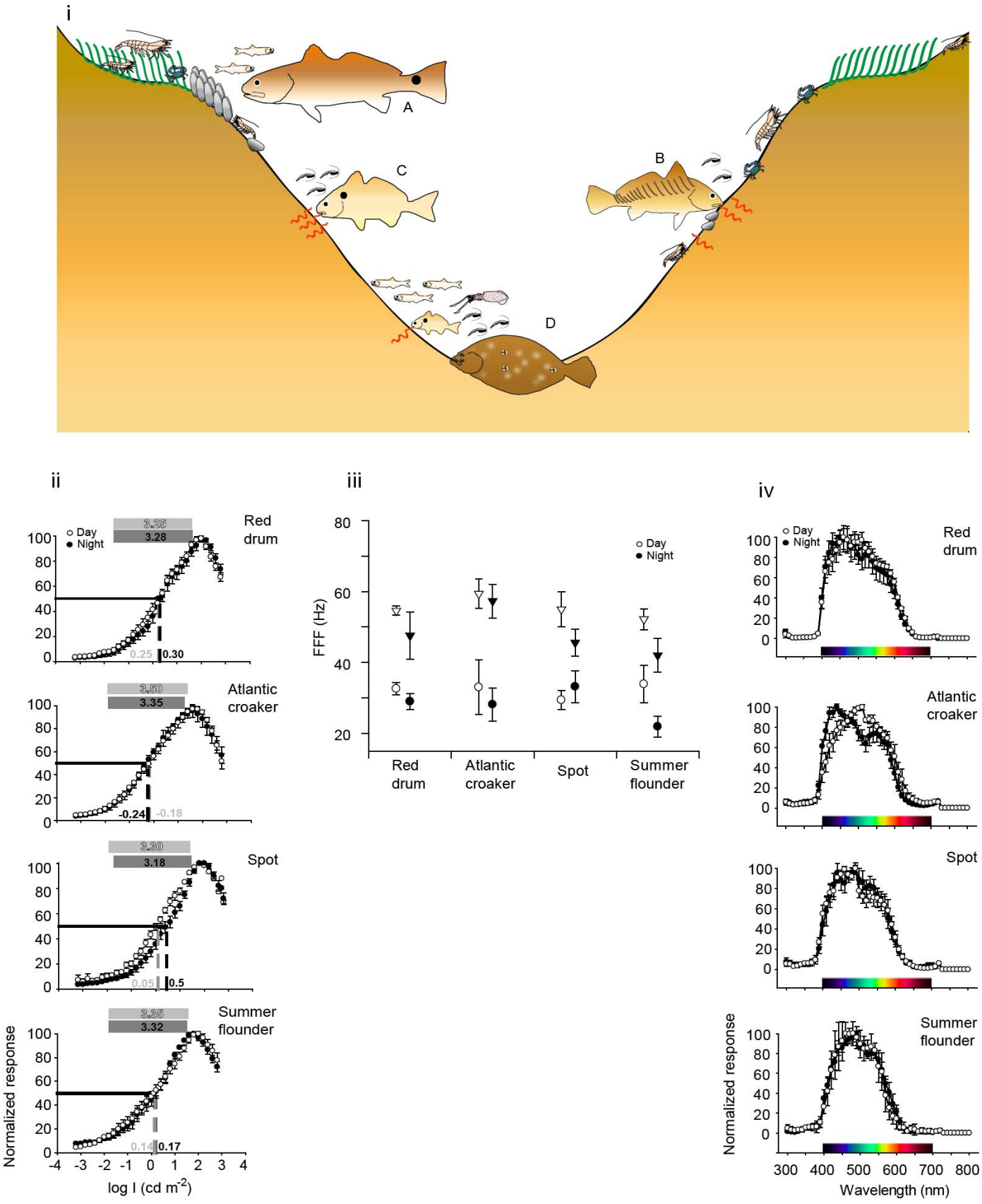
i
A
B
C
D
ii
Day
Night
Red drum
3.25
3.28
0.25
0.30
Atlantic croaker
3.50
3.35
-0.24
-0.18
Spot
3.30
3.18
0.05
0.5
Summer flounder
3.35
3.32
0.14
0.17
Normalized response
log I (cd m-2)
iii
FFF (Hz)
Red drum
Atlantic croaker
Spot
Summer flounder
iv
Wavelength (nm)

CHAPTER 4: METABOLIC RATES OF SCIAENID FISHES COMMON TO CHESAPEAKE BAY, VIRGINIA

INTRODUCTION

The acquisition and allocation of energy by fishes are fundamental processes that integrate organismal physiology, behavior, and biophysics. Ingested energy is apportioned to metabolic requirements and wastes before surpluses can be routed to processes including growth and reproduction (Winberg, 1956; Hewett and Kraft, 1993). Interest in the description, quantification, and prediction of energy acquisition and allocation patterns of fishes among physiological compartments including catabolism and anabolism (i.e. somatic and gonadal growth) has led to the development of bioenergetic and individual-based models (Kitchell et al., 1977; Boisclaire and Tang, 1993; Jobling 1994). These models can link fish physiology, behavior, and environmental conditions with population dynamics to provide system-level estimates of production and consumption (Kitchell et al., 1977; Brandt and Hartman, 1993). However, catabolism, generally the largest and most labile component of the energy budgets of fishes, must be understood for such models to generate valid results (Ney, 1993; Bosclair and Sirois, 1993).

Aerobic metabolism ranges over a metabolic scope from the lower limit set by the standard metabolic rate (SMR), the rate of oxygen consumption (VO_2) of an inactive, unfed, thermally-acclimated subject at rest (Krogh, 1914; Brett and Groves, 1979) to the upper limit set by maximum aerobic metabolic rate (AMR: Fry, 1947). The standard metabolic rates of fishes have been obtained using a variety of techniques, including

repeated measurements on the same individual until a minimum rate of oxygen consumption is observed (Ferry-Graham and Gibb, 2001; Steffensen et al., 1994), regressing active metabolic rate back to zero activity to obtain the Y-intercept (Bushnell et al., 1984; Sepulveda and Dixon, 2002), or via the use of paralytic agents to isolate minimum costs of organ function (Brill, 1979). More commonly, researchers measure resting metabolic rates (RMR), which include the oxygen consumption of fishes exhibiting minimum minor spontaneous activity (Beamish, 1964; Prosser, 1973). Active metabolic rate (AMR) is generally measured as the oxygen consumption at increments of enforced activity leading up to or immediately following the maximum sustainable swimming speed and exhaustive exercise (Brett, 1964; Soofiani and Priede, 1985).

Environmental and biological factors influence the metabolic rates of fishes. The environmental factors affecting metabolism include temperature and salinity (Moser and Hettler, 1989; Wuenschel et al., 2004), dissolved oxygen (Fitzgibbon, 2007), and photoperiod (Boef and Le Bail, 1999; Jonassen et al., 2000). The interactive effects of temperature and dissolved oxygen have received considerable attention because of their spatial and temporal variability in aquatic systems (Taylor and Peck, 2004). Biological factors affecting metabolic rates of fishes include body mass (Brett and Groves, 1979; Clarke and Johnston, 1999), ontogeny (Oikawa et al., 1991; Post 1996), life history (Metcalfe et al., 1995), individual disposition (McCarthy, 2001), stress (Barton and Schreck, 1987), and nutritional condition (Alsop and Wood, 1997). Additionally, the assimilation and biochemical transformation of food, termed specific dynamic action (SDA), elevate oxygen consumption and reduce the metabolic scope of an organism (Beamish, 1974; Secor, 2009).

Comparative methods have provided novel insights into the form-function-environment relationships of teleost metabolic systems and how they affect behavior (Metcalfe et al., 1995), habitat utilization (Chapman et al., 1995, 2002), distribution and movement (van Dijk et al., 1999), tolerance to environmental variables (MacIsaac et al., 1997; Pichavant et al., 2001), interspecific, intraspecific, and predator-prey interactions (Morris and North, 1984), aquaculture (Brougher et al., 2005), and bioenergetics (Hartman and Brandt, 1995; Burke and Rice, 2002). However, despite the rich literature on teleost metabolic physiology (Clarke and Johnston, 1999), such data are sparse for many managed neritic fishes such as teleosts of the family Sciaenidae that support valuable commercial and recreational fisheries along the US East Coast. Sciaenid fishes occupy a myriad of habitats in freshwater, estuarine, neritic, and reef-associated marine systems, but are most speciose in neritic waters, where species-specific ecomorphologies and microhabitats result in niche separation (Myers, 1960; Chao and Musick, 1977). Temperature, salinity, and dissolved oxygen levels in estuaries used by sciaenid fishes are highly variable (Breitburg, 2002). Previous studies have demonstrated that sciaenid fishes are good candidates for comparative study by virtue of their taxonomic, morphological, and microhabitat diversity (Chao and Musick, 1978; Horodysky *et al.*, 2008a,b), but there has been little comparative study of their metabolic rates. We therefore used stop-flow respirometry to assess resting metabolic rates (RMR) in four sciaenid species and active metabolic rates (AMR) and costs of transport (COT) in two species.

METHODS

Animal collection and husbandry

Hook and line gear was used to capture Atlantic croaker (*Micropogonias undulatus* Linnaeus, 1766), spot (*Leiostomus xanthurus* Lacepede, 1802), northern kingfish (*Menticirrhus saxatilis* Bloch and Schneider, 1801) and southern kingfish (*Menticirrhus americanus* Linnaeus, 1758). Animals were maintained in recirculating 1855 L aquaria at 15°C ± 1°C (winter) or 25°C ± 2°C (summer) and fed a combination of frozen Atlantic menhaden (*Brevoortia tyrannus*), squid (*Loligo* sp.), and commercially-prepared food (AquaTox flakes; Zeigler, Gardners, PA, USA) (Table1). Prior to each trial, subjects were isolated and fasted for 48 h to ensure complete gastric evacuation. Experimental and animal care protocols were approved by the College of William and Mary's Institutional Animal Care and Use Committee and followed all relevant laws of the United States.

Automated intermittent-flow respirometry (IFR)

Automated intermittent-flow respirometry (IFR) was used to determine the RMR of six sciaenid species and the AMR of Atlantic croaker and spot. In this technique, a respirometer submerged in a flow-through outer bath experiences repeated cycles of two computer-driven flow regimes over a ~36-48 h period: flow-through chamber ventilation (5-10 min), when fresh seawater from the outer bath is flushed through the metabolic chamber, and closed-chamber VO_2 recording (5-60 min) intervals, where flushing ceases, effectively sealing the respirometer (Fig. 1A, B, C). Accordingly, IFR eliminates washout problems of traditional flow-through respirometry and avoids the carbon dioxide

and metabolite accumulation issues that plague closed respirometry (Steffensen, 1989). Further, this computer-driven technique records metabolic rates with high temporal resolution over several days without the constant presence of a researcher, facilitating high data yields with reduced potential for human movement/noise biasing VO_2 upwards (Steffensen, 2002).

Resting metabolic rate (RMR)

RMR was assessed as the oxygen consumption (VO_2, mg kg^{-1} h^{-1}) of a thermally-acclimated, unfed subject at low-level spontaneous motor activity. For each experiment, a subject was netted from its holding tank, weighed (g), and transferred depending on body mass to a 0.35 or 7.4 L acrylic respirometer (Loligo Systems, Copenhagen, Denmark) that was submerged in a flow-through outer bath (Fig. 1B). Temperature-controlled, aerated, and filtered seawater was delivered to the bath with an approximate system-wide seawater turnover rate of 20-30% hr^{-1} (Dowd et al., 2006). VO_2 was measured during closed-respirometer intervals that were temporally adjusted until a subject extracted ~20-30% of the dissolved oxygen from the seawater. At predetermined intervals, the respirometer was flushed with fresh seawater by a small pump submerged in the outer bath, forcing the oxygen-depleted water through a PVC chimney to be re-aerated and mixed in the outer bath. During both recording and flushing cycles, water within the respirometer was continually mixed by a small recirculating pump external to the chamber (Steffensen, 1989). Flushing and recirculating flows were diffused by baffles within the respirometer, and the entire assembly was covered with black plastic to

minimize visual disturbance. Respirometer turnover rates were 200-500% per flushing cycle. RMR experiments were conducted at 10, 15, 20, and 25ºC. To overcome low sample sizes, 10ºC data were adjusted to 15ºC while 20ºC data were adjusted to 25ºC using a Q_{10} of 1.65 (White et al., 2006).

Calculation of VO_2

The partial pressure of oxygen (PO_2, mm Hg) in respirometers was continuously measured with a polarographic electrode (Radiometer A/S, Copenhagen, Denmark) mounted in a water-jacketed cuvette (Loligo Systems) and connected to a digital oxygen meter (either Radiometer A/S or Cameron Instruments Company, Port Aransas, TX). Water temperature, time, and PO_2 were oversampled, averaged to 1 sec^{-1} to remove electronic noise, and recorded with a computerized data acquisition system by a custom Dasylab 7.0 worksheet interfacing with a QuattroPro 11.0 spreadsheet. PO_2 values were converted to oxygen content (mg O_2 L^{-1}) for a given temperature and salinity following Richards (1965) and Dejours (1975). To help ensure the linearity of the rate of change of oxygen concentration with time, data from the first 60-180 seconds at the conclusion of the flush cycle were excluded from calculations. Oxygen uptake (VO_2, mg h^{-1}) for a given measurement period was calculated from the time course of PO_2 change (Steffensen et al., 1984):

$$VO_{2m} = V \cdot \frac{\Delta PO_2}{\Delta t \cdot \alpha}, \qquad \text{(Eq. 1)}$$

where V is the respirometer volume (L) corrected for fish volume, $\Delta PO_2 \cdot \Delta t^{-1}$ is the slope of the linear regression of PO_2 versus time, α is the oxygen solubility coefficient. The mass-specific RMR (mg O_2 kg^{-1} hr^{-1}) were calculated by dividing absolute VO_2 (mg h^{-1}) by the mass of the fish (in kg).

After being placed in the respirometer, most individuals displayed some degree of agitation and increased oxygen consumption due to handling. These typically lasted < 1-3 hr and were removed from analyses. Additionally, regressions of PO_2 vs. time with r^2 values less than 0.9 were excluded from consideration (Hölker, 2002). Resting metabolic rates for each species were calculated by fitting a normal distribution to the frequency distribution of VO_2 measurements (Steffensen et al., 1994).

RMR analyses

Allometric equations were fitted via nonlinear least squares to the sciaenid RMR data following the formula:

$$RMR = a * M^b, \quad \text{(Eq. 2)}$$

where *RMR* is the resting metabolic rate (in mg O_2 hr^{-1}), M is body mass (kg), and a and b are estimated parameters with the latter representing the allometric scaling exponent that may vary between 0.5 and 1.0 in fishes (Clarke and Johnston, 2006). Data for northern and southern kingfish were combined into a single group (i.e., 'kingfishes') for analyses due to small sample sizes. Interspecific differences in the RMRs of spot, croaker, and kingfishes were assessed via ANCOVA performed on $\log_{10}$-transformed data as 25°C with body mass as the covariate. The effects of temperature on the metabolic rates of spot and croaker were similarly evaluated via ANCOVA performed

separately for each species on log_{10}-transformed data. To place sciaenid data in context of other fishes, interspecific comparisons to other taxa were performed by first standardizing oxygen consumption data from the literature to absolute VO_2 (mg O_2 hr^{-1}), converting the oxygen consumption to 25°C where necessary via a Q_{10} of 1.65 (White et al., 2006), and regressing against body mass (kg). The VO_2 data of all species were allied graphically in three groups separated by energy demand. Allometric models (Eq. 2) were fitted separately to these groups and parameter estimates were tested with a Hotelling's T^2 test to evaluate their equality.

Active metabolic rate (AMR)

For AMR experiments, the fish were weighed, total length (TL) and standard lengths (SL) were measured and then fish were immediately transferred to a modified Blazka-type (Blazka et al., 1960) swimming respirometer (Fig. 1C). Water temperature was maintained at 25 (± 0.9) º C. Animals were allowed to acclimate to the chamber for 12 h with water velocity set to 0.5 body lengths (BL) s^{-1} during which time RMR was measured as described previously During swimming trials, water flow within the chamber was increased for 20 min that included 10 min flushing (open) phase and a 10 min (closed) recording phase. Water velocity was increased every 20 min, in steps that corresponded to 0.25 or 0.5 BL s^{-1} increments, until the subject was no longer able to continue sustained swimming and made contact with the rear chamber grate for > 3 s twice within the same swimming velocity's measurement interval. At this point, water velocity was reduced to 0.5 BL s^{-1} and maintained for 8 hrs, during which time recovery VO_2 was measured.

For AMR experiments, the relationship between swimming velocity and VO_2 was investigated by fitting power functions of the form:

$$VO_2 = a + bU^c \quad \text{(Eq. 3)}$$

where *a*, *b*, and *c* are constants and *U* is the swimming velocity (BL s^{-1}). Standard metabolic rate (SMR) was estimated by extrapolating the VO_2 relationship back to a constant swimming velocity of 0 BL s^{-1} and interpreting the y-intercept (i.e., the constant *a* in Eq. 3) (e.g., Dewar and Graham 1994).

AMR experiments in which the oxygen consumption of a swimming individual is recorded repeatedly at increasing swimming speeds may violate several fundamental assumptions of standard nonlinear regression, including independence and constant variance (i.e., homoscedasticity) (Underwood, 2002). To consider each VO_2 measurement as independent within subjects is tantamount to pseudoreplication (Hurlbert, 1984); doing so may lead to biased parameter estimates (i.e., intercept, slope, and shape parameters), standard errors, and metrics of model fit (Littell et *al.*, 2006). Further, AMR measurements may be more variable among subjects at higher vs. lower swimming speeds, resulting in violation of the regression assumption of homoscedasticity. We therefore fitted repeated measures nonlinear mixed effects models that considered the within-individual autocorrelation (Pinheiro and Bates, 2004) and weighted the data by the inverse of the variance at each level of the *x*-variable (BL s^{-1}). These mixed models contained fixed (swimming speed) and random variables (fish). Subjects were a random sample from the wild population, thus "fish" was modeled as a random variable. For each species, the best fitting covariance structure was objectively

selected using an Information Theoretic approach (Burnham and Anderson, 2002) following Akaike's Information Criterion (AIC):

$$\mathrm{AIC} = -2\ln(\hat{L}) + 2p, \text{ where} \qquad \text{(Eq. 4)}$$

AIC: Akaike's Information Criterion

$\hat{L}$: the estimated value of the likelihood function at its maximum

p: number of estimated parameters

AIC is a parsimonious measure that strikes a balance between model simplicity and complex overparameterization (Burnham and Anderson, 2002). Accordingly, AIC provided a quantitative metric to evaluate the simplest, most likely estimates given our data. All statistical analyses were conducted using the software package *R* version 2.7.1 (R Development Core Team, 2008).

Costs of transport (NCOT, GCOT) and optimum swimming speeds (U_{opt}) were calculated separately for spot and croaker from the AMR model parameters and VO_2 data (following Claireaux et al., 2006; Videler, 1993). For each individual, oxygen consumption at each swimming speed was converted from mg O_2 kg^{-1} hr^{-1} to J kg^{-1} hr^{-1} using an oxycalorific coefficient of 3.24 cal mg O_2 (Beamish, 1978) and converting calories to J (4.18 J cal^{-1}). The net cost of transport (NCOT) was determined by subtracting the SMR estimate from each VO_2, dividing by the U (BL s^{-1}) at which it was obtained, canceling time units, and plotting. Using parameter estimates from the best fitting power model, a predictive line was calculated from the equation:

$$\text{NCOT (J kg}^{-1}\text{ km}^{-1}\text{)} = \hat{b} \cdot U^{(\hat{c}-1)} \qquad \text{(Eq. 5)}$$

Gross cost of transport (GCOT) was determined by dividing each VO_2 by the U (BL s^{-1}) at which it was obtained and canceling time units. A predictive line was calculated using the equation:

$$\text{GCOT (J kg}^{-1}\text{ km}^{-1}) = \frac{\hat{a}}{U} + \hat{b}U^{(\hat{c}-1)} \qquad \text{(Eq. 6)}$$

The optimum swimming speed (U_{opt}) for spot and croaker was calculated according to the following equation:

$$U_{opt}\text{ (BL s-1)} = \left(\frac{\hat{a}}{(\hat{c}-1)\cdot\hat{b}}\right)^{(1/\hat{c})} \qquad \text{(Eq. 7)}$$

Finally, $NCOT_{min}$ and $GCOT_{min}$ were calculated by inserting the U_{opt} for each species into equations 5 and 6 and canceling time units.

RESULTS

The RMRs of Atlantic croaker and spot increased significantly with body mass and temperature at 15 and 25ºC (Fig. 2, Table 2). Interactions terms in this ANCOVA analysis were not significant. As expected, estimates of the constant *a* in allometric functions increased with temperature for both species, but the scaling parameter *b* did not. At 25ºC, ANCOVA with mass as a covariate revealed that kingfishes have a significantly higher RMR than Atlantic croaker or spot ($F=286.9$, $p<0.0001$, Table 2).

Relative to standard nonlinear regression, nonlinear mixed effects models fitted to the croaker and spot AMR data that accounted for repeated measures (by specifying the within-individual covariance) and adjusted for heteroscedasticity improved fit and reduced standard errors of parameter estimates including the y-intercept (Table 3, Fig. 4). Specifically, autoregressive first order (AR(1)) and autoregressive moving average

(ARMA) covariance models significantly outfit all other models considered for both spot and croaker. ARMA models slightly outfit AR(1) models (Table 3); estimates from the former were therefore used in subsequent calculations. For both species, ARMA model y-intercepts fit neatly within the confidence intervals of the RMR at 25ºC calculated for each species by substituting the mean mass of individuals used in the swim trials into equation 2. Maximum metabolic rates (AMR_{max}) were 869.2 mg O_2 kg^{-1} hr^{-1} for croaker and 1274.9 mg O_2 kg^{-1} hr^{-1} for spot, which suggest metabolic scopes (AMR_{max} SMR^{-1}) of 7.2 and 10.6 times SMR respectively (Table 4).

Gross and net costs of transport (GCOT and NCOT) were calculated from the Atlantic croaker and spot AMR data and Eq. 3 parameters resulting from ARMA models (Table 4). For both species, GCOT assumed a J-shaped curve with initial high costs and subsequently reduced costs at intermediate swimming velocities (Figure 5). The optimal swimming speeds (U_{opt}), calculated via equation 7, were 3.5 BL s^{-1} for croaker and 3.6 BL s^{-1} for spot. Substituting U_{opt} into Eqs. 5 and 6, the minimum net costs of transport ($NCOT_{min}$) were 0.54 J kg^{-1} BL^{-1} for croaker and spot, while the minimum gross costs of transport ($GCOT_{min}$) were 0.66 and 0.79 J kg^{-1} BL^{-1} respectively.

DISCUSSION

Resting metabolism

The resting metabolic rates of Atlantic croaker and spot, like those of a wide variety of species, increase significantly with body mass and temperature. Our RMR measurements likely overestimate SMR due to the spontaneous movements of subjects to maintain position and posture. Nonetheless, our results agree with previous

investigations of RMR in larvae and juveniles of both species (Hoss et al., 1988; Moser and Hettler, 1989). Interspecific comparisons to a wide array of taxa suggest that Atlantic croaker and spot have RMRs that are very typical for most freshwater, anadromous, and marine teleost fishes (Fig 3). When compared to other taxa, the RMRs of Atlantic croaker and spot align with the RMR of rainbow trout (*Oncorhynchus mykiss*), brown trout (*Salmo trutta*) and Atlantic cod (*Gadus morhua*), as well as several other sciaenid species including weakfish (*Cynoscion regalis*), silver seatrout (*Cynoscion arenarius*), spotted seatrout (*Cynoscion nebulosus*), and mulloway (*Argyrosomus japonicus*) (this study; Vetter, 1982; Fitzgibbon et al., 2007). At 25ºC, the metabolic rates of this group of "standard energy demand" teleosts were significantly lower than those observed in "high energy demand" species such as tunas and dolphinfish ($p < 0.01$).

An unexpected finding in this study was the significantly "elevated energy demand" of the two kingfish species that was significantly higher ($p < 0.01$) than standard energy demand fishes (including Atlantic croaker and spot) and significantly lower ($p < 0.01$) than the high energy demand fishes (i.e. tunas). The RMR of kingfishes was similar to that of bluefish (Bushnell, unpubl., Fig 3.), a highly active, fast-growing coastal pelagic species. Kingfishes frequent high energy littoral zones where dissolved oxygen levels are likely at or near saturations. By contrast, croaker and spot can be found in a myriad of lower energy aquatic habitats (Chao and Musick, 1977). It is likely that the elevated RMR of kingfishes is linked to their substantially faster growth rates relative to other sciaenids (Miller et. al, 2002; Waggy et al., 2006). High SMRs allow high maximum metabolic and growth rates, which are supported by higher rates of oxygen extraction and delivery made possible by larger gill surface areas (Pauly, 1981; Boggs

and Kitchell, 1991; Brill, 1996). While gill surface areas have not been examined in sciaenids, kingfishes demonstrate substantially higher heart rates than either croaker or spot (R.W. Brill and P. Bushnell, upubl.), suggesting high oxygen and metabolite distribution capabilities that could support the elevated energy demands and higher metabolic rates. However, the physiological mechanisms and ecological consequences of elevated RMR in *Menticirrhus* remain unclear, and further study within the genus is warranted.

Active metabolism

The active metabolic rates and costs of transport in fishes are typically determined by measuring oxygen consumption of individuals at increasing swimming velocities, yet few studies have accounted for the within-individual autocorrelation or heteroscedastic variance that generally results from such experiments. Failure to consider these fundamental violations of regression assumptions can result in biased or invalid parameter estimates, standard errors, and metrics of fit as well as inflated probability of Type I errors (falsely concluding significance; Underwood, 2002). Further, by treating subjects as truly random samples of the larger population, mixed effects models account for variability in the global population and increase the scope of inference to the larger wild population from which subjects were sampled Conversely, considering "fish" as fixed effects (i.e. not specifying random variables) limits inference to specific experimental subjects only (Davidian and Giltinan 1995). In this study, repeated measures nonlinear mixed effects models with AR(1) and ARMA covariance structures that accounted for heteroscedacity, applied to the croaker and spot AMR data,

significantly improved model fits and reduced parameter standard errors relative to standard nonlinear regression. Both AR(1) and ARMA covariance structures assume that the correlation between observations is a function of their lag in time; adjacent observations (in this case, VO_2 at adjoining swim velocities) are more likely to be strongly correlated than those taken further apart (i.e, at dissimilar swimming velocities) within an individual (Pinheiro and Bates, 2004). ARMA models include an additional moving average smoothing parameter and may outperform AR(1) models when data are particularly noisy (Pinheiro and Bates, 2004), such as in AMR experiments with wild fish that may vary in body condition and size. Information Theoretic model selection via AIC provides an objective balance between model simplicity (fewer parameters) and fit; models are penalized for additional parameters (Burnham and Anderson, 2002). Collectively, these methods hold great potential for improving the analyses of data resulting from AMR and other repeated measures metabolic experiments.

Resting and standard metabolic rates converge when within-chamber activity is low. Regressing our ARMA power performance curves to the y-intercept (0 m s^{-1}) generated estimates of SMR that neatly aligned within the confidence intervals of our experimental measurements of RMR for croaker and spot (Table 4, Fig. 4). The lack of significant differences in these two complimentary techniques demonstrate that our RMR estimates are likely close to true SMR and confirm the veracity of our approach and the utility of repeated measures methods for SMR estimation from AMR experiments.

Swimming respirometry revealed that spot had higher maximum metabolic rates (AMR_{max}), and broader metabolic scopes than Atlantic croaker. Maximum metabolic rates of our wild croaker and spot were 2.3 and 3.5 times higher than those of cultured

mulloway, a Pacific sciaenid (Fitzgibbon et al., 2007), comparable to those of sockeye salmon (corrected to 25º, Brett 1965), but less than half of the AMR_{max} of yellowfin tuna (Korsmeyer et al., 1996). Metabolic scopes of croaker (7.2) and spot (10.6), defined as (AMR_{max}/SMR) were similar to those observed in sockeye salmon (4-16, Brett, 1965), lower than those observed in yellowfin tuna (11.5, Korsmeyer et al., 1996, 2000), and higher than those observed in Atlantic cod (3.1, Schurmann and Steffensen, 1997), rainbow trout (3.9, Bushnell et al., 1984), Pacific yellowtail (4.04, Clark and Seymour, 2006), and mulloway (5, Fitzgibbon et al., 2007). These results suggest that the metabolic scopes of Atlantic croaker and spot are typical for standard energy demand fishes of similar morphologies and life styles. Finally, U_{opt} values for croaker (3.5 BL s^{-1}) and spot (3.6 BL s^{-1}) were higher than those of several sciaenid fishes including red drum (3.0 BL s^{-1}), spotted seatrout (2.7 BL s^{-1}), and mulloway (1.3 BL s^{-1}) (Videler, 1993; Fitzgibbon et al., 2007). Additionally, U_{opt} likely approximates routine swimming velocity in highly migratory fishes, but the routine swimming velocities of more sedentary species are likely much less than U_{opt} (Videler, 1993, Steinhausen et al., 2005). Interspecific comparisons of U_{opt} are, however, complicated by the use of numerous testing protocols (velocity increments and durations), study temperatures, individual status (wild vs. culture), body conditions and sizes, and variable life histories (Fitzgibbon et al., 2007).

Active metabolic rates in fishes range widely due to diverse biochemical, morphological, and physiological adaptations among taxa, allowing insights into the bounds of energy requirements and costs of transport. GCOT is a measure of the energy required to travel a unit difference and frequently assumes a J-shaped function with high

initial costs when SMR dominates total oxygen consumption, low intermediate costs, and increasing values above U_{opt} due to steeply increasing hydrodynamic resistance with U. The net cost of transport (NCOT) is a measure of the cost of transport excluding SMR; the proportional contribution of NCOT to GCOT thus increases with increasing speeds. The GCOT and NCOT of croaker and spot are classic examples of this pattern, though increases above U_{opt} are slight (Fig 5). Gross transport costs for spot and croaker appear only marginally affected over a broad range of intermediate and higher swimming velocities (fairly unsubstantial cost increases with speed), typical of low-drag swimming and foraging generalist fishes that have adapted for swimming performance at higher swim velocities (Pettersson and Anders Hedenström, 2000). By contrast, less efficient swimmers with higher drag, such as flatfishes, have pronounced increases in GCOT and NCOT with increasing speed above U_{opt} (Duthie, 1982). Juvenile croaker and spot may not move great distances within estuarine nursery habitats at 25ºC; however, adults of these and many other fishes undertake pronounced offshore migrations when inshore and estuarine temperatures decline to 10-15ºC (Murdy et al., 1997). Future AMR experiments conducted at 10 and 15ºC will permit the estimation of the energetic costs of these winter migrations.

The biotic and abiotic properties of many coastal ecosystems that serve as key habitats for managed aquatic organisms have changed dramatically over the past century of industrialization and population expansion (Beck et al., 2001; Kemp et al., 2005). Specifically, anthopogenic degradation of coastal waters has resulted in ever-increasing eutrophication, hypoxia, and even anoxia events, with major implications for aquatic flora and fauna (Breitburg, 2002). These concerns, coupled with and potentially

exacerbated by potential warming of aquatic habitats as a result of climate change (Perry et al., 2005) demonstrate the need for comparative studies that examine the relationships between metabolic physiology, performance, behavior, and ecology in fishes. Such studies can greatly benefit the management of aquatic resources by mechanistically linking processes from the cellular to the individual to the population level.

LITERATURE CITED

Alsop, D. and Wood, C. (1997). The interactive effects of feeding and exercise on oxygen consumption, swimming performance and protein usage in juvenile rainbow trout (*Oncorhynchus mykiss*). *J. Exp. Biol.* **200(17)**, 2337-2346.

Barton, B. A., and Schreck, C. B. (1987). Metabolic cost of acute physical stress in juvenile steelhead. *Trans. Am. Fish. Soc.* **166**, 257-263.

Benetti, D. D., Brill, R. W., Kraul, S. A. (1995). The standard metabolic rate of dolphin fish. *J. Fish. Biol*. **46**, 987-996.

Blaczka, P., Volf, M., Cepela, M. (1960). A new type of respirometer for the determination of the metabolism of fish in an active state. *Physiologia Bohemoslovenica*. **9**,553-558.

Boef, G. and Le Bail, P-Y. (1999). Does light have an influence on fish growth? *Aquaculture*. **177**, 129-152.

Boggs, C. H.; Kitchell, J. F. (1991) Tuna metabolic rates estimated from energy losses during starvation. *Physiol. Zool*. **64**,502-524.

Boisclair, D. and Sirois, P. (1993). Testing assumptions of fish bioenergetics models by direct estimation of growth, consumption, and activity rates. *Trans. Am. Fish. Soc*. **122**, 784-796.

Brandt, S. B. and Hartman, K. J. (1993). Innovative approaches with bioenergetics models: future applications to fish ecology and management. *Trans. Am. Fish. Soc.* **122**, 731-735.

Breitburg, D. 2002. Effects of hypoxia, and the balance between hypoxia and enrichment, on coastal fishes and fisheries. *Estuaries*. 25(4), 767-781.

Brett, J. R. (1965). The relation of size to rate of oxygen consumption and sustained swimming speed of sockeye salmon (*Oncorhynchus nerka*). *J. Fish Res. Board. Can.* **22**, 1491-1501.

Brett, J. R., and Groves, T. D. D. (1979). Physiological energetics. *In* Fish Physiology (W. S. Hoar, D. J. Randall, and J. R. Brett, eds.) p 279-352. Academic Press, NY.

Brill, R. W. (1979). The effect of body size on the standard metabolic rate of skipjack tuna, *Katsuwonus pelamis*. *Fish. Bull.* **77**, 494-498.

Brill, R. W. (1987). On the standard metabolic rates of tropical tunas, including the effects of body size and acute temperature change. *Fish Bull*. **85**, 25-35.

Brill, R. W. (1996). Selective advantages conferred by the high performance physiology of tunas, billfishes, and dolphin fish. *Comp. Physiol. Biochem. A*. **113**, 3-15.

Brougher, D. S., Douglass, L. W., and Soares, J.H. (2005). Comparative oxygen consumption and metabolism of striped bass *Morone saxatilis* and its hybrid *M. chrysops* x *M. saxatilis*. *J. World Aquacult. Soc.* 36(4), 521-529

Burke, B. J., and Rice, J. A. (2002). A linked foraging and bioenergetics model for southern flounder. *Trans. Am. Fish. Soc.* **131**, 120-131.

Burnham, K. P. and D. R. Anderson. (2002). Model selection and multimodel inference: a practical information-theoretic approach. 2nd edition. 488 Pp. N.Y, N.Y., U.S.A.: Springer Science and Business Media, LLC.

Bushnell, P. G., Steffensen, J. F., and Johansen, J. (1984). Oxygen consumption and

swimming performance in hypoxia-acclimated rainbow trout *Salmo gairdneri*. *J. Exp. Biol.* **113**, 225-235.

Claireaux, G., Couturier, C., and Groison, A-L. (2006). Effect of temperature on maximum swimming speed and cost of transport in juvenile European sea bass (*Dicentrarchus labrax*). *J. Exp. Biol*. **209**, 3420-3428.

Clarke, A. and Johnston, A.M. (1999). Scaling of metabolic rate with body mass and temperature in teleost fish. *J. Anim. Ecol.* **68**, 893-905.

Chapman, L. J., Kaufman, L. S., Chapman, C. A., and McKenzie, F. E. (1995). Hypoxia tolerance in twelve species of east African cichlids: potential for low oxygen refugia in Lake Victoria. *Conserv. Biol.* **9(5)**, 1274-1287.

Chapman, L. J., Chapman, C. A., Nordlie, F. G., and Rosenberger, A. E. (2002). Physiological refugia: swamps, hypoxia tolerance, and maintenance of fish diversity in the Lake Victoria region. *Comp. Biochem. Physiol. A* **133**, 421-437.

Dewar, H. and Graham, J. B. (1994). Studies of tropical tuna swimming performance in a large water tunnel. I. Energetics. *J. Exp. Biol.* **192**, 12-31.

Dowd, W. W., Brill, R. W., Bushnell, P. G., and Musick, J. A. (2006). Standard and routine metabolic rates of juvenile sandbar sharks (*Carcharhinus plumbeus*), including effects of body mass and acute temperature change. *Fish Bull*. **104**, 323-331.

Drud Jordan, A., Jungersen, M., and Steffensen, J. F. (2001). Oxygen consumption of East Siberian cod: no support forthe metabolic cold adaptation theory. *J. Fish. Biol*. **59**, 818-823.

Duthie, G. G. (1982). The respiratory metabolism of temperature-adapted flatfish at rest

and during swimming activity and the use of anaerobic metabolism at moderate swimming speeds. *J. Exp. Biol.* **97**, 359-373.

Evans, D.O. (1990). Metabolic thermal compensation by rainbow trout: effects on standard metabolic rate and potential usable power. Trans. Am. Fish. Soc. 119, 585-600.

Fitzgibbon, Q. P., Strawbridge, A. and Seymour, R. S. (2007). Metabolic scope, swimming performance, and the effects of hypoxia in the mulloway, *Argyrosomus japonicus* (Pisces: Sciaenidae). *Aquaculture*. **270**, 358-368.

Hettler, W. F. (2006). Influence of temperature and salinity on routine metabolic rate and growth of young Atlantic menhaden. *J. Fish. Biol.* **8(1)**, 55-65.

Hewett, S. W., and Kraft, C. E. (1993). The relationship between growth and consumption: comparisons across fish populations. *Trans. Am. Fish. Soc.* **122**, 814-821.

Hoss, D. E., Coston-Clements, L., Peters, D.S., and Tester, P.A. (1988). Metabolic responses of spot, *Leiostomus xanthurus*, and Atlantic croaker, *Micropogonias undulatus*, larvae to cold temperatures encountered following recruitment to estuaries. *Fish Bull.* **86(3)**, 483-488.

Jobling, M. (1994) *Fish Bioenergetics*. Chapman and Hall, New York.

Kitchell, J. F., Stewart, D. J., and Weininger, D. (1977). Applications of a bioenergetics model to perch (*Perca flavescens*) and walleye (*Stizostedion vitreum*). *Fish. Res. Board Can*. **34**, 1922-1935.

Korsmeyer, K. E., Dewar, H., Lai, N. C., and Graham, J. B. (1996). The aerobic

capacity of tunas: adaptation for multiple metabolic demands. *Comp. Biochem. Phys. A.* **113**, 17-24.

Krogh, A. (1914). The quantitative relation between temperature and standard metabolism in animals. *Internationale Zeitschrift für Physikalisch-Chemische Biologie.* 1, 491-508.

MacIsaac, P. F., Goff, G. P., and Speare, D. J. (1997). Comparison of routine oxygen consumption rates of three pleuronectids at three temperatures. *J. Appl. Ichthyol*. **13**,171-176.

McCarthy, I. D. (2001). Competitive ability is related to metabolic asymmetry in juvenile rainbow trout. *J. Fish. Biol.* 5**9(4)**, 1002-1014.

Metcalfe, N. B., Taylor, A. C., and Thorpe, J. E. (1995). Metabolic rate, social status and life-history strategies in Atlantic salmon. *Anim. Behav.* **49(2)**, 431-436.

Miller, M. J., Rowe, P. M., and Able, K. W. (2002). Occurrence and growth rates of young-of-year northern kingfish, *Menticirrhus saxatilis*, on ocean and estuarine beaches in southern New Jersey. *Copeia*. 2002(3), 815-823.

Morris, D. J., and North, A. W. (1984). Oxygen consumption of five species of fish from south Georgia. *J. Exp. Mar. Biol. Ecol.* **78**, 75-86.

Moser, M.L. and Hettler, W. F. (1989). Routine metabolism of juvenile spot, *Leiostomus xanthurus* (Lacepede), as a function of temperature, salinity, and weight. J. Fish Biol. 35, 703-707.

Ney, J. J. (1993). Bioenergetics modeling today: growing pains on the cutting edge. *Trans. Am. Fish. Soc.* **122**, 736-748.

Oikawa, S., Itazawa, Y., and Gotoh, M. (1991). Ontogenetic change in the relationship

between metabolic rate and body mass in a sea bream *Pagrus major* (Temminck & Schlegel). *J. Fish. Biol.* **38**,483-496.

Pauly, D. (1981). The relationships between gill surface area and growth performance in fish: a generalization of von Bertalanffy's theory of growth. *Berichte der Deutschen Wissenchaftlichen Kommission für Meersforschung* **28(4)**,251-282.

Perry, A. L., Low, P. J., Ellis, J. R., and Reynolds, J.D. (2005). Climate change and distribution shifts in marine fishes. *Science*. **308(5730)**, 1912 – 1915.

Petterson, L.B. and Hetterström, A. (2000). Energetics, cost reduction and functional consequences of fish morphology. *Proc. R. Soc. Lond*. B. **267**, 759-764

Pichavant, K., Person-Le-Ruyet, J., Le Bayon, N., Severe, A., Le Roux, A., and Bouef, G. (2001). Comparative effects of long term hypoxia on growth, feeding, and oxygen consumption in juvenile turbot and European sea bass. *J. Fish. Biol.* **59**, 875-883.

Pinheiro, J. C. and Bates, D. M. (2004). Mixed effects models in S and S-PLUS. (New York: Springer), 528 pp.

Post, J. R. and Lee, J. A. (1996). Metabolic ontogeny of teleost fishes. Can. J. Fish. Aquat. Sci. **53(4)**, 910-923.

Schurmann, H., and Steffensen, J. F. (1997). Effects of temperature, hypoxia, and activity on the metabolism of juvenile Atlantic cod. *J. Fish. Biol*. **50**,1166-1180.

Secor, S. M. (2009). Specific dynamic action: a review of the postprandial metabolic response. *J. Comp. Physiol. B*. 179, 1-56.

Sepulveda, C. and Dickson, K. A. (2002) Maximum sustainable speeds and cost of

swimming in juvenile kawakawa tuna (*Euthynnus affinis*) and chub mackerel (*Scomber japonicus*). *J. Exp. Biol.* **203**, 3089-3101.

Sepulveda, C., Dickson, K.A., and Graham, J. B. (2003) Swimming performance studies on eastern Pacific bonito *Sarda chilensis*, a close relative of the tunas (family Scombridae). *J. Exp. Biol*. **206**, 2739-2748.

Sloman. K.A., Motherwell, G., O'Connor, K. I. and Taylor, A. C. (2000). The effect of social stress on the standard metabolic rate (SMR) of brown trout. *Fish Physiol. Biochem*. **23**,49-53.

Soofani, N. M. AND Priede I. G. (1985). Aerobic metabolic scope and swimming performance in juvenile cod, *Gadus morhua* L. *J. Fish Biol*. **26**, 127–138.

Steinhausen, M. F., Steffensen, J. F., and Andersen, N. A. (2005). Tail beat frequency as a predictor of swimming speed and oxygen consumption of saithe (*Pollachius virens*) and whiting (*Merlangius merlangus*) during forced swimming. *Mar. Biol.* **148**, 157-204.

Steffensen, J. F. (1984). An automated swimming respirometer. *Comp. Physiol. Biochem.* **79A(3)**, 437-440.

Steffensen, J. F. (1989). Some errors in respirometry of aquatic breathers: how to avoid them and correct for them. *Fish. Physiol. Biochem*. **6**,49-59.

Steffensen, J. F., Bushnell, P. G. and Schurmann, H. (1994). Oxygen consumption in four species of teleosts from Greenland: no evidence of metabolic cold adaptation. Polar Biology 14(1), 49-54.

Steffensen, J. F. (2002). Metabolic cold adaptation of polar fish based on measurements

of aerobic oxygen consumption: fact or artefact? Artefact! *Comp. Phys. Biochem. A.* **132**. 789–795.

Van Dijk, P. L. M., Tesch, C., Hardewig, I., and Pörtner, H. O. (1999). Physiological disturbances at critically high temperatures: a comparison between stenothermal Antarctic and eurythermal temperate eelpouts (Zoarcidae). *J. Exp. Biol.* **202**, 3611-3621.

Videler, J.J. (1993). *Fish swimming*. Fish and Fisheries Series 10. London: Chapman Hall. 260 pp.

White, C.R., Phillips, N. F., and Seymour, R.S. (2006). The scaling and temperature dependence of vertebrate metabolism. *Biol. Lett.* **2(1)**, 125-127.

Winberg, G. G. (1956). Rate of metabolism and food requirements of fishes. *Fish. Res. Bd Can*. (transl. ser. no. 194).

Table 1. Species, sample size (n), and mass of the sciaenid fishes investigated in resting (A) and active (B) metabolic rate experiments.

A) Resting metabolic rate

Species	*n*	Mass (g)
Croaker (*Micropogonias undulatus*)	42	30 – 790
Spot (*Leiostomus xanthurus*)	39	4 – 240
Northern kingfish (*Menticirrhus saxatilis*)	9	105 – 475
Southern kingfish (*Menticirrhus americanus*)	6	130 – 250

B) Active metabolic rate

Species	*n*	Mass (g)
Croaker (*Micropogonias undulatus*)	15	75 – 480
Spot (*Leiostomus xanthurus*)	12	55 – 196

Table 2. Summary of resting metabolic rate equations and ANCOVA analyses for Atlantic croaker (*Micropogonias undulatus*), spot (*Leiostomus xanthurus*), and kingfish (*Menticirrhus* spp.). Mass and VO_2 data were log-transformed for ANCOVA analyses, but not for the fitting of allometric models.

Species	RMR Equation	Factor	F	p
Croaker	$RMR_{15C} = 44.8(\pm 5.7) \cdot M^{0.78(\pm 0.08)}$	mass	673.80	< 0.001
	$RMR_{25C} = 82.9(\pm 4.6) \cdot M^{0.81(\pm 0.05)}$	temperature	121.61	<0.001
		interaction	0.21	0.65
Spot	$RMR_{15C} = 44.9(\pm 13.2) \cdot M^{0.58(\pm 0.13)}$	mass	169.29	< 0.001
	$RMR_{25C} = 66.3(\pm 6.6) \cdot M^{0.50(\pm 0.05)}$	temperature	37.46	< 0.001
		interaction	1.29	0.26
Kingfish	$RMR_{25C} = 149.7(\pm 38.5) \cdot M^{0.54(\pm 0.17)}$	species	341.51	<0.001
		mass	57.50	<0.001
		interaction	0.23	0.80

Table 3. Summary statistics for nonlinear mixed effects models fit to Atlantic croaker (A) and spot (B) AMR data obtained at 25ºC via maximum likelihood. Models were of the form: $VO_2 = a + bU^c$ (Eq. 4). Repeated measures were considered only where indicated (RM), and covariance structures were: D (default), autoregressive first order (AR(1)), autoregressive moving average (ARMA), and compound symmetry (CS). AIC – Akaike's Information Criterion (Eq. 4: lower value denotes better fit). ΔAIC was calculated by subtracting each model's AIC from the best fitting model's AIC (ΔAIC = 0 denotes best fit). Models with ΔAIC < 2 have strong support, those with ΔAIC > 10 have little to no support (Burnham and Anderson, 2002).

A. Atlantic croaker

Model	*a* (± s.e.)	*b* (± s.e.)	*c* (± s.e.)	AIC	ΔAIC
NO	133.1 (± 43.3)	88.7 (± 28.0)	1.34 (± 0.17)	1910.0	69.3
RM, D	139.7 (± 24.5)	82.1 (± 17.6)	1.39 (± 0.13)	1864.2	23.5
RM, AR(1)	**126.0 (± 27.2)**	**93.5 (± 24.8)**	**1.32 (± 0.16)**	**1841.5**	**0.8**
RM, ARMA	**115.3 (± 28.4)**	**106.1 (± 28.0)**	**1.23 (± 0.16)**	**1840.7**	**0**
RM, CS	130.8 (± 24.8)	88.0 (± 20.6)	1.34 (± 0.14)	1863.7	23

B. Spot

Model	*a* (± s.e.)	*b* (± s.e.)	*c* (± s.e.)	AIC	ΔAIC
NO	13.0 (± 116.4)	246.4 (± 95.4)	0.89 (± 0.17)	2085.3	89.7
RM, D	193.1 (± 23.0)	69.8 (± 15.6)	1.60 (± 0.12)	2005.0	9.4
RM, AR(1)	**167.2 (± 41.2)**	**117.1 (± 40.2)**	**1.26 (± 0.16)**	**1995.8**	**0.2**
RM, ARMA	**176.6 (± 37.8)**	**108.0 (± 36.5)**	**1.31 (± 0.18)**	**1995.6**	**0**
RM, CS	193.0 (± 22.1)	67.6 (± 15.5)	1.66 (± 0.12)	2007.4	11.8

Table 4. Summary of the estimated standard metabolic rate (SMR), mean resting metabolic rate (RMR), active metabolic rate (AMR_{max}), metabolic scope, optimum swimming velocity (U_{opt}), and the minimum net ($NCOT_{min}$) and gross ($GCOT_{min}$) costs of transport for Atlantic croaker and spot at 25 ºC. SMR values were estimated by obtaining the y-intercept (0 BL s^{-1}) of the best fitting AMR power function (equation 3), while mean RMR was calculated by inserting the mean AMR experimental subject mass into the appropriate 25 ºC equations from Table 2. Metabolic scope was calculated by dividing AMR_{max} by the mean RMR.

Parameter	Atlantic croaker	Spot
SMR_{25C} estimate ($mg\ O_2\ kg^{-1}\ hr^{-1}$)	115.3 ± 28.4	176.6 ± 37.8
mean RMR_{25C} ($mg\ O_2\ kg^{-1}\ hr^{-1}$)	102.4 ± 8.2	184.1 ± 17.9
AMR_{max} ($mg\ O_2\ kg^{-1}\ hr^{-1}$)	869.2 ± 71.7	1274.9 ± 55.3
Scope ($mg\ O_2\ kg^{-1}\ hr^{-1}$)	7.2	10.6
U_{opt} ($BL\ s^{-1}$)	3.5	3.6
$NCOT_{min}$ ($J\ kg^{-1}\ BL^{-1}$)	0.54	0.54
$GCOT_{min}$ ($J\ kg^{-1}\ BL^{-1}$)	0.66	0.79

Figure 1. Schematic representation of the metabolic chambers used in experiments. A. computing equipment and oxygen electrodes. B. Experimental stop-flow respirometry chamber for resting metabolic rate (RMR) experiments. The letters 'F' and 'R' refer to flushing and recirculating pumps, and the illustrated species is a spot (*L. xanthurus*). C. Experimental stop-flow Blaczka swim chamber for active metabolic rate (AMR) experiments. The letter 'F' denotes the flush pump, and the illustrated species is an Atlantic croaker (*M. undulatus*). Filtered, oxygenated seawater was introduced to the system via the spigot on the left of B and C (denoted by blue arrow) and exited the system via thru-hull fitting (B) or standpipe (C).

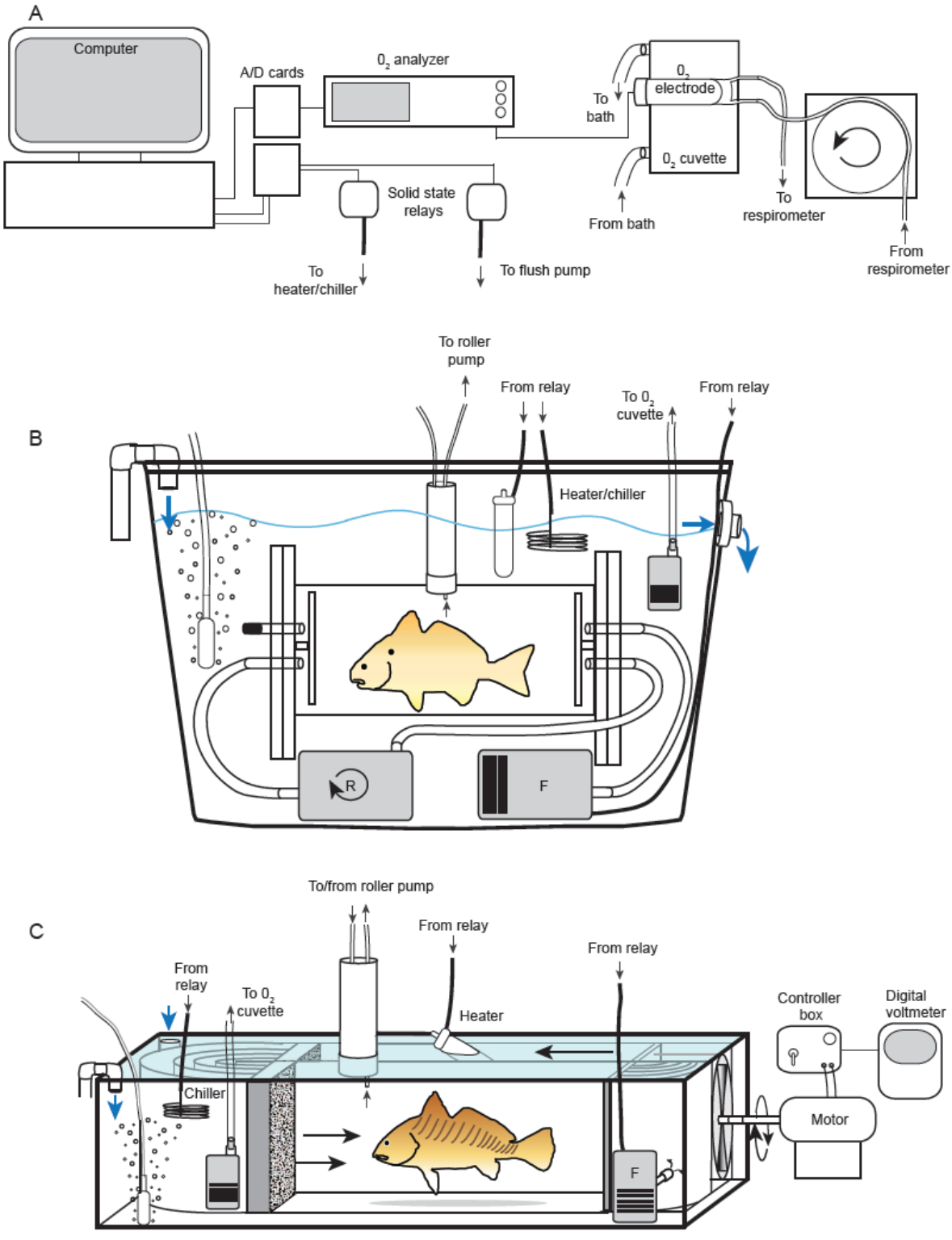
A
Computer
A/D cards
0_2 analyzer
Solid state relays
To heater/chiller
To flush pump
To bath
0_2 electrode
0_2 cuvette
From bath
To respirometer
From respirometer
B
To roller pump
From relay
To 0_2 cuvette
From relay
Heater/chiller
R
F
C
To/from roller pump
From relay
From relay
From relay
To 0_2 cuvette
Heater
Chiller
Controller box
Digital voltmeter
Motor
F

Figure 2. Resting metabolic rates of Atlantic croaker (*M. undulatus*), spot (*L. xanthurus*), and kingfish (*Menticirrhus sp.*). For croaker and spot, open symbols denote Q_{10} adjusted values (using a Q_{10} value of 1.65, White et al., 2006), solid symbols represent experiments conducted exactly at 15 and 25 ºC. For kingfishes, open triangles denote southern kingfish (*Menticirrhus americanus*), solid triangles denote northern kingfish (*M. saxatilis*). Allometric equations (Table 2) are represented by blue lines for spot and croaker at 15 ºC and by red (spot, croaker) or black (kingfishes combined) lines at 25 ºC.

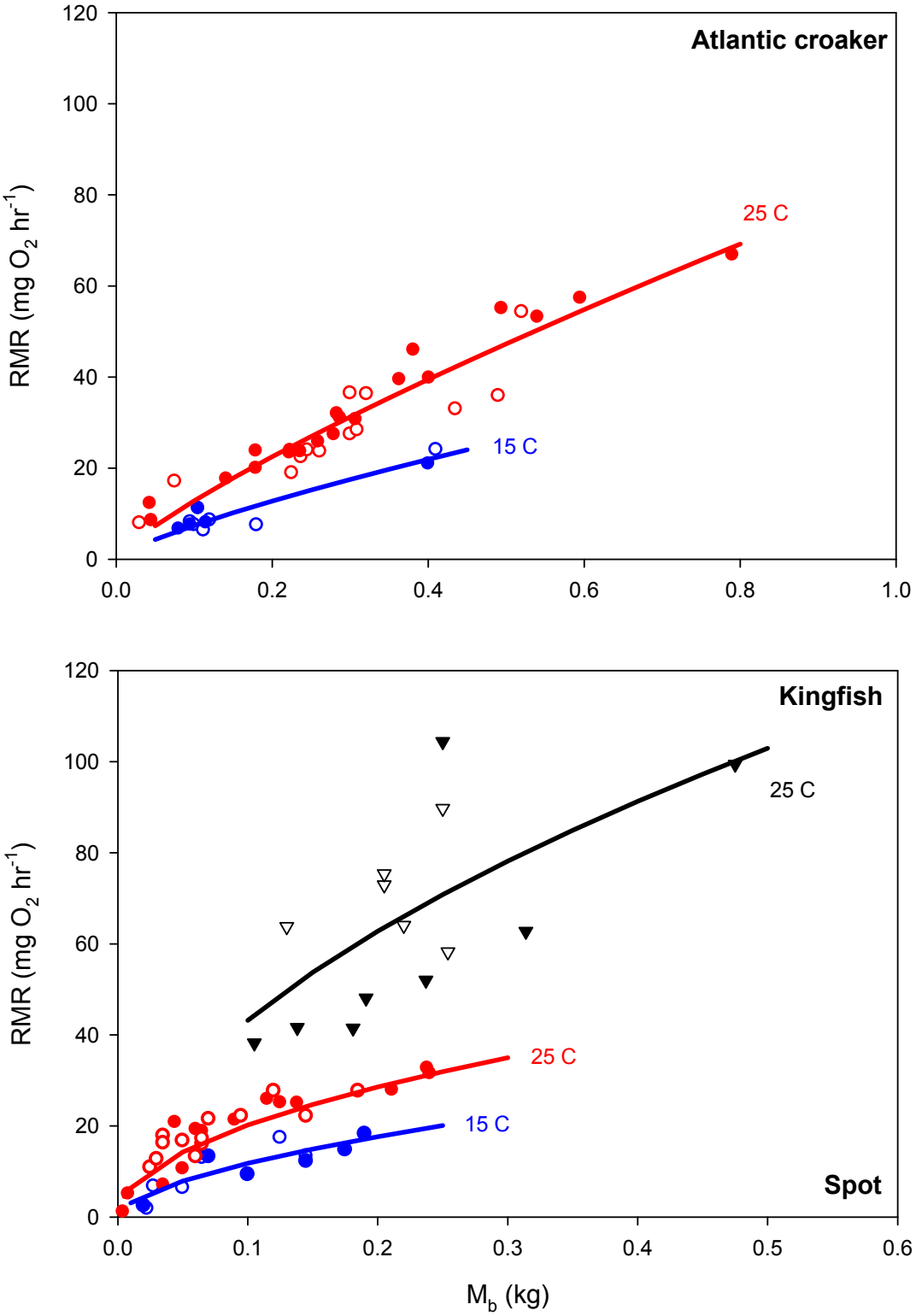
Atlantic croaker
25 C
15 C
RMR (mg O_2 hr^{-1})
0
20
40
60
80
100
120
0.0
0.2
0.4
0.6
0.8
1.0
Kingfish
25 C
25 C
15 C
Spot
RMR (mg O_2 hr^{-1})
0
20
40
60
80
100
120
0.0
0.1
0.2
0.3
0.4
0.5
0.6
M_b (kg)

Figure 3. Interspecific comparison of the relationship between standard metabolic rate (SMR) and body mass (M_b) of three groups of fishes categorized by oxygen demand: (A, black line) standard oxygen demand, (B, blue line) elevated oxygen demand, and (C, red line) high oxygen demand. All data were standardized to 25 ºC via a Q_{10} of 1.65 (White et al., 2006). Standard oxygen demand teleosts include: [1]spot, [2]croaker, [4]weakfish (this study, S1), [5]spotted seatrout (this study, S1; Vetter, 1982), [6]mulloway (Fitzgibbon et al., 2007), •rainbow trout (Evans, 1990), ▲brown trout (Sloman et al., 2000) and ▪Atlantic cod (Schurmann and Steffensen, 1997). Elevated oxygen demand teleosts include: [3]kingfishes *Menticirrhus* spp. (this study), and [PSA]bluefish (Bushnell, unpubl). High oxygen demand teleosts include: [SKJ]skipjack tuna, [YFT]yellowfin tuna, [KAW]kawakawa, and [CHI]mahi mahi (Benetti et al., 1995; Brill, 1979; Dewar and Graham, 1994; Sepulveda and Dickson, 2000). Note that log axes are used for graphical portrayal, but data were not log-transformed for model fitting and hypothesis testing.

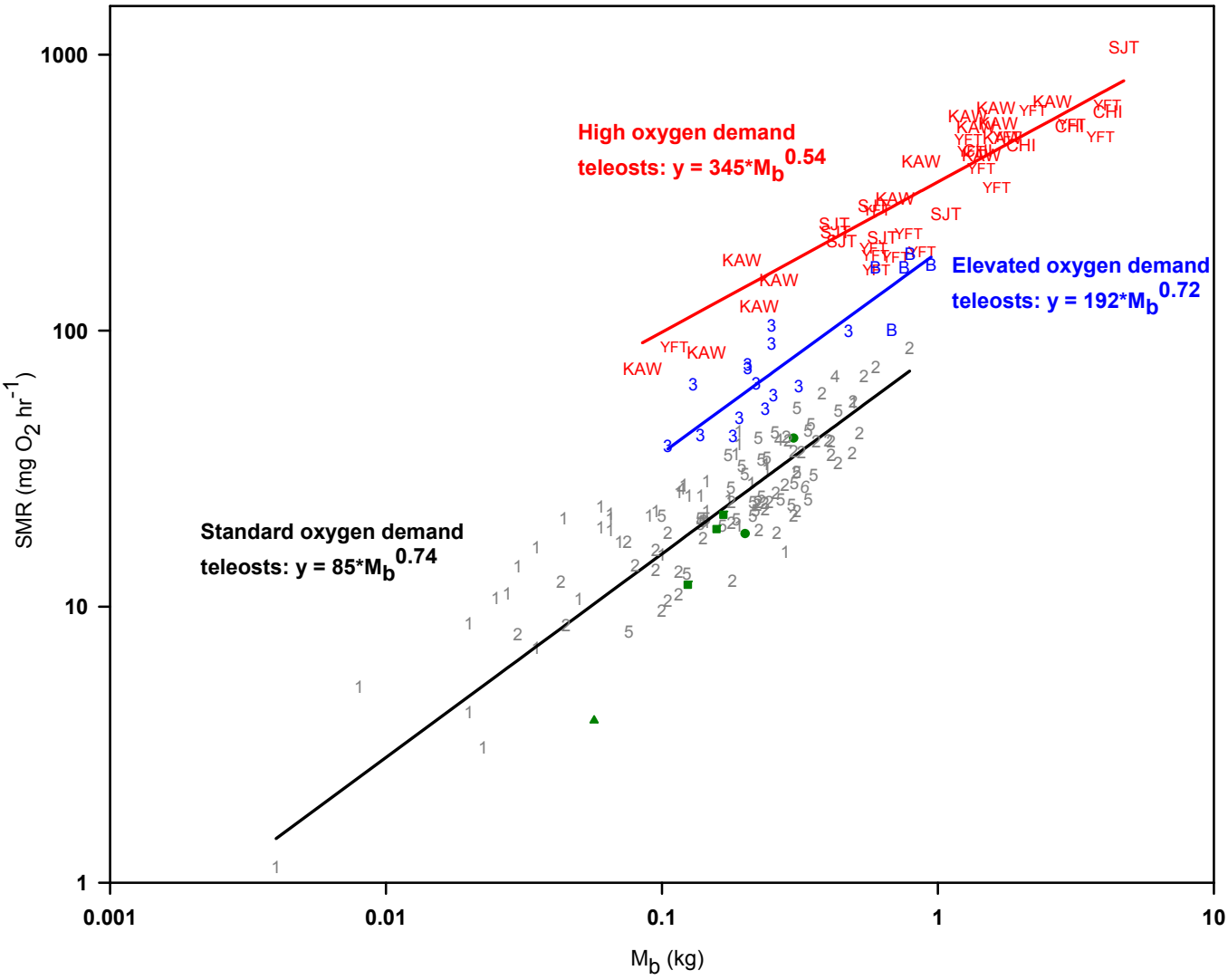
High oxygen demand
teleosts: y = 345*M_b^0.54
Elevated oxygen demand
teleosts: y = 192*M_b^0.72
Standard oxygen demand
teleosts: y = 85*M_b^0.74
SMR (mg O2 hr-1)
Mb (kg)
1000
100
10
1
0.001
0.01
0.1
1
10

Figure 4. Oxygen consumption (mg O_2 kg^{-1} hr^{-1}) as a function of swimming velocity (BL s^{-1}) of Atlantic croaker (*n*=15) and spot (*n*=12) at 25ºC. The solid black line represents the best fitting equation (Eq 4: $VO_2 = a + bU^c$). For both species, repeated measures linear mixed effects models using the ARMA covariance matrix best fit the AMR data; corresponding parameter estimates and AIC model fits are given in Table 3. Red lines denote 95% CI of RMR for a fish with mean mass of all swum individuals (eq. 2), blue lines denote 95% CI of y-intercept estimated by the best fitting ARMA model (eq. 3) for each species (Table 3).

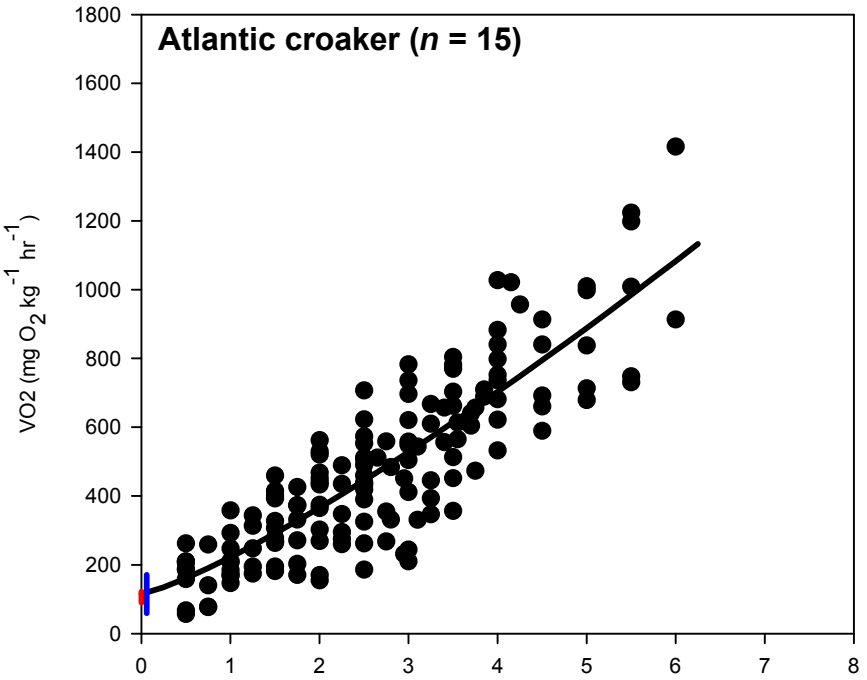
Atlantic croaker (*n* = 15)
VO2 (mg O_2 kg^{-1} hr^{-1})
0
200
400
600
800
1000
1200
1400
1600
1800
0
1
2
3
4
5
6
7
8

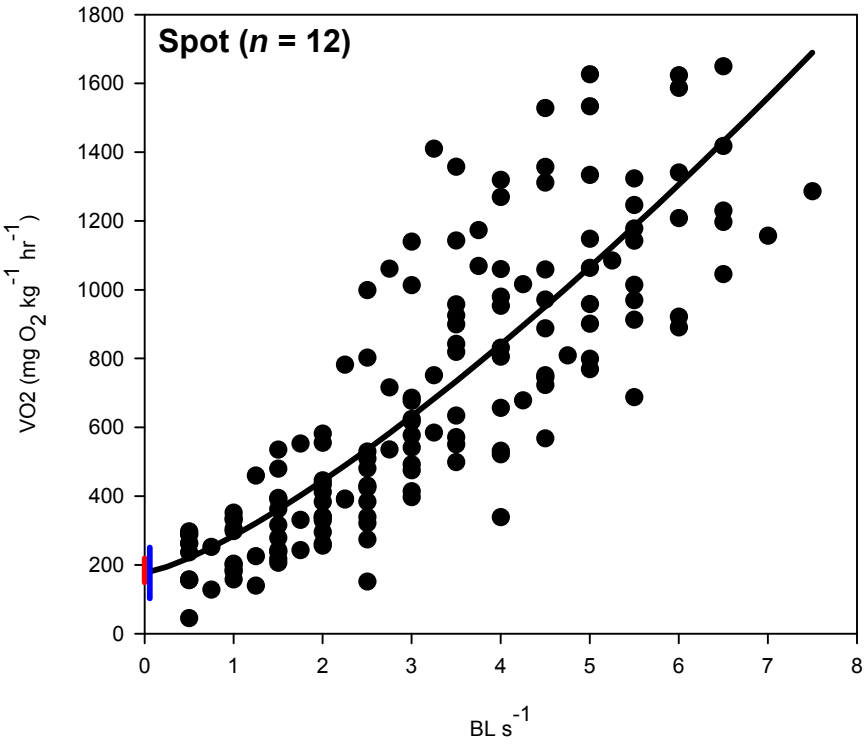
Spot (*n* = 12)
VO2 (mg O_2 kg^{-1} hr^{-1})
0
200
400
600
800
1000
1200
1400
1600
1800
0
1
2
3
4
5
6
7
8
BL s^{-1}

Figure 5. Gross cost of transport (GCOT: J kg^{-1} BL^{-1}) and net cost of transport (NCOT: J kg^{-1} BL^{-1}) for Atlantic croaker (*n* = 15) and spot (n = 12) swum at 25°C. Note different X-axis scale for spot. Solid lines represent predicted values calculated from parameter estimates from equations 5 and 6. Dashed vertical lines represent $GCOT_{min}$ and $NCOT_{min}$ at the U_{opt} of each species, calculated from equation 7.

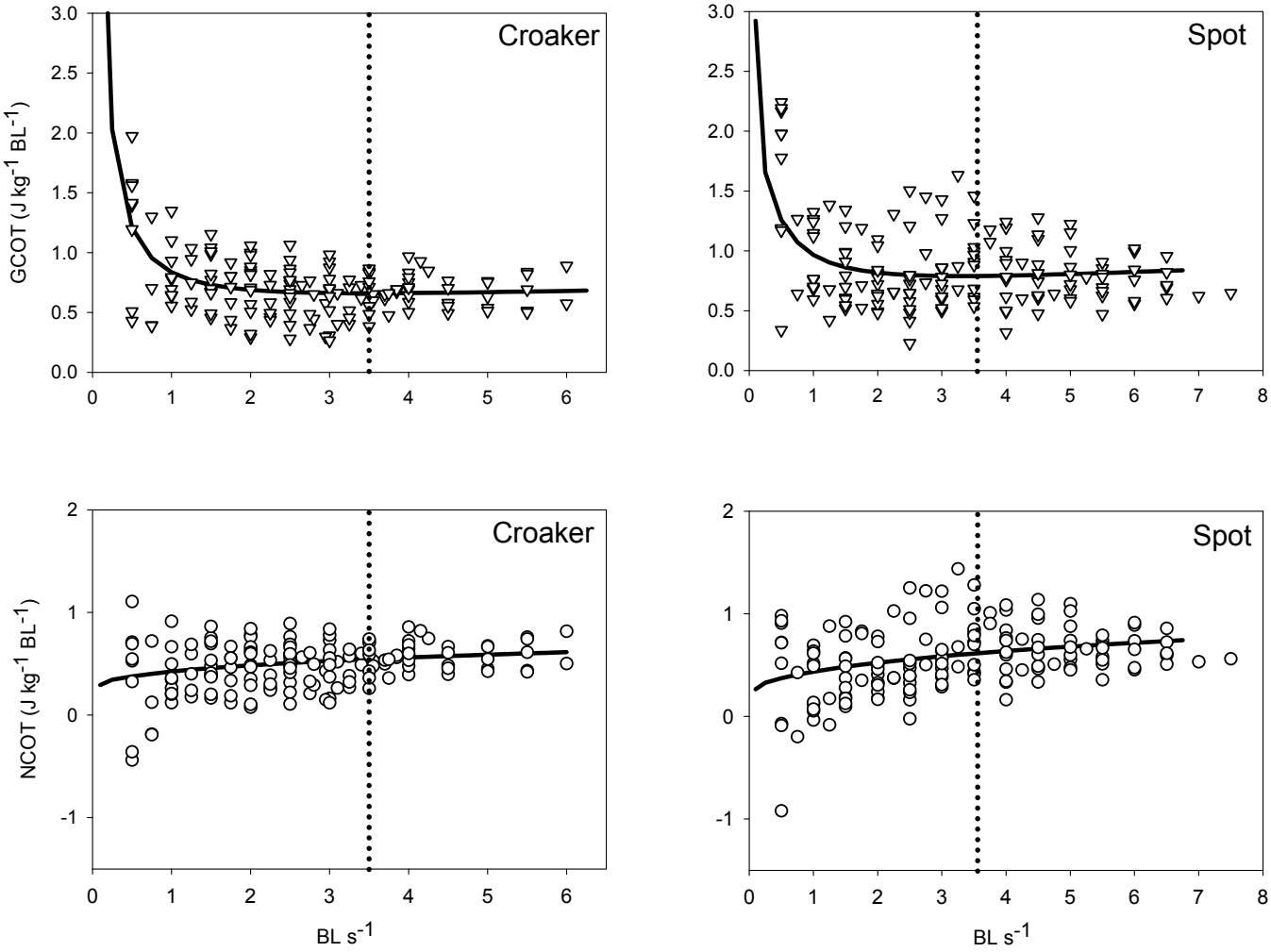
Croaker
Spot
GCOT (J kg-1 BL-1)
NCOT (J kg-1 BL-1)
BL s-1
BL s-1

PROJECT CONCLUSION AND FUTURE WORK

This dissertation applied comparative, multidisciplinary ecophysiological methods to investigate aspects of the sensory and energetic ecology of sciaenid fishes and several competing piscivores in Chesapeake Bay. The physical properties of Chesapeake Bay and other coastal and estuarine habitats, such as temperature, salinity, dissolved oxygen and light levels, demonstrate hyperdynamic lability on a variety of temporal and spatial scales (Kemp et al., 2005). Many of these waters are key nursery, forage, or reproductive habitats for the majority of managed coastal aquatic fauna, and have undergone significant anthropogenic alteration over the past century (Beck et al., 2001). The physiology of coastal organisms is thus an important and complex field, yet remains surprisingly underinvestigated.

The physiology of an organism represents its *internal* ecology – a study of the properties and reactions of cells, the organs they comprise, and the individual organisms that house them to chemical and physical stimuli. An organism's behavior is an expression of its *external* ecology as enabled by the physical bounds of its habitat and the constraints of its own (*internal*) physiology. The interface between the processes occurring within organisms and those occurring between organisms and their environment is the discipline of ecophysiology, which seeks to understand the abilities and limitations of an organism's form and function to gain insights into ecological interactions that, in turn, determine fundamental properties of populations of organisms and communities. As such, ecophysiology is a transfer function wherein the energetic needs and responses to physical stimuli on a cellular level, as affected by biotic and abiotic factors, are transformed into ecological effects via behavioral acts by animals.

Ecophysiology is thus the currency of organismal behavior, much as individual behavior is the currency of population and ecosystem ecology. (*sensu* Weissburg, 2005)

This dissertation not only provides important initial investigations into the sensory and energetic ecophysiology of managed aquatic fishes common to neritic zones in the western North Atlantic, such as Chesapeake Bay, but also demonstrates the potential power and utility of physiological techniques to provide a wide variety of information that may complement more traditional techniques used in fisheries science. Many questions in fisheries science are addressed at the scope of populations, fishery-wide dynamics, and anthropomorphic perspectives (management regulations and benchmarks). Ecophysiological methods, by contrast, approach fisheries problems from the perspectives of cells and individual fish. Physiologists have a great deal to learn from traditional fisheries scientists about critical data needs for models to assess populations and processes, socioeconomic dynamic underlying management, and species of concern. Likewise, traditional fisheries scientists have a great deal to lean from physiologists regarding the mechanisms underlying behavior and ecology, the physical and physiological limitations of a species, and optimal conditions for growth and reproduction. Combining these two research universes can result in mutually beneficial, complimentary investigations that attack real-world fisheries problems from the perspective of fish and man simultaneously, leading to mechanistic insights into the dynamics of behaviors, ecology, ecosystems, and populations. The major findings of my research and suggestions for future research directions follow below.

Sciaenid audition

This project applied auditory brainstem response (ABR) to assess the pressure and particle acceleration thresholds of six sciaenid fishes commonly found in Chesapeake Bay. Sciaenid fishes are important models of fish sound production, but substantially less is known about their hearing abilities. The results of this project demonstrate that the six species are hearing generalist fishes attuned to frequency bandwidths < 2 kHz. Sound pressure and particle acceleration thresholds varied significantly among species and between frequencies, with lower thresholds generally observed in species with morphological auditory adaptations (e.g. anteriorly-projecting swim bladder diverticulae). Such adaptations are expressed in *Cynoscion* and *Micropogonias* that are among the most derived within the Sciaenidae (Sasaki, 1989), suggesting that these species may be evolving towards becoming hearing specialists. Enhanced auditory abilities and sonifery are fairly common strategies among piscine taxa that frequent turbid environments (Ramcharitar et al., 2006; Rountree et al., 2006). Sciaenids were most sensitive at low frequencies that overlap the peak frequencies of their vocalizations, which may propagate between 8-128 m from soniferous spawning aggregations in coastal and estuarine environments.

Sciaenid audition remains a fruitful field for future study, and the results of this project may be used to guide several future research avenues. Several anthropogenic impacts may deleteriously affect soniferous spawning aggregations. Specifically, anthropogenic noise (Wahlberg and Westerberg, 2005; Rountree et al., 2006) and decreased auditory neural function due to the increased prevalence of neurotoxin-producing dinoflagellate blooms in eutrified waters (Lu and Tomchick, 2002) have strong

potential to impact both audition and sonifery, key adaptations in the reproductive ecology of sciaenid species. However, these anthropogenic impacts, along with potential effects of contaminant bioaccumulation on auditory performance, have received little research attention. Similarly, sex-specific differences in audition seem likely in some sciaenids because of species-specific difference in sonifery among the sexes. Sonifery occurs in both sexes in many sciaenid genera (*Sciaenops*, *Leiostomus*, *Micropogonias*), only in males in *Cynoscion*, and not at all in other genera (*Menticirrhus*). Ontogenetic differences in sciaenid auditory and soniferous abilities have likewise not been described for the family despite changes in microhabitat use in different lifestages. Additionally, sonifery intensifies in spawning seasons and during the administration of steroid hormones to some sciaenids (Connaughton et al. 1997), but is unclear if temporal changes in auditory abilities likewise occur during spawning seasons as has been demonstrated in other taxa (Sisneros et al., 2004). Finally, intriguing questions remain in topics such as the particle motion components of sciaenid vocalizations, directional hearing via particle motion component of sound, the role of the lateral line in encoding low frequency sounds, masked auditory thresholds for pressure and particle motion, receptor-level auditory morphology (hair cell orientation patterns) and neural encoding and processing mechanisms.

Vision in coastal teleosts

This study used electroretinographic techniques to describe the light sensitivities, temporal properties, and spectral characteristics of the visual systems of five sciaenids and four nonsciaenid piscivores common to Chesapeake Bay and other western North

Atlantic neritic waters: weakfish, spotted seatrout, red drum, Atlantic croaker, spot, striped bass, bluefish, cobia, and summer flounder. Maintaining optimal visual performance in these habitats is a difficult task because of unavoidable tradeoffs between visual sensitivity and resolution. Benthic and nocturnal foragers exhibited higher sensitivities, broader dynamic ranges, and higher temporal summation (i.e. slower vision) than pelagic piscivores, consistent with lifestyle and habitat. Collectively, these results suggest that dim-dwelling (i.e. benthic and nocturnal) foragers are well adapted to the turbid photoclimate of the coastal and estuarine habitats they utilize. Conversely, pelagic foragers exhibited more diel plasticity in sensitivity, temporal properties, and spectral responses of their eyes, consistent with foraging in their diurnal light niches. However, the recent anthropogenic degradation of water quality in coastal environments has occurred at a pace faster than the evolution of visual systems, amplifying the importance of characterizing visual function in managed aquatic fauna.

The visual ecology of neritic fishes remains a fruitful field for future study, and the results of this project may be used to guide several future research avenues. From a structure-function perspective, although microhabitat use changes in larval, juvenile, and adult neritic fishes, little is known about how ontogenetic changes in their visual systems. Further, although this dissertation models the chromatic mechanisms most likely in our ERG data, behavioral and photopigment isolating experiements (such as extractions, MSP, or chromatic adaptation) would greatly improve insights into ecology and performance throughout ontogeny. Similarly, morphological techniques would provide important information regarding visual fields, spatial resolution, and receptor sensitivity, as well as how these change with ontogeny. Experiments manipulating light levels would

shed insights into the plasticity of visual systems and rates of adaptation to environmental change in light fields. Intriguing questions remain in topics such as the visual communication in conspecifics, neural encoding, processing, and integration mechanisms and rates, the effects of comparative sensory deprivation on foraging,

Several anthropogenic impacts on optical habitats may deleteriously affect the visual systems of neritic fishes, with potentially major implications for the structure and function of coastal ecosystems, yet little experimental work has addressed these issues. The effects of dinoflagellate neurotoxins (*sensu* Lu and Tomchick, 2002) and/or anthropogenic contaminants (Blaxter and Hallers-Tjabbes, 1992) on visual development and thresholds in fishes are exciting fields with little study at present. The fusion of electrophysiological techniques with experimental manipulations and traditional fisheries techniques could improve insights into ecosystem structure and function for resource management. Field measurements of aquatic light fields and how they and faunal communities change in space and time, combined with experimentally-derived sensitivity thresholds for key species, would allow far-reaching insights into the physical and physiological boundaries of fish visual systems (*sensu* Johnsen and Sosik, 2003; Johnsen, 2007). A better understanding of temporal and spatial variations in light fields, combined with physiological thresholds, may provide a key environmental predictor variable for studies investigating habitat use, movement, migration, abundance, aggregation, predator-prey dynamics, and gear efficiency. The identification of sensitivity thresholds combined with laboratory or field investigations of predator-prey reaction distances as a function of light level and turbidity is a powerful fusion of ecophysiological and behavioral techniques, particularly if it can extended to the formation of habitat

envelopes, as has been done with other environmental variables (Luo et al., 2006). These experimental data could result in the development of powerful visual foraging and resource-use models for key managed species (*sensu* Mazur and Beauchamp, 2006); integrated over habitats and multiple species, such approaches could be used to investigate the effects of light on benthic-pelagic resource dynamics.

Energetic ecology

This project examined the resting metabolic rates (RMR) of four wild-caught sympatric sciaenid species (Atlantic croaker, spot, and northern and southern kingfish) as well as the active metabolic rate (AMR) of two species (croaker and spot) to gain insights into the energetic ecology of these fishes and facilitate inter- and intraspecific comparisons. Croaker and spot had RMRs and AMRs comparable to the majority of non-scombroid and non-thunniform teleost fishes. By contrast, the RMRs of the kingfishes were significantly higher than croaker and spot, but significantly lower than tunalike fishes. Additionally, the nonlinear mixed effects models used for analyses of AMR data in this project used separate techniques to account for the repeated sampling of individuals and the heteroscedastic variance resulting from AMR methodology. The inclusion of both analytical techniques significantly improved fits of resulting models and demonstrate a quantitative advancement for the analyses of these data.

The metabolic and energetic ecology of fishes, though well-studied (Clarke and Johnston, 1999), remains a field of burgeoning research potential given recent interest in bioenergetic and individual-based models in support of ecosystem-based fisheries management. In the absence of data on relevant species, many such models use data

from related or ecologically-similar taxa (Ney, 1993). Data for specific dynamic action (SDA, the costs of protein assimilation) are especially sparse in the literature (Secor, 2009), and metabolic rate data are lacking across ontogenetic life stages for many managed neritic fishes common to the western North Atlantic (Post and Lee, 1996). Little is also known about the magnitude of additional metabolic costs due to toxins, contaminants, and disease. Investigations of the direct effects of hypoxia and temperature on metabolic rate are likewise of increasing importance given recent anthropogenic degradation of water quality and warming of coastal seas resulting from climate change. Coastal eutrophication and sedimentation may also increase metabolic rate directly via respiratory mucus production and indirectly by increasing stress levels (Abrahams and Kattenfield, 1997; Utne-Palm, 2002). Additionally, turbidity-induced shifts from visual foraging to encounter-rate feeding approaches in piscivores would increase the energetic costs of predation via increased activity levels (i.e., a predaotr's AMR), potentially decreasing the caloric gain from consumed prey. Finally, given that only 32 of Chesapeake Bay's 267 species are residents (12%: Murdy et al., 1997), AMR data at temperatures key to emigration of seasonal visitors are needed to assess the costs of migration.

Sciaenids as model organisms

This dissertation has revealed important initial insights into structure-function-environment relationships in the ecophysiology of coastal teleosts, focusing most heavily on teleosts of the family Sciaenidae common to Chesapeake Bay. Sciaenid fishes have long served as models of teleost bioacoustics (Roundtree et al., 2006), but the collective results of this dissertation demonstrate the potential utility of this group as models for a

variety of ecophysiological and ecological studies. Sciaenids are taxomonically, ecomorphologically, trophically, and ecologically diverse, inhabiting a myriad of niches in estuarine, coastal neritic and reef-associated marine systems (Myers, 1960). In neritic zones, sciaenid fishes support large commercial, recreational, and subsistence fisheries, thus serve as useful models of fisheries-relevant resources. Additionally, this dissertation has demonstrated that many sciaenid fishes are hardy captive subjects adaptable to a variety of handling, experimental manipulation, and even surgical techniques. In fact, global aquaculture of sciaenid fishes is rapidly expanding (Hong and Zhang, 2003), further suggesting their adaptability as captive research subjects.

Today's applied fisheries issues are broad in scale, frequently affecting legions of interacting organisms, and potentially involving many stakeholders and jurisdictions, requiring multidisciplinary approaches with an emerging emphasis on mechanisms to identify and reduce anthropogenic impacts on managed aquatic fauna. As new techniques and technologies both inspire and facilitate new directions of research, new groups of fishes will be needed to serve as model organisms, particularly in neritic environments. Sciaenid fishes are ideal prospective models for basic and applied fisheries problems.

REFERENCES

Abrahams, M. and Kattenfeld, M. (1997). The role of turbidity as a constraint on predator-prey interactions in aquatic environments. *Behav. Ecol. Sociobiol.* **40**, 169-174.

Blaxter, J.H.S., and Hallers-Tjabbes, C.C.T. (1992). The effect of pollutants on sensory systems and behaviour of aquatic animals. *Aquatic Ecology*. **26**, 43-58.

Clarke, A. and Johnston, A.M. (1999). Scaling of metabolic rate with body mass and temperature in teleost fish. *J. Anim. Ecol.* **68**, 893-905.

Connaughton, M. A., Fine, M. L. and Taylor, M. H. (1997). The effects of seasonal hypertrophy and atrophy on fiber morphology, metabolic substrate concentration and sound characteristics of the weakfish sonic muscle. *J. Exp. Biol.* 200, 2449–2457.

Hong, W. and Zhang, Q. (2003). Review of captive bred species and fry production of marine fish in China. *Aquaculture*. **227**, 305-318.

Johnsen, S. (2007). Does new technology inspire new directions? Examples drawn from pelagic visual ecology. *Integr. Comp. Biol*. **47**, 799-807.

Johnsen, S. and Sosik, H.M. (2003). Cryptic coloration and mirrored sides as camouflage strategies in near-surface pelagic habitats: implications for foraging and predator avoidance. Limnol. Oceanogr. **48**, 1277-1288

Lu, Z. and Tomchick, S.M. (2002). Effects of a red-tide toxin on fish hearing. *J. Comp. Physiol. A.* **188**, 807-813.

Luo, J., Prince, E.D., Goodyear, C.P., Luckhurst, B.E., and Serafy, J.E. (2006).

Vertical habitat utilization by large pelagic animals: a quantitative framework and numerical method for use with pop-up satellite tag data. *Fish. Oceanogr*. **15**, 208-229.

Mazur, M.M. and Beauchamp, D.A. (2006). Linking piscivory to spatial–temporal distributions of pelagic prey fishes with a visual foraging model. *J. Fish. Biol.* **69(1)**, 151-175.

Myers, G.S. (1960). Restriction of the croakers (Sciaenidae) and anchovies (Engraulidae) to continental waters. *Copeia*, 1960(1): 67-68.

Ney, J. J. (1993). Bioenergetics modeling today: growing pains on the cutting edge. *Trans. Am. Fish. Soc.* **122**, 736-748.

Post, J. R. and Lee, J. A. (1996). Metabolic ontogeny of teleost fishes. Can. J. Fish. Aquat. Sci. **53(4)**, 910-923.

Ramcharitar, J.U., Gannon, D.P., and Popper, A.N. (2006). Bioacoustics of fishes of the family Sciaenidae (croakers and drums). *Trans. Am. Fish. Soc.* **135**, 1409-1431.

Roundtree, R. A., Gilmore, R. G., Goudey, C. A., Hawkins, A. D., Luczkovitch, J. J., and Mann, D.A. (2006). Listening to fish: applications of passive acoustics to fisheries science. *Fisheries.* **31(9)**, 433-446.

Sasaki, K. (1989). Phylogeny of the family Sciaenidae, with notes on its zoogeography (Teleostei: Perciformes), *Memoirs of the Faculty of Fisheries, Hokkaido University, Hakodate, Japan* **36**, Serial 53, pp. 1–137.

Secor, S. M. (2009). Specific dynamic action: a review of the postprandial metabolic response. *J. Comp. Physiol. B*. 179, 1-56.

Sisneros, J.A., Forlano, P.M., Deitcher, D.L., and Bass, A.H. (2004). Steroid-dependent auditory plasticity leads to adaptive coupling of sender and receiver. *Science*. **305**, 404-407.

Utne-Palm, A. C. (2002). Visual feeding of fish in a turbid environment: physical and behavioural aspects. *Mar. Freshwater Behav. Physiol.* **35**,111 -128.

Wahlberg, M. and Westerberg, H. (2005). Hearing in fish and their reactions to sounds from offshore wind farms. *Mar. Ecol. Prog. Ser.* **288**, 295-309.

VITA

Andrij Zenon Horodysky

Born in Bordentown, NJ on February 11, 1978. Graduated from Bordentown Regional High School, Bordentown, NJ in 1996. Graduated with Honors from Eckerd College, St. Petersburg, FL with a Bachelor of Science in Marine Science in 2000. Received the Barry M. Goldwater Scholarship in 1999. Conducted a senior honors thesis entitled "Larval Ingress and Subadult Mortality in Two Populations of Ladyfish (Elops) (Teleostei: Elopidae) in the Indian River Lagoon, Florida."

Entered the Master of Science program at the School of Marine Science, Virginia Institute of Marine Science, College of William and Mary in August 2001 and obtained said degree in May 2004. Became a member of Umpqua Feather Merchants' Signature Fly Designer Program in 2001. Entered the Doctor of Philosophy program at the School of Marine Science, Virginia Institute of Marine Science, College of William and Mary in August 2004 and received the Matthew Fontaine Maury Student Fellowship Award in May 2008. Lost a fly rod to an Alaskan grizzly bear in 2005, and served as a postgame effects specialist for Super Bowls XXXIX, XLI, and XLIII.